To the Graduate Council:

I am submitting herewith a thesis written by Robert Earl Gatlin entitled "Numerical Modeling and Analysis of Reinforced Residential Foundations Subjected to Mining-Induced Subsidence." I have examined the final copy of this thesis for form and content and recommend that it be accepted in partial fulfillment of the requirements for the degree of Masters of Science, with a major in Civil Engineering.

Richard M. Bennett

Richard M. Bennett, Major Professor

We have read this thesis
and recommend its acceptance:

Eric C. Drumm

Edwin G. Burdette

Accepted for the Council:

C W Minkel

Associate Vice Chancellor
and Dean of the Graduate School

STATEMENT OF PERMISSION TO USE

In presenting this thesis in partial fulfillment of the requirements for a Master's degree at The University of Tennessee, Knoxville, I agree that the Library shall make it available to borrowers under rules of the Library. Brief quotations from this thesis are allowable without special permission, provided that accurate acknowledgement of the source is made.

Permission of extensive quotation from or reproduction of this thesis may be granted by my major professor, or in his absence, by the Head of Interlibrary Services when, in the opinion of either, the proposed use of the material is for scholarly purposes. Any copying or use of the material in this thesis for financial gain shall not be allowed without my written permission.

Signature Robert E. Gatten

Date 2/25/93

NUMERICAL MODELING AND ANALYSIS OF REINFORCED RESIDENTIAL FOUNDATIONS SUBJECTED TO MINING-INDUCED SUBSIDENCE

A Thesis

Presented for the

Master of Science

Degree

The University of Tennessee, Knoxville

Robert Earl Gatlin

May, 1993

DEDICATION

This thesis is dedicated to my Family.

ACKNOWLEDGEMENTS

I first want to thank my major professor, Dr. Richard M. Bennett, for his guidance, suggestions, and support. This thesis would be far from complete without his assistance. I would also like to thank Dr. Eric C. Drumm and Dr. Edwin G. Burdette for their contributions as members of my committee. Additionally, the help and advice from the entire staff of the Subsidence Group of the Institute of Geotechnology at UTK is greatly appreciated. Finally, this thesis would not be possible if not for the financial support and opportunity to participate in this research given from the U.S. Bureau of Mines, Twins Cities Research Center. Thank You Larry, Ted, and Mark.

ABSTRACT

Numerical techniques are used to investigate the behavior of reinforced residential foundations subjected to mine-induced subsidence. The foundation and subsidence event are modeled after test foundations constructed near West Frankfort, Illinois. Parametric analyses are performed to evaluate reinforcing amounts and location within the footing, soil-structure interface, the thickness of the footing, and masonry wall construction techniques.

The finite element analysis established that the combination of the masonry wall and footing contribute greatly to foundation response. There was no reduction in damage and curvature for increased amounts of reinforcing placed in the footing. More damage occurred in the reinforced footing as its depth was gradually increased; however, larger increases of footing depth reduced damage. If typical masonry is used for foundation wall construction, only one layer of reinforcing in the top of the footing is required. Cracking and curvature can be reduced if a bond beam is utilized in the masonry wall or if the masonry wall is replaced by a reinforced concrete wall. Decreasing the friction angle at the interface resulted in larger amounts of tension and curvature in the footing.

TABLE OF CONTENTS

LIST OF TABLES

PAGE

LIST OF FIGURES

PAGE

PAGE

CHAPTER 1

INTRODUCTION

1.1 Introduction

Coal mining production causes many problems due to the extraction of coal beneath the surface. When coal is being extracted at sub-surface levels, subsidence occurs at the ground level. The effect of this subsidence inflicts damage to structures residing in mining areas. The results of this damage have caused great concerns among mining industries, land owners, insurance agencies, and government officials (Bennett, 1990).

There are different methods for extracting coal. One of the oldest methods is room and pillar mining. This technique involves extracting only a portion of coal thereby leaving the rest behind to serve as pillars to hold up the overburden. However, over a period time these pillars may gradually collapse causing subsidence. The time at which this subsidence will occur is very hard to predict (Treworgy and Hindman, 1991). A more efficient way of extracting coal is longwall coal mining. All coal is extracted at one time. This causes somewhat immediate subsidence which is easier to predict both with respect to timing and magnitudes. Due to the relative predictability of this type of subsidence it is easier to examine the forces that cause damage to overlying structures. The results, however, will be equally applicable to abandoned room and pillar mine subsidence.

Some of the most affected structures from subsidence are residential homes. Foundation response from subsidence is a major factor for superstructure damage. The degree of damage induced in the structure depends upon the relative motion and behavior of the foundation and subgrade (Kane et al., 1989). Several techniques and methods for the alleviation or prevention of structural damage have been proposed; however, more research in this area is needed as more information is being compiled about foundation response.

The construction of various types of foundations of different designs and techniques is one way of observing soil-structure interaction behavior during subsidence; however, this approach is very expensive and time consuming. A more efficient approach is through numerical techniques (Kane et al., 1989). The growing use of the computer has greatly increased our ability to evaluate foundation response during subsidence. Numerical techniques serve as a powerful tool to simulate mining-induced subsidence. Foundations can be incorporated into models in which parameters can be changed in order to better understand mechanisms associated with soil-structure interaction (Drumm et al., 1988). This will in turn allow for a more efficient and effective design of foundations for residential type structures in mining areas.

1.2 Scope

A finite element program was utilized to examine the response of residential concrete foundations subjected to subsidence. The program used is ABAQUS (HKS, 1989). This program permits the appropriate modeling of inelastic materials, the cracking of concrete, behavior of reinforcing, and vertical and horizontal relative movements at the interface.

The foundations analyzed consist of strip footings with and without rebar reinforcing. On top of the footings sits a four course masonry wall unit. The foundations are subjected to an actual subsidence wave in the centerline of a longwall coal panel through finite element analysis. Results from ABAQUS are compared to the results taken from test foundations constructed and monitored near West Frankfort in southern Illinois. A parametric study is conducted to determine the location and optimum amount of reinforcing bars to be placed within the footing. Furthermore, various footing dimensions and masonry wall construction are also analyzed. Recommendations are made to give an efficient and cost effective foundation for residential construction.

1.3 Subsidence

1.3.1 Coal Mining Effects

Damage inflicted to structures during subsidence is caused by the interaction between the ground surface and structure. This interaction is related to vertical and horizontal movements of the ground in relation to the position of the structure's foundation to subsidence. The size and type of the structure as well as the type of subsidence event also contribute to the structure's response (Boscardin and Ahmed, 1992).

The type of damage caused by the structure's response can be categorized into three specific areas (Marino et al., 1988). The first type of damage considered is structural damage in which a supporting member such as the foundation has been damaged beyond its capabilities of supporting the superstructure to a sufficient level of performance. The second type of damage is called functional damage. This type of damage causes a reduction in the "non-structural" function of an element within a structure. Stuck windows and doors, ground water entry in cracked basements, and tilting are some examples. The last type of damage considered is aesthetic damage. This type of damage is more of a personal decision by the home owner as to whether there is an unacceptable amount of deformation or shifting to their residence. The limits associated with these types of damage are not well defined.

In Table 1.1, Boscardin and Cording (1989) present a classification of visible damage which was modified from Burland et al. (1977).

Reducing structural damage is the primary focus as it relates to foundation stability. Typical residential foundations are not designed to accommodate ground movements associated with subsidence. As the foundation tries to conform to the ground movements, excessive stresses and strains may be produced thereby causing damage (Geddes, 1977a). According to Marino et al. (1988) structural damage occurs when cracks are produced in the masonry walls and the footing has completely ruptured. However, the stresses and strains produced in the foundation from subsidence are not necessarily the same as that induced in the ground (Geddes, 1977c). Relating exactly how these ground movements cause damage in foundations is a difficult and on going process (Drumm et al., 1988).

Much attention has been given to the effects that ground movements induce in structures. Settlement is one these effects which is produced by vertical movement. There are two types of settlement to consider. The first type is total settlement which corresponds to maximum vertical displacement of the structure. The second type is differential settlement which is the relative vertical displacement of the structure. Differential settlement causes slope in the foundation and tilting in the superstructure (Geddes, 1977a). This tilting

Table 1.1 Classification of Visible Work (Boscardin et al., 1989)

Class of Damage	Description of Damage[a]	Approximate width[b] of cracks,mm
Negligible	Hairline cracks	< 0.1
Very Slight	Fine cracks easily treated during normal redecoration. Perhaps isolated slight fracture in building. Cracks in exterior brickwork visible upon close inspection.	< 1
Slight	Cracks easily filled. Redecoration probably required. Several slight fractures inside building. Exterior cracks visible, some repointing may be required for weathertightness. Doors and windows may stick slightly.	< 5
Moderate	Cracks may require cutting out and patching. Recurrent cracks can be masked by suitable linings. Tuck-pointing and possible replacement of a small amount of exterior brickwork may be required. Doors and windows sticking. Utility service may be interrupted. Weathertighness often impaired.	5 to 15 or several cracks > 3 mm
Severe	Extensive repair involving removal and replacement of sections of walls, especially over doors and windows required. Windows and door frames distorted, floor slopes noticeably. Walls lean or bulge noticeably, some loss of bearing in beams. Utility service disrupted.	15 to 25 also depends on No. of cracks
Very Severe	Major repair required involving partial or complete re-construction. Beams lose bearing, walls lean badly and require shoring. Windows broken by distortion. Danger of instability.	usually > 25 depends upon No. of cracks

[a]Location of damage in the building or structure must be considered when classifying degree of damage.

[b]Crack width is only one aspect of damage and should not be used alone as a direct measure of it.

action usually does not cause any actual structural damage (Drumm et al., 1988). However, functional damage may be a problem depending on the amount of tilt involved.

Curvature is another effect from structure-soil interaction. According to Karmis et al. (1990) curvature is a critical criteria in establishing superstructural damage. It is suggested that if the structure experiences a curvature greater than .000082 rad/m, architectural damage may occur. This curvature develops in the foundation as the foundation tries to conform to the ground profile (NCB, 1975). Curvature is defined by Triplett et al. (1986) as the change in tilt over a distance. The curvature may be either concave or convex depending upon where the foundation resides in relation to the soil profile (Geddes, 1984). Moreover, the foundation's curvature will not be the same as the curvature produced in the ground. This is due to the fact that slippage or bridging may occur at the interface (Boscardin and Ahmed, 1992).

The curvature produced in the foundation will cause bending effects. Tension and compression regions in the foundation are a product of these bending effects (Drumm et al., 1988). Since concrete cannot take high tensile forces, cracking will develop in the footing (Johnson, 1992). In addition, cracking in masonry walls will develop from the shear and tensile stresses induced by the bending. This will result in failure of the wall or in water entry (Drumm et al., 1988).

Even though horizontal movements are associated with subsidence, not much information has been compiled about the damage associated with their effects. Horizontal movements produced by the ground may be as important as vertical movements (Geddes, 1977a; Geddes, 1984). This is due to tensile and compressive forces in the foundation that are produced by the shearing action at the soil-structure interface. These forces are dependent upon soil and interface properties, contact pressures, the friction angle and adhesion, and the relative displacement or slip between the ground and foundation. If these movements and resulting stresses are occur an area of contact, in-plane rotation and bending will occur. However, if a foundation is able to move relatively slowly in a horizontal direction with a uniform displacement of soil without restraint, no horizontal shear forces will develop at the interface. As the foundation becomes restrained from the moving process, forces will be produced from shearing action at the interface.

1.3.2 Foundation Construction Techniques

Much attention has been given to the design of structures to resist the damage induced by subsidence. "Conventional" construction does not consider the movements associated with subsidence (Geddes, 1984). Since most residential damage occurs primarily at the foundation level, it is important to establish some kind of residential construction specification for the foundation to minimize deformations associated with subsidence. This in turn decreases repair costs associated with the damage (Basham et al., 1989).

Many designs and techniques have been proposed for residential construction. Two solutions for design are to make the structure relatively flexible or relatively rigid (Peng, 1986). For a flexible design, the foundation is constructed to bend in order to comply with the ground profile (NCB, 1975). A sufficient amount of reinforcing should be placed in the footing only to hold the foundation together during subsidence. Too much reinforcing would not allow the foundation to follow the ground movements due to added rigidity (Drumm et al., 1988). A rigid approach would allow the foundation to ride or bridge over the ground movement producing smaller curvatures in the footing. A rigid foundation is usually designed with larger members containing increased amounts of reinforcing (Peng, 1986). The structure can be jacked to its original position to correct for tilt after subsidence (NCB, 1975). To reduce horizontal strains, the bottom of the footing should be smooth and free of projections and should be placed on a piece of polyethylene sheeting (Chen et al., 1974). Also basements should have compressible material backfilled in trenches on the outside of the walls to alleviate compressive strains.

One of many problems created during subsidence is cracking of a typical plain concrete footing. The footing can not handle the curvature produced by the soil profile. Reinforcing steel gives the footing increased curvature and moment capacity after cracking (Park and Paulay, 1975).

A reinforced concrete footing with 1% reinforcing was monitored during subsidence in southern Illinois (Triplett et al., 1986). Cracks formed in the footing as the subsidence wave passed but closed after subsidence was complete. This suggests that the reinforcing may not have yielded (Kane et al. 1989).

Post-tensioning placed in footings is another way of minimizing structural damage during subsidence. Post-tensioning places the footing in a state of initial compression which helps to prevent cracking. By preventing cracking, the footing acts in a more rigid manner. This type of footing has primarily been used only for floors lying on expansive and compressive soils where subgrade movement usually occurs (Freyermuth, 1987).

Masonry walls constructed on footings usually have severe cracking at the mortar joints during subsidence due to tensile stresses induced by subsidence (Johnson, 1992). These tensile stresses exceed the low tensile strength of the masonry materials. The use of bond-beams would help prevent cracking by serving as a tension chord (Schneider and Dickey, 1987). Reinforcement is placed in the hollow section of the bond-beam unit and then grouted in place. It should remain continuous for the entire structure. Vertical and horizontal reinforcement in the masonry wall unit has also been suggested (Hall, 1978). The vertical reinforcement should be anchored in the footing with dowels. The juncture of masonry wall units at the corners should be adequately connected. This could be accomplished by using standard hooks provided by specifications in the ACI-318 Building Code (1989).

A completely rigid approach is to make the foundation footing and wall act as a composite unit to resist ground movements. One of the main concerns is to design the foundation wall unit strong enough to resist lateral pressures. To accomplish this reinforcing is used throughout the foundation. Recommendations and specifications by Basham et al. (1989) are made according to how severe the ground movements are in relation to subsidence. Ground movements associated with a differential vertical settlement of 3/4 inch or less are classified as slight ground movements in this case. The minimum design criterion for this type of movement is a soil pressure of 30 psf, equivalent fluid pressure, per foot of depth. The construction details for reinforced concrete and masonry foundations are given in Figure 1.1 and Figure 1.2 respectfully. Moderate ground movements are classified according to maximum differential vertical

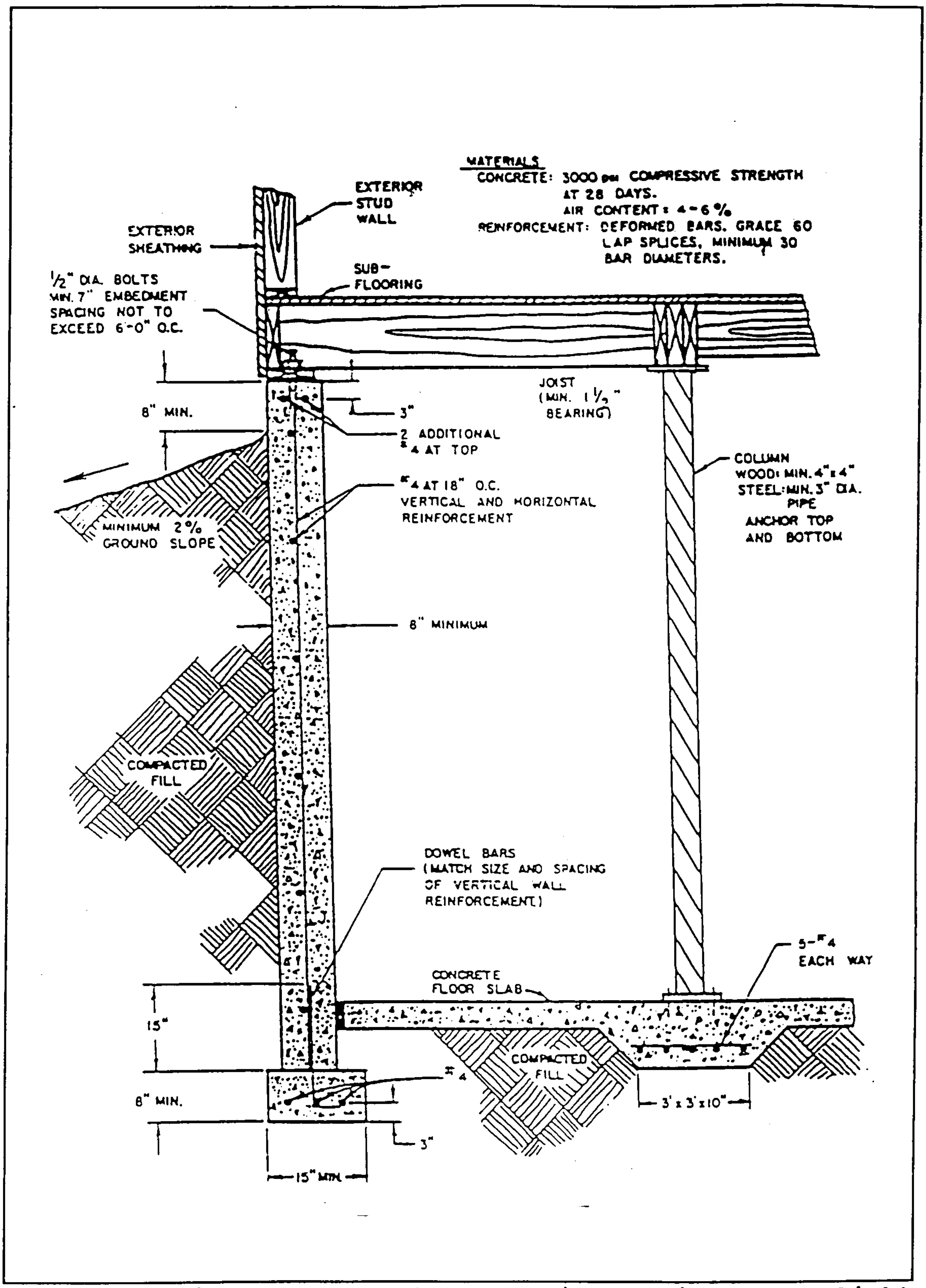

Figure 1.1 Reinforced Concrete Foundation: Designed for Slight Ground Movements (Basham et al., 1989)

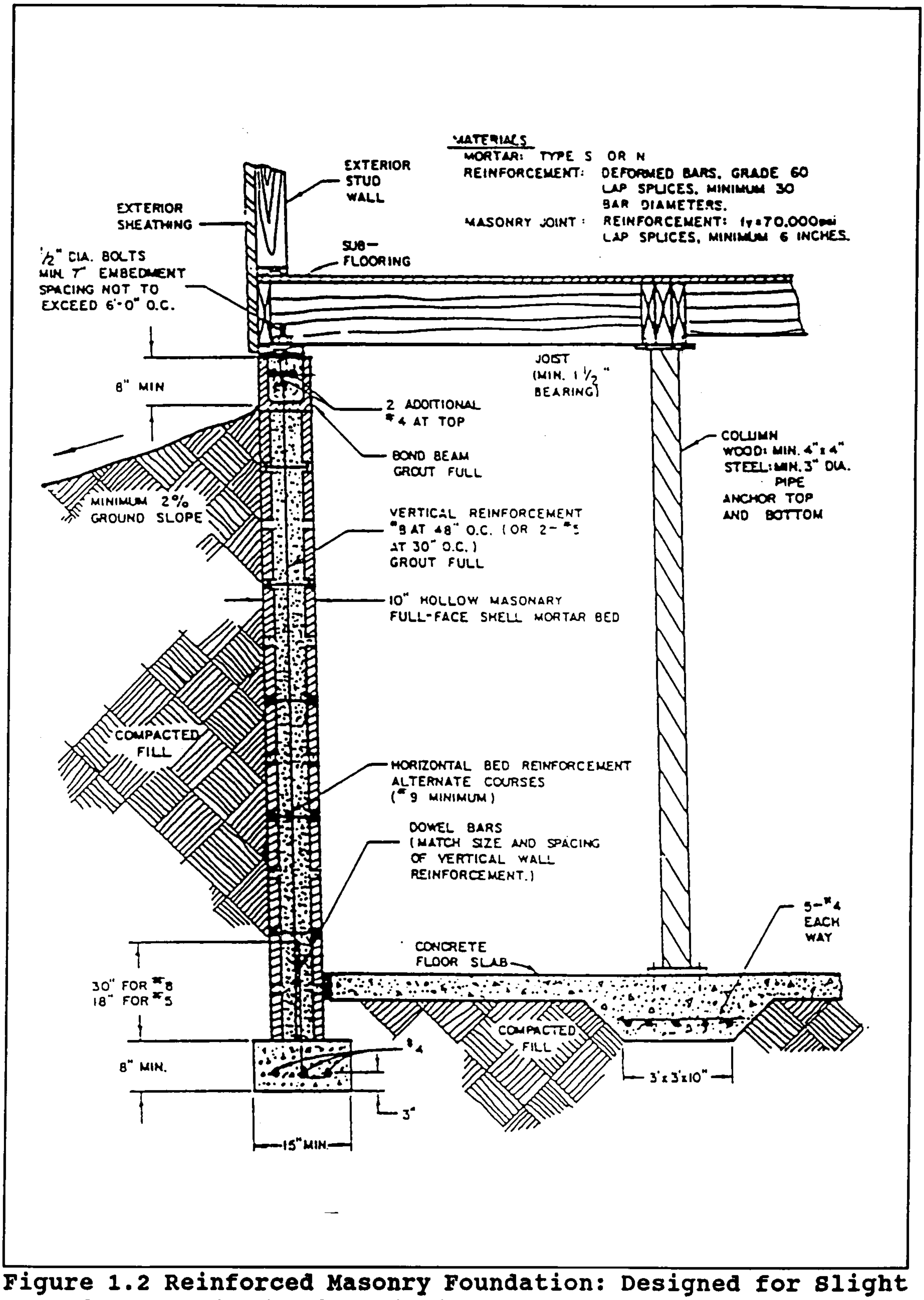

Figure 1.2 Reinforced Masonry Foundation: Designed for Slight Ground Movements (Basham et al., 1989).

settlement not exceeding 3 inches. There may be some minor structural damage produced in the foundation; however, repairing the damage should be easy. The foundations constructed for this case may not be designed for a soil pressure less than 100 psf, equivalent fluid pressure, per foot of depth. Figure 1.3 gives a recommended design for a reinforced concrete wall and footing type foundation. Since severe ground movements are associated with differential vertical settlement in excess of 3 inches, a design criterion is not specified due to the uncertainty of how much settlement may occur in this classification.

A flexible approach to the design of structures in subsidence prone areas would be the CLASP (Consortium of Local Authorities Special Program) system (Bell, 1977; Heathcoate, 1965; Geddes, 1977b). This system is usually used for light commercial buildings. This system was invented and widely used in England. It allows the structure to move freely with minimum resistance to ground movement. Gaps and joints allow cladding, partitions, and similar features to move without angular and longitudinal distortions due to the vertical ground movement. Diagonal spring bracing placed in specific bays allows the structure to withstand horizontal forces such as wind loads while allowing the structure to follow ground curvature. This bracing also aids in the recovery of the structure's original shape.

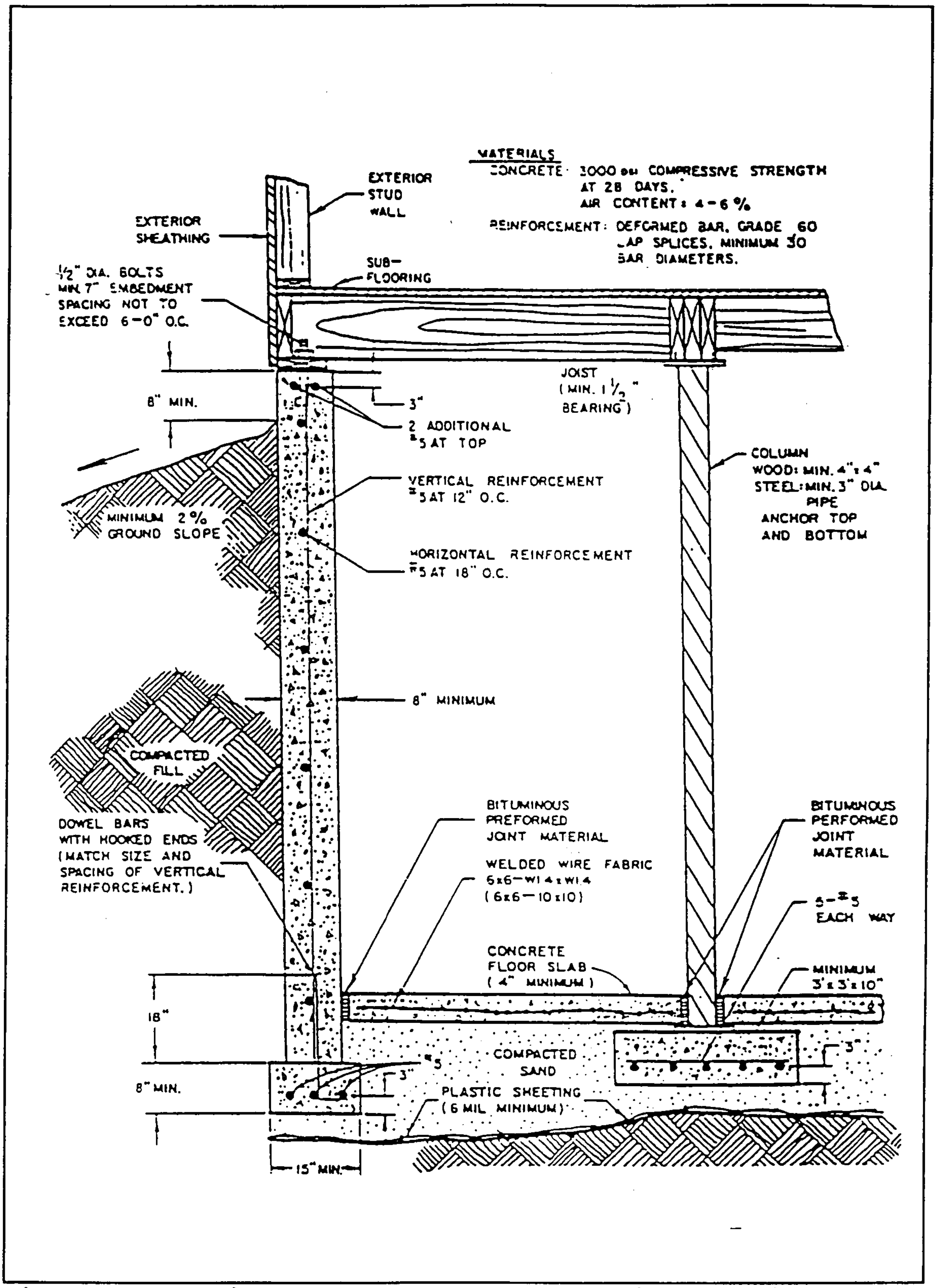

Figure 1.3 Reinforced Concrete Foundation: Designed for Moderate Ground Movements (Basham et al., 1989).

The CLASP system uses a slab foundation so that there are no superstructure projections in the ground. This allows minimum horizontal strains to be produced in the structure. The slab foundations are usually five inches thick and no more than 300 square feet. The slabs are connected together by reinforcing to transfer shear and tension.

In a reported case history by Geddes (1977b), the CLASP system was used in a school in England. The school was constructed as five inter-connected buildings. After monitoring the structure for three years after subsidence, it was found that a maximum settlement of 580 mm and a differential settlement of 339 mm had taken place. Ordinarily these vertical movements would cause considerable damage; however, only a small amount of repairable damage took place.

CHAPTER 2

TEST FOUNDATIONS

2.1 Introduction

The purpose of this chapter is to compare reinforced and plain concrete foundation behavior as observed in test foundations. Using reinforcing bars in foundation construction for mitigation purposes was utilized in one of the test foundations constructed near Sesser, Illinois (Triplett et al., 1986). The effects of the reinforcing showed promising results; however, due to complicated three dimensional effects induced in the foundations, it was decided to construct a more basic type of foundation. Two-dimensional foundations were constructed at Herron Road in West Frankfort, Illinois, based on the plane stress behavior proposed by Drumm et al. (1988). Six different types of foundations were constructed at West Frankfort. One was constructed using conventional construction practices in the area which was an unreinforced concrete footing. The other five foundations utilized different mitigation techniques. One mitigation technique was reinforcing rebars in the footing. The effectiveness of the reinforcing was established through extensive instrumentation, monitoring, testing, and observations. The data collected at the Herron Road site has been used to help construct the numerical models developed in this study.

2.2 Sesser Foundations

Two 9 m by 12 m (30 X 40 ft) foundations were constructed over the center of a high extraction retreat room-and-pillar panel near Sesser, Illinois (Powell et al., 1988). This was a combined effort between the U.S. Bureau of Mines and the Illinois Mine Subsidence Insurance Fund to study the mechanisms associated with the response of structures produced from soil-foundation interaction during subsidence. This was achieved by instrumenting and monitoring both the soil and foundations during the subsidence event.

Since one of the objectives at Sesser was to observe the effects of mitigation techniques, two different types of foundations were constructed. The first foundation, referred to as foundation A, was constructed using a typical plain strip footing with a masonry wall on top. The footing consisted of plain concrete 40.6 cm (16 in.) wide and 25.4 cm (10 in.) thick. The masonry wall used 20.3 cm (8 in.) blocks stacked three courses high. The second foundation, referred to as foundation B, consisted of the same masonry wall construction and footing dimensions; however, several mitigation techniques were incorporated. Four No.4

reinforcing bars were placed in both the top and bottom of the footing to increase the tensile capacity of the foundation. A trench was excavated around the foundation and backfilled with vermiculite to reduce compressive stresses induced in the footing and masonry wall. A plastic drain pipe was placed within the vermiculite to remove surface water. To reduce frictional forces and adhesion transmitted at the interface, sand covered with a 0.1 mm (.004 in.) thick polyethylene sheet was placed between the ground and footing. Load bins filled with soil were placed on the foundations to simulate typical house loads. The second foundation was basically the same construction as the first foundation except for the added mitigation techniques which added an increase of $2,400 to construction cost.

Monitoring of the foundations began in November 1984 and ended in July 1985. Both foundations tended to cantilever as subsidence began. Eventually the structures responded to the ground curvature causing cracking initially in their corners on January 19, 1985 (Triplett et al., 1986). As subsidence continued, cracks widened in the footings and extended up into the block walls (Powell et al., 1988). Within a month of initial cracking, cracks began to form horizontally in the blocks at the mortar joints as well as in the footings of both foundations. When monitoring was complete, foundation A experienced cracking that led to 10 major segments. Most of the major cracking and separation occurred at the corners.

Foundation B also showed major cracking in its corners; however, only hairline cracks formed throughout the rest of the foundation with no separation at the corners. Foundation B acted more as a unit due to the added reinforcing. This in turn allowed it to respond more uniformly while foundation A exhibited an uneven distribution of movement.

Bending and torsion were the primary causes of cracking patterns observed in the foundations. Horizontal cracks were produced by the torsional effects of the foundations while the bending stresses contributed to the vertical cracks. The torsion produced in the foundation was a contribution from skew movements in three dimensional behavior provided by horizontal and vertical displacements. These skew movements were expected given the position and geometry of the foundations in relation to the mined out area. Foundation B experienced more torsional movements than foundation A; however, the added resistance to torsion provided by the reinforcing placed in foundation B allowed it to undergo less structural damage than foundation A.

In conclusion, both foundations first exhibited weakness in their corners resulting in cracking (Tripllet et al., 1986). This resulted from torsional and bending effects. Only hairline cracks formed in the reinforced foundation and closed after subsidence was complete, while fewer larger cracks developed in the plain concrete foundation and remained open after subsidence. The performance of the reinforced foundation proved to be very effective when compared to standard foundation construction. The mechanisms associated with three dimensional effects have not completely been analyzed due to their complicated nature.

2.3 Herron Road Foundations

Two sets of six foundations were constructed on a site at Herron Road which is located approximately three miles east of West Frankfort, Illinois in Franklin County. They were placed above an advancing longwall panel with six constructed parallel to mining in the center-line and the other six perpendicular to mining located in a predicted zone of maximum tension, Figure 2.1.

One foundation was constructed according to conventional practices while the others incorporated mitigation techniques. These mitigation techniques addressed both footing design and soil-foundation interface treatment. A four course masonry wall was placed on top of the footings. Double wood sill plates were anchored to the top of the masonry wall. Wood load bins placed on top of the foundation walls were filled with soil to simulate a typical house bearing pressure at the interface. The dimensions of the foundations and loading scheme is shown in Figure 2.2.

A summary of the mitigation techniques used in the project are given in Table 2.1. The behavior of the added

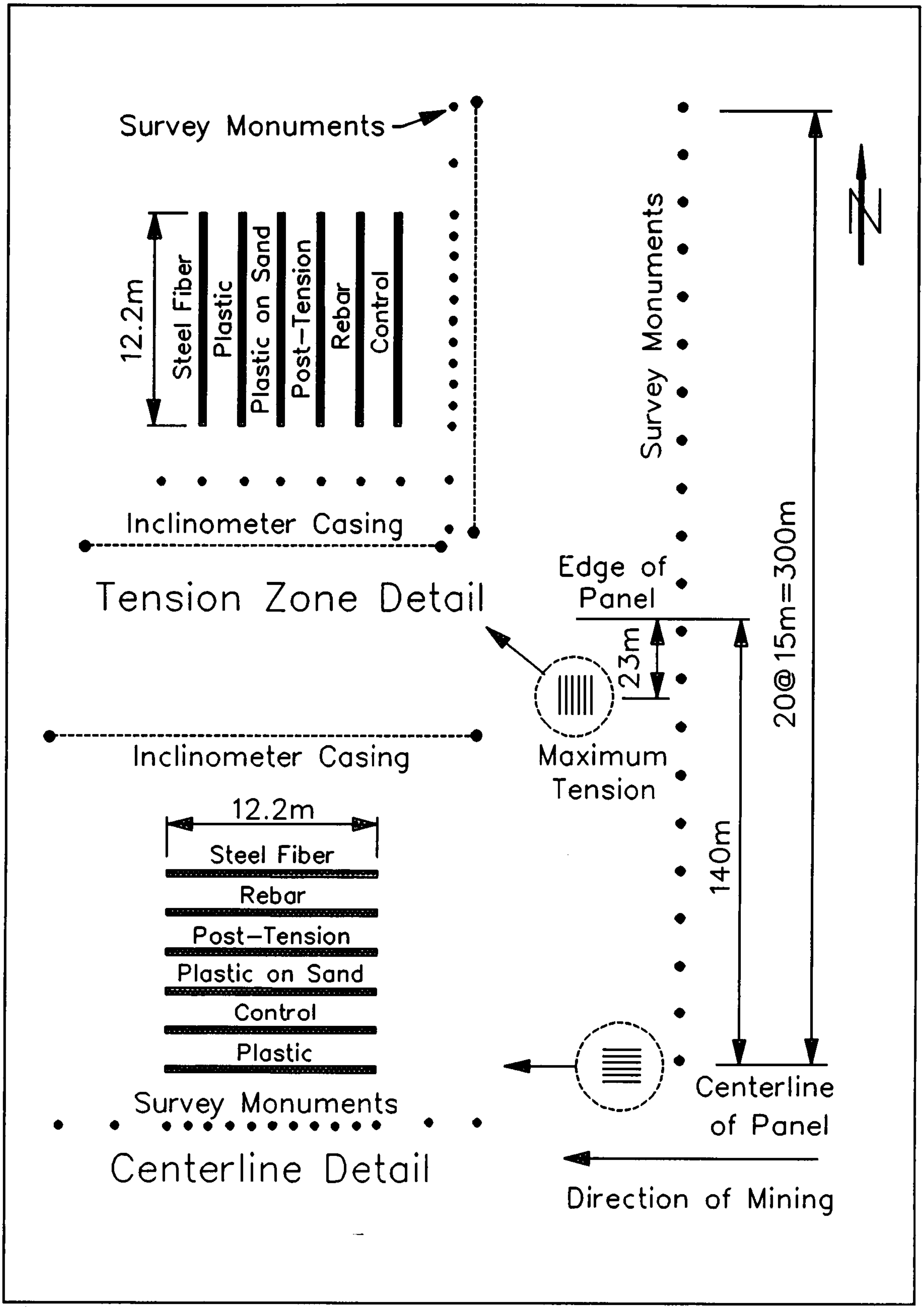

Figure 2.1 Test Foundation Position

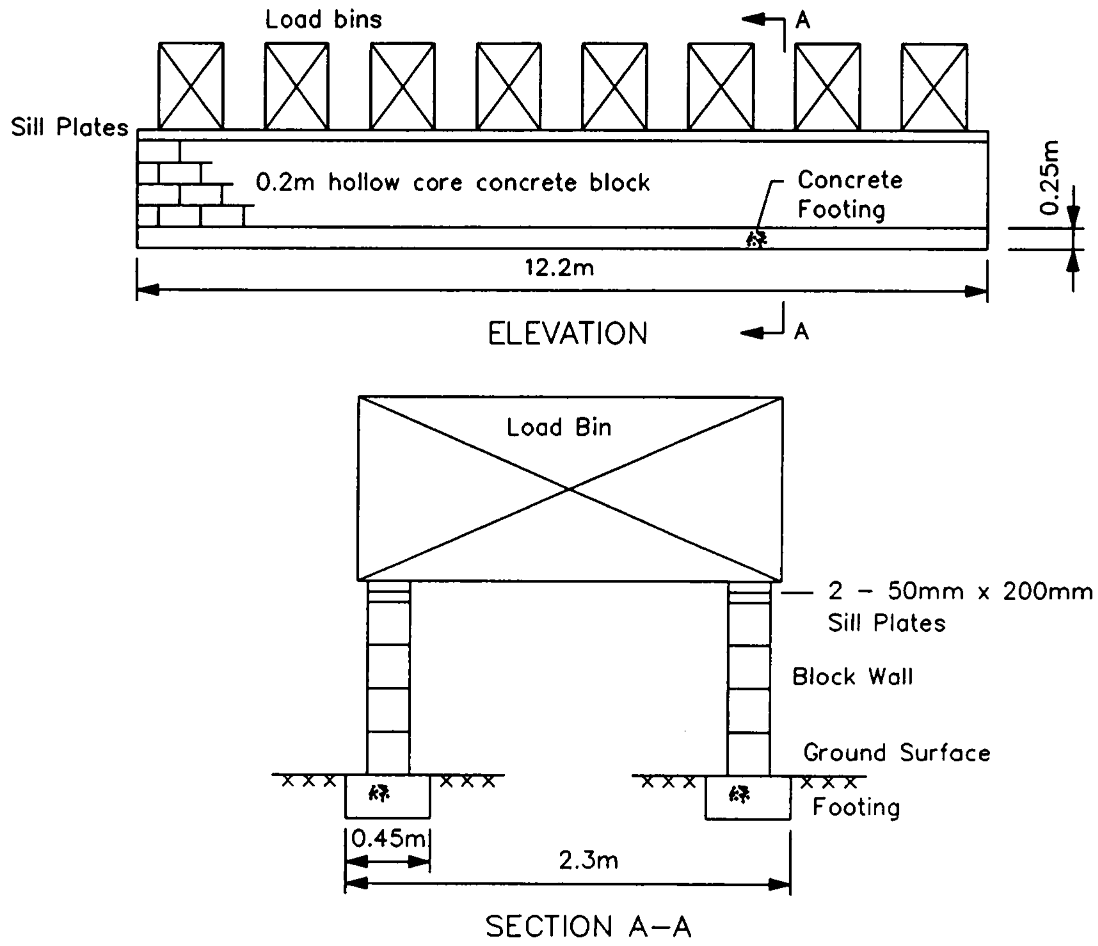

Figure 2.2 Foundation and Loading Scheme Concept

reinforcing bars in the footing as well as the control foundation is of primary interest for this study. A complete description of other mitigation techniques and foundation construction can be ascertained from Drumm and Bennett (1992).

Table 2.1 Summary of Test Foundations

Footing	Interface	Reinforcing
1	Soil-Concrete (control)	None
2	Soil-Plastic-Concrete	None
3	Sand-Plastic-Concrete	None
4	Soil-Concrete	4-#4 Rebar
5	Soil-Concrete	6-270K &-wire Post-tensioning Strands
6	Soil-Concrete	Steel Fibers

The design for the reinforcing bars for these foundations came from preliminary FEM analysis conducted by Hudgings (1989). Unlike plain concrete, reinforced concrete is able to support loading after cracking. Hudgings (1989) concluded that bending stresses and not axial stresses are the primary stresses induced in concrete footings during subsidence. Bennett (1990) recommended that a reinforced footing be designed to produce a yield moment slightly greater than the cracking moment. This is because Hudgings' (1989) analyses showed that the amount of reinforcing did not affect the amount of curvature induced in the footing. It was also recommended that reinforcing be placed in both the top and bottom of the footing to design for reverse curvature effects from subsidence (Bennett, 1990). From these conclusions and recommendations, two No.4 standard reinforcing bars were placed in the top and bottom of the footings which corresponds to 0.44% reinforcing.

Since the foundations located in the center-line experienced both compression and tension phases during subsidence, the behavior of the control foundation as compared to the deformed bar foundation in this area is of primary interest. Material properties were gathered and tested for these foundations by Johnson (1992).

An array of instrumentation was utilized to give sufficient amounts of information about the behavior associated with the foundations. For a complete description of instrument usage, placement, and data refer to Bennett and Drumm (1992). The behavior of the foundations is given with respect to observations made as well as to instrumentation utilization. Subsidence initially began May 10, 1990 which is referred to as Day 0. Monitoring of the foundations and free field continued through August 1990.

The tiltmeter and the inclinometer were used to measure tilt and slope in which curvature was calculated in the footings of the foundations (Awasthi, 1992). From tiltmeter and inclinometer results, Awashti concluded that the overall behavior of the footings in the centerline can be explained in three major phases, Figure 2.3. The first phase, which occurred on Day 12, is the phase at which tension was produced in the top of the foundations in order to produce the first cracking in the footings. The second phase is rigid body tilt and compression in the top of the footing which was noticed on Day 14. The third phase is a relaxation phase that results in tension forming in the top of the footing again. This phase occurred around Day 20 of monitoring. Table 2.2 gives maximum curvature values during the three major phases. Comparing maximum curvature values from inclinometer data at Day 12 from Table 2.2 to the theoretical cracking curvatures of .0008 rad/m of the plain and reinforced concrete footings indicates that cracking should have formed during this stage. The curvatures produced from the tiltmeter data showed the same behavior of the phase shifts even though the magnitude of values were different. This is due to tiltmeter readings being spaced farther apart which affected the calculation procedure to determine curvature.

The horizontal strain measured by Johnson (1992) through extensometer readings showed the same phase behavior as Awashti (1992). The maximum elongation associated with each phase for both footings and blocks is given in terms of total strain in Table 2.3. Even though Day 20 was the start of the relaxation phase, Johnson produced values for Day 48 which produced the highest values of strain in this phase as well as the entire subsidence event. Johnson compared readings

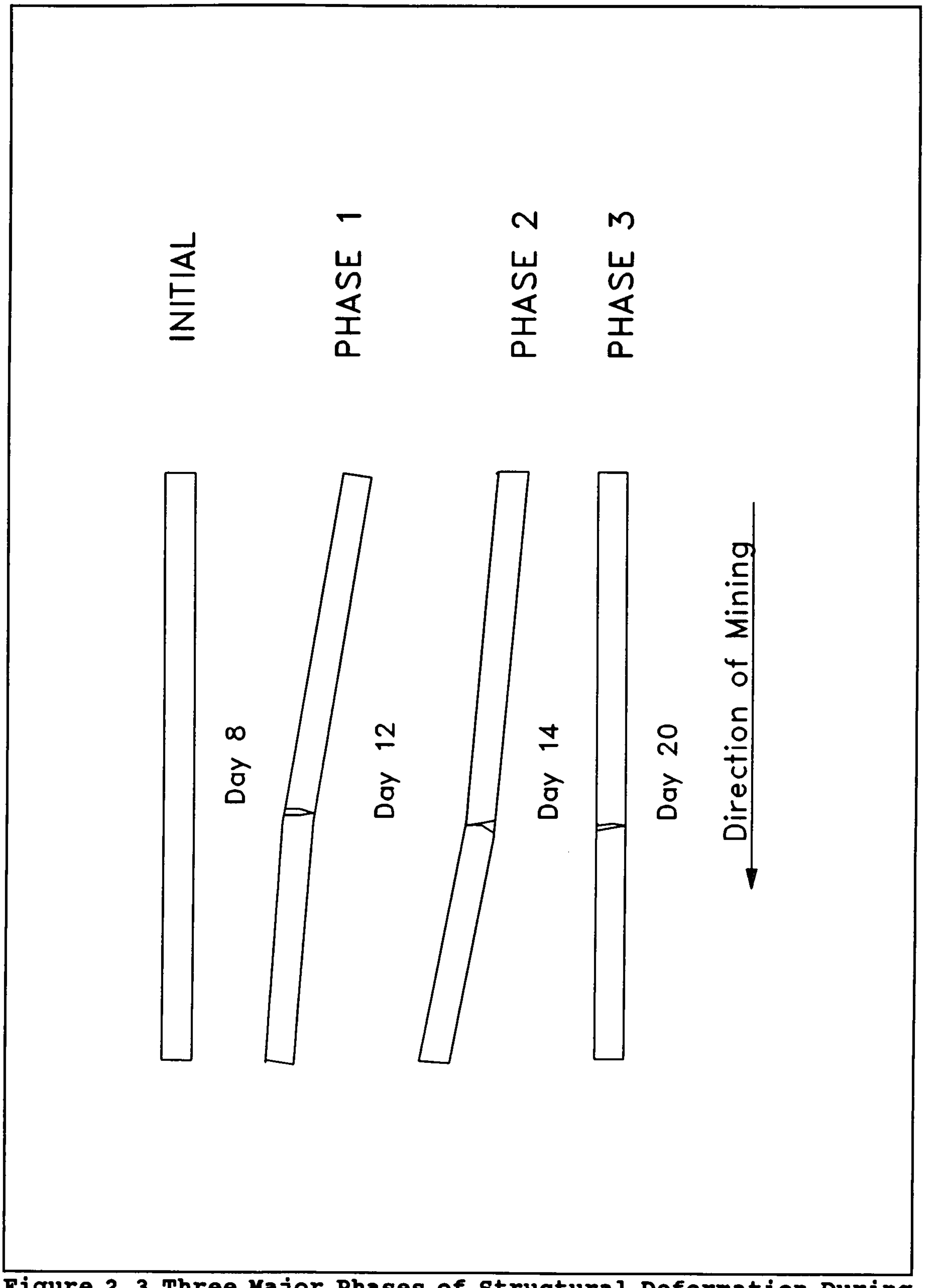

Figure 2.3 Three Major Phases of Structural Deformation During Subsidence (Awashti, 1992)

throughout the subsidence event between the reinforced concrete footing and a footing with plain concrete construction. He concluded that the reinforced footing maintained more stiffness in post cracking behavior than plain concrete construction due to the increase of curvature capacity.

Table 2.2 Calculated Curvature of Footings

Data Used	Footing Type	Curvature (rad/m)		
		Day 12	Day 14	Day 20
Inclinometer	Plain	-.00086	.000504	-.00022
	Reinforced	-.00098	.00048	-.000082
Tiltmeter	Plain	-.00067	.00046	-.00026
	Reinforced	-.00103	.00033	.00032

Table 2.3 Maximum Strain of Reinforced and Plain Concrete Foundations Located in Centerline

Foundation Type		Strain (m/m)		
		Day 12	Day 14	Day 48
Plain	Footing	.00065	.00033	.00188
	Wall	.00094	.00015	.00218
Rebar	Footing	.00018	.00008	.00092
	Wall	.00081	.00012	.00099

Strain gages incorporated within the footing provided useful information about axial and bending effects from subsidence. Unfortunately strain gage data recorded in the reinforced footing was useless. However, since the post-tensioned footing did not crack in the center-line, data obtained from its strain gage behavior can be used to produce an axial force-moment interaction diagram, Figure 2.4 (Lin, 1992a). This diagram illustrates that bending forces are of greater interest rather than axial forces which corresponds to Hudgings' (1989) conclusions. Even though bending forces exceeded the cracking limit of the reinforced footing, the tensile forces were still able to be taken by the reinforcing bars whereas failure will occur in the plain concrete after cracking.

Structural damage assessment was performed by Lin (1992b). A detailed description of the initial cracks forming in the foundations for Day 12 is given in Table 2.4. This table gives crack location in the terms of the number of blocks in the masonry wall from the trailing edge (west end) of the foundation. Table 2.4 shows that cracks developed rapidly between Day 12 am and Day 12 pm. Both foundations initially cracked at around their third points of the trailing section. The plain concrete footing broke into two distinct sections while the reinforced footing produced only a hairline crack and remained intact. Both foundations produced cracks in the masonry wall at this juncture. By the evening of Day 14, cracks that had formed in the upper courses of foundation blocks had closed. The crack in the reinforced footing had

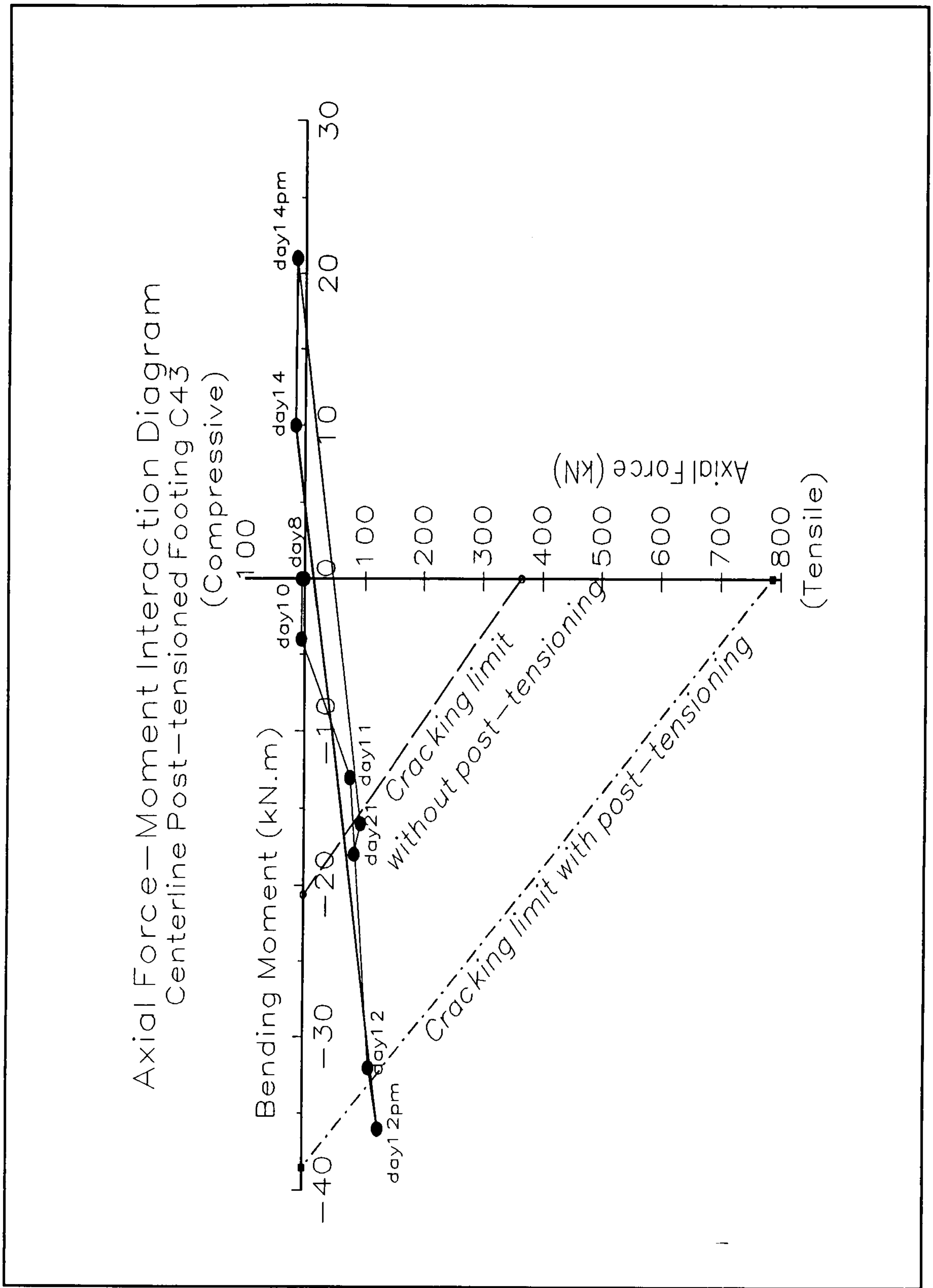

Figure 2.4 Axial Force-Moment Interaction Diagram for Centerline Post-tensioned Footing (Lin, 1992a)

Table 2.4 Cracks in Plain and Reinforced Foundations at Day 12 am and Day pm (after Lin, 1992b)

Foundation Type		Major Cracks		
		Location (W-block)	Width (mm)	Depth (block)
Day 12 AM				
Plain	Footing	11.5	3	-
	Wall	12.5	6	4
Rebar	Footing	-	-	-
	Wall	11.5	1	4
Day 12 PM				
Plain	Footing	11.5	10	-
	Wall	12.5	10	4
Rebar	Footing	11.5	Hair	-
	Wall	11.5	2	4

closed while the crack in the plain concrete footing did not completely close. During the relaxation phase of Day 20, cracks had reopened. The final crack pattern, mapped on Day 90, is shown in Figure 2.5 and 2.6 for the footings and masonry walls respectively. These Figures show that cracking patterns occurred at about the same locations in both footings and masonry walls. The behavior observed and recorded by Lin (1992b) corresponds to behavior produced by instrumentation used during the subsidence event.

An economic analysis was performed for the mitigation practices used in this project (Johnson, 1992). Several assumptions were made in the analysis. For a complete

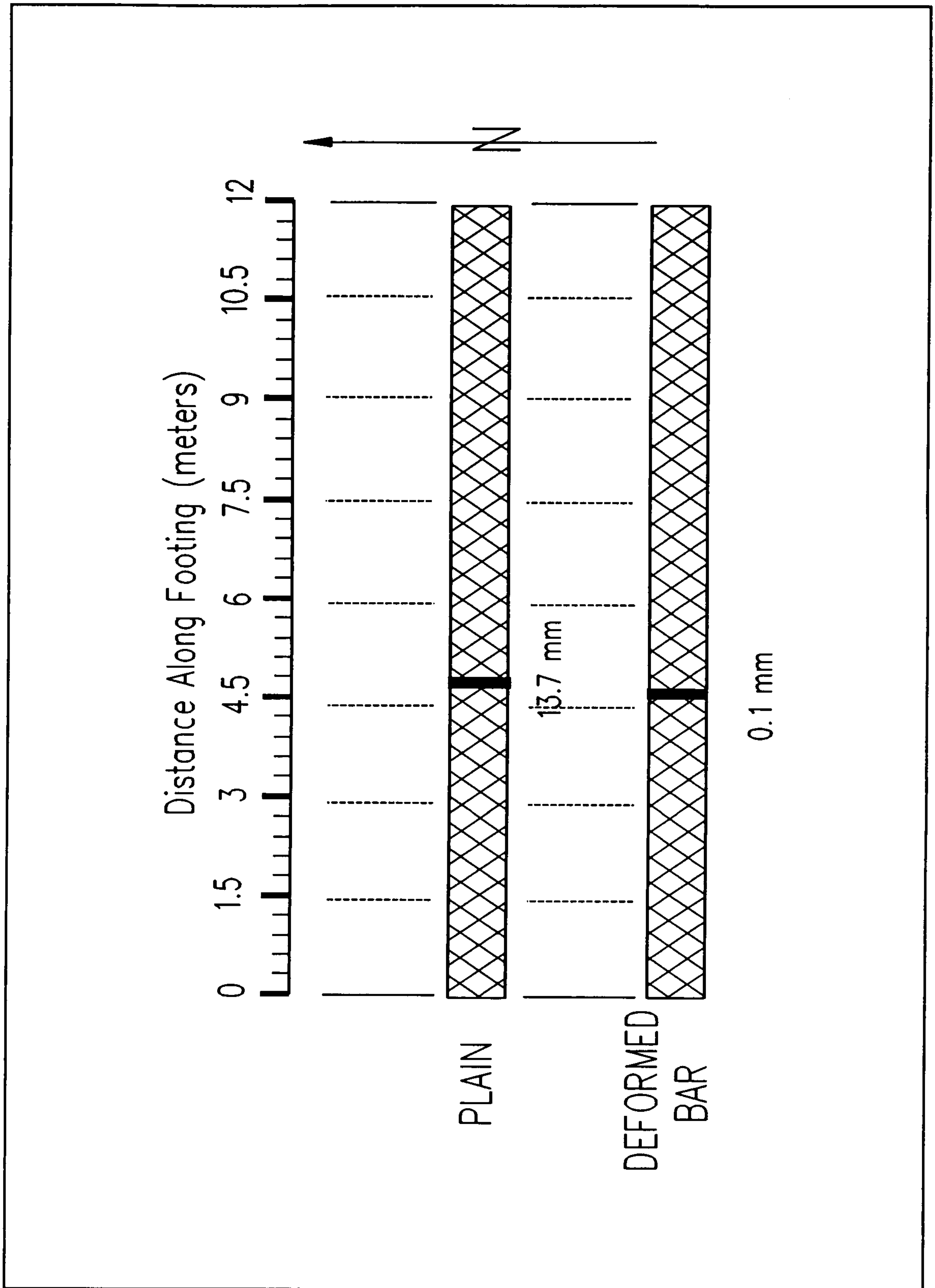

Figure 2.5 Crack Locations for Footings, Day 90 (after Lin, 1992b)

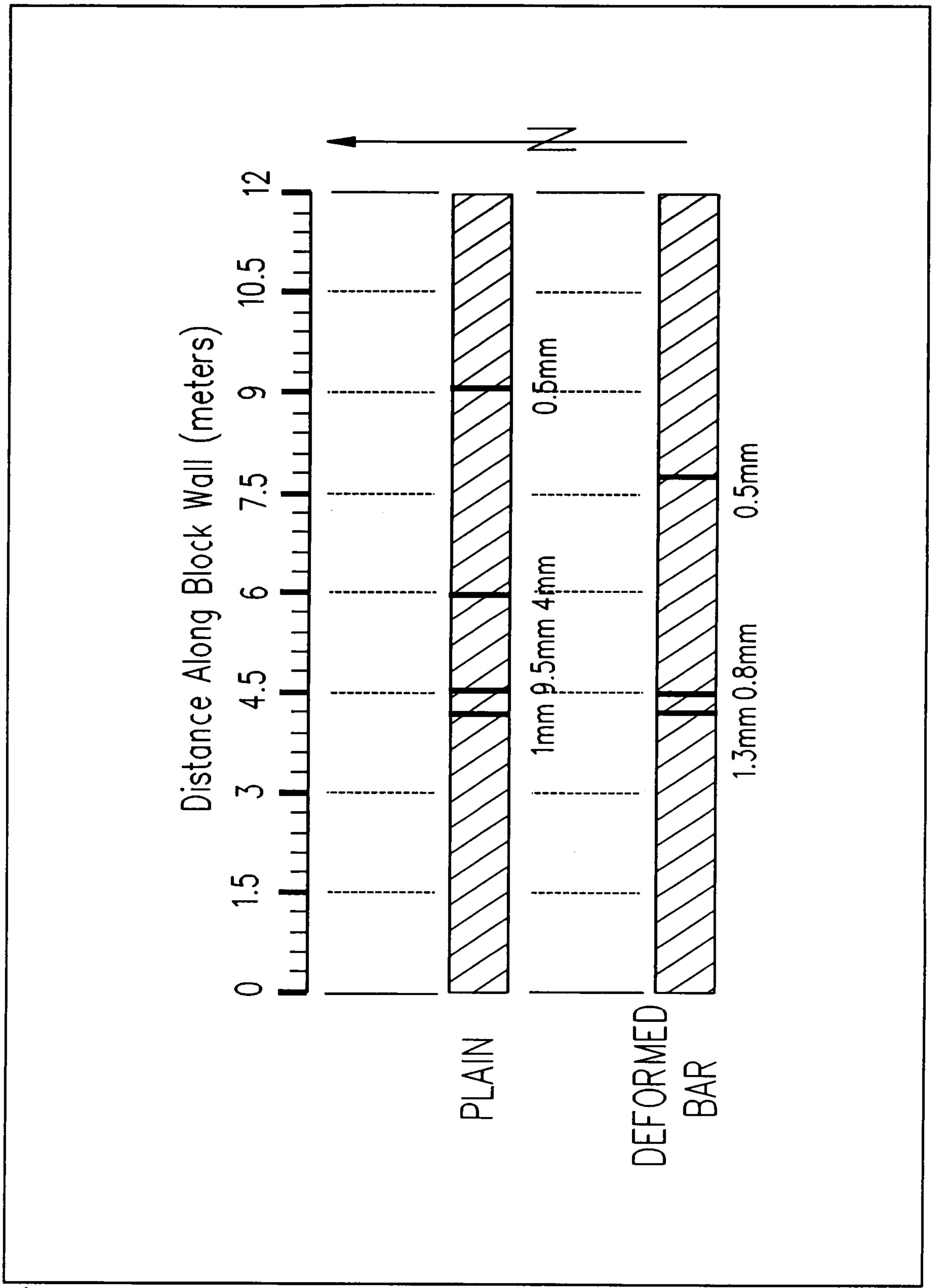

Figure 2.6 Crack Locations for Masonry Walls, Day 90 (after Lin, 1992b)

description of assumptions refer to Johnson (1992). Johnson shows in Table 2.5 an increase in base price per linear foot of foundation for mitigation techniques used at Herron Road. This table corresponds to housing with a length to width ratio of 2:1. Comparing the construction of the deformed bar to other mitigation techniques in Table 2.5 shows that this construction practice is quite economical.

In conclusion, the use of reinforcing bars is an economic and efficient way to relieve damage associated with subsidence. The material properties and field data obtained in this project will be used to help numerically model a reinforced concrete foundation subjected to subsidence in the center-line of a longwall panel. The subsidence history associated with the center-line foundations was used in the numerical analysis.

Table 2.5 Footing Damage Mitigation Techniques Costs for Various Houses (Johnson, 1992)

Living Space Floor Area (sf)	Footing Damage Mitigation Techniques Cost (dollars)					
	Plastic-Soil	Plastic-Soil	Steel Fiber	Rebar	(F) Post-Tensioning	(O) Post-Tensioning
800	86	216	330	106	1,020	612
1000	97	241	369	118	1,140	684
1200	106	265	404	129	1,249	750
1400	114	286	437	140	1,349	810
1600	122	305	467	149	1,442	865
1800	130	324	495	158	1,530	918
2000	137	342	522	167	1,613	968
2400	150	374	572	183	1,767	1,060
2800	162	404	617	198	1,908	1,145
3200	173	432	660	211	2,040	1,224

(F) - First Timer
(O) - Experienced

CHAPTER 3

FINITE ELEMENT MODELING

3.1 Introduction

Numerical modeling is an efficient and cost effective way of analyzing foundation response from subsidence; however, it is important to model the occurrence as close as possible in order to obtain accurate results. Parameters obtained in the field through extensive material testing are incorporated in numerical models. These models are tested and compared to known behavior characteristics to verify that ABAQUS is utilizing material parameters correctly.

The models were constructed with only two-dimensional elements. Since the foundation consists of several components, they are modeled individually to insure adequate behavior. The footing and masonry wall unit consist of plane stress elements while the soil is composed of plane strain elements. The intersection of the soil and foundation incorporates interface elements to allow for the effects of slippage and gapping.

3.2 Soil Modeling

All of the soil modeling was performed by Lawrence (1992). Soil samples were taken from the field in West Frankfort for laboratory testing. Drained triaxial laboratory tests were performed and proved to be appropriate for this particular subsidence event. The material parameters used for his analysis depended upon which constitutive relationship that was being utilized. Three general constitutive relationships were considered. They were linear elastic, non-linear elastic, and elastoplastic. The elastoplastic constitutive relationship was chosen because a plasticity model accounts for the permanent deformations associated with the loading and unloading process relative to this subsidence event.

Several models with different elastoplastic constitutive relationships were reviewed in order to give an appropriate soil model. The models reviewed were Drucker-Prager, Cam-Clay, and cap. Two finite element codes were used for this analysis. The cap model was performed using a two-dimensional code developed at the University of Tennessee called UTGTECH (Ben Hassine and Drumm, 1991). The Drucker-Prager and Cam-Clay models were implemented by the ABAQUS finite element code (HKS, 1989a). Appropriate soil parameters were given to each model. Verification of the soil models was accomplished by the backprediction of the laboratory tests.

After comparing results from each model, Lawrence (1992) concluded that either the Cam-Clay model or the cap model should be used to represent soil behavior associated with this particular subsidence event. He also conducted free field FEM analysis using the Cam-Clay modeling and obtained sufficient results. This free field analysis will be discussed in more detail in chapter 4. Since the Cam-Clay modeling is performed by ABAQUS, this soil model is used in foundation analysis. The material parameters associated with this soil model is given in Table 3.1.

3.3 Plain Concrete Footing

3.3.1 Modeling

Numerical modeling of the concrete is difficult due to cracking from tensile stresses and post cracking behavior. The concrete model used by ABAQUS (HSK, 1989a) incorporates a smeared cracked model to simulate the effect of cracking. This smeared crack model does not produce individual "macro" cracks, rather the presence of cracks are given to integration points in the model, from which they affect the stress and material stiffness at a particular integration point. This leads to a concern of mesh sensitivity of the model. Finite element predictions using the concrete model may not converge to a unique solution as the mesh is refined (HSK, 1989a).

Table 3.1 Soil Model Parameters (after Lawrence, 1992).

Physical Significance	Parameter	Value
Logarithmic Elastic Bulk Modulus	κ	0.0045
Poisson's Ratio	ν	0.28
Elastic Tensile Limit	p_t	0.0
Logarithmic Plastic Bulk Modulus	λ	0.045
Stress Ratio at the Critical State	M	1.52
Initial Yield Surface Size	a_o	ABAQUS Determined
Defines Yield Surface Size to the right of the Critical State Line	β	0.75
Flow Stress (Triaxial Extension to Compression)	K	1.0
Initial Void Ratio	e_o	0.60

Since there was no available information for a mesh size for this particular concrete footing in relation to this subsidence event, a mesh was arbitrarily constructed. The mesh consists of two rows of 16 elements and has the same dimensions constructed in the field. The mesh is illustrated in Figure 3.1. Two-dimensional plane stress, eight node, biquadratic interpolation elements were chosen for this model. This type of element has been shown to be suitable for concrete modeling (HSK, 1989b).

Material properties of the footings from the field were gathered and tested by Johnson (1992). ABAQUS allows the

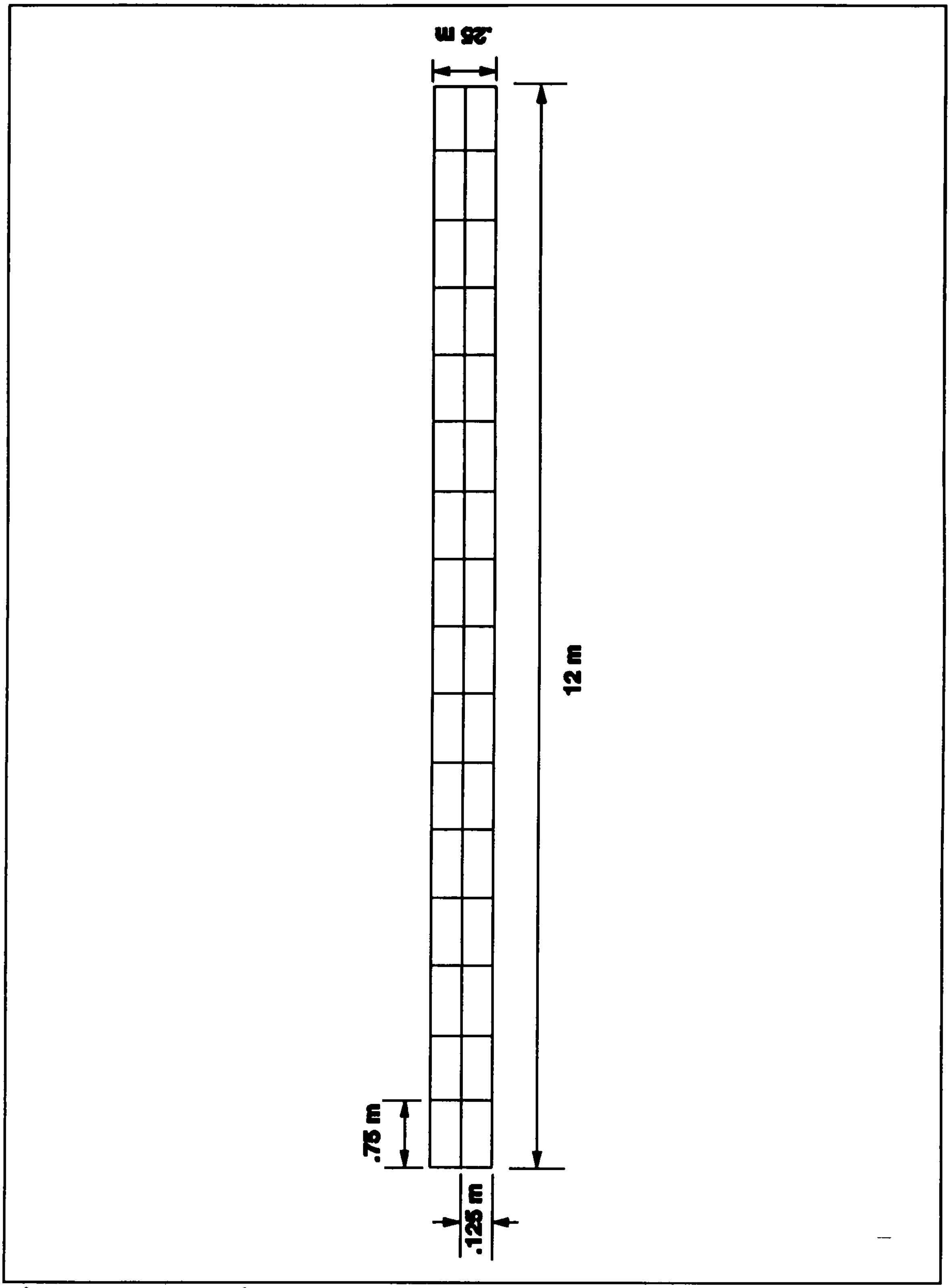

Figure 3.1 Footing FEM Mesh (not to scale)

input of the compressive stress-strain behavior in its concrete option. Johnson (1992) tested several concrete cylinders from batches of concrete poured for both the plain and reinforced concrete footings. An average compressive stress-strain curve for each of these footing was obtained from his raw data, Figure 3.2. Both of these curves produce similar values in the lower portion of the curves. The compressive strains induced in both the plain and reinforced footings were relatively small for the centerline footings, less than 200 $\mu\varepsilon$ (Lin, 1992a); therefore, the reinforced concrete stress-strain curve was used for all concrete models. Also, since small compressive strains were produced in the field, an initial tangent modulus of 42,700 MPa (6200 ksi) is used which would best describe the elastic portion of the curve. This curve is also shown in Figure 3.2.

Tension induced by subsidence caused cracking in the footings (Lin, 1992b). The modulus of rupture defines the point at which the footing cracks. ABAQUS uses a failure ratio of maximum tensile strength to absolute compressive strength. The average maximum tensile strength obtained from testing of material of the centerline reinforced concrete footing was 4.25 MPa (617 psi) and an average value of 34.9 MPa (5060 psi) was obtained as the maximum compressive strength (Johnson, 1992). This gives a failure ratio of .122. The failure ratio produced from the plain concrete footing was the same; therefore, the use of the reinforced concrete

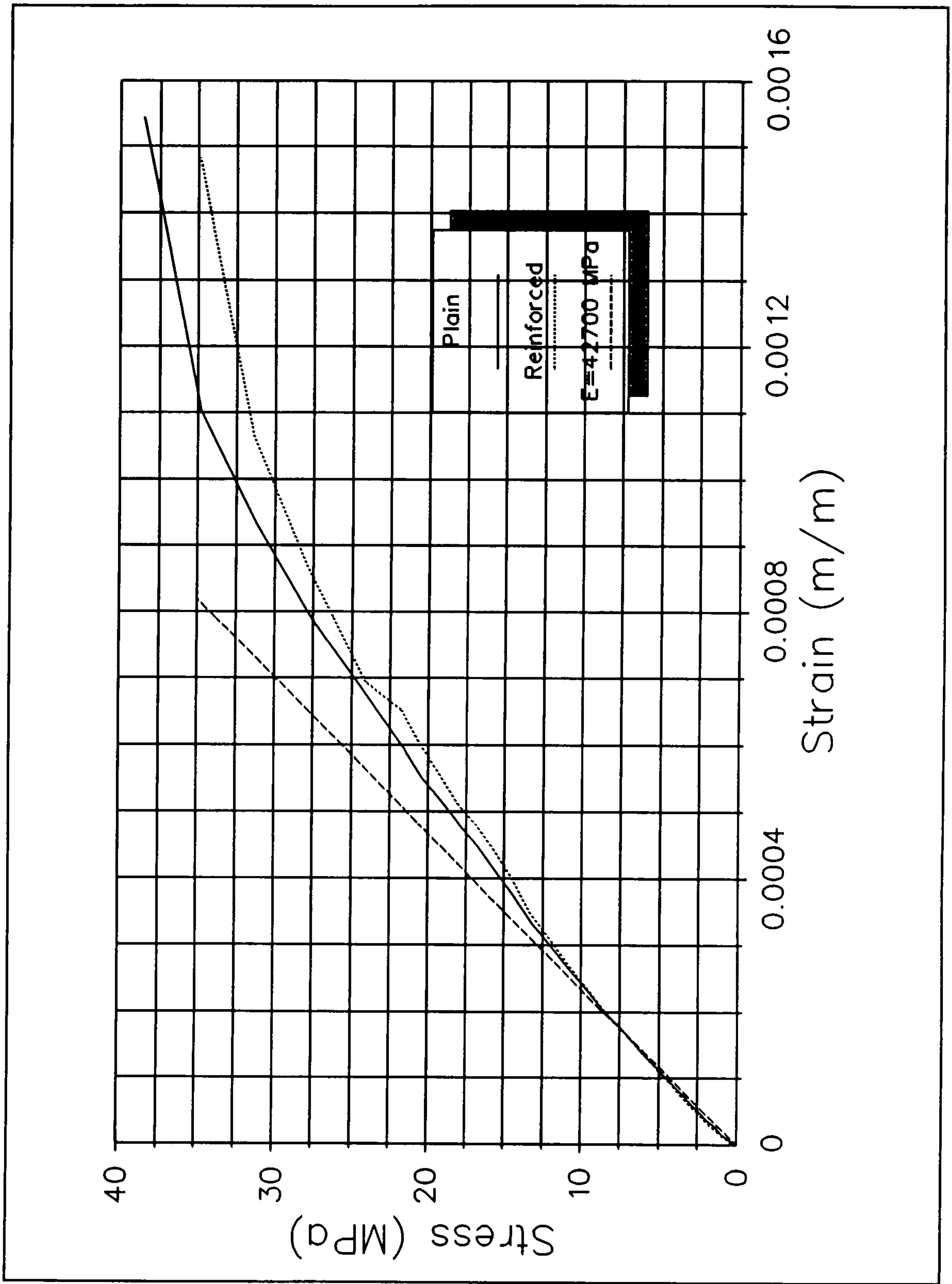

Figure 3.2 Compressive Stress-Strain Curves for Concrete Poured in Both Plain and Reinforced Concrete Footings

stress-strain curve also proves adequate.

ABAQUS's concrete option uses other failures ratios as a part of the input. They are as follows:

1. Ratio of ultimate biaxial compressive stress to the uniaxial compressive ultimate stress.

2. Ratio of the magnitude of a principal component of plastic strain at ultimate stress in biaxial compression to the plastic strain at ultimate stress in uniaxial compression.

3. Ratio of the tensile principal stress value at cracking, in plane stress, when the other non-zero principal stress component is at the ultimate compressive stress value, to the tensile cracking stress under uniaxial tension.

Since not enough information was obtained from material testing for these values, the default values provided by ABAQUS (HSK, 1989a) were used.

A tension stiffening sub-option is provided by ABAQUS to define the relationship of the retained tensile stress normal to a crack and the strain in the same direction. As concrete cracks, there is some remaining tensile strength that exits between the cracks. This option allows for this retained tensile strength. This option requires the input of the remaining stress at the absolute value of direct strain minus the direct strain at cracking, which are assumed to be zero and .0005 respectively.

A suggested value of .15 for Poisson's ratio is used for this model (Park and Paulay, 1975). A density of 2.32 Mg/m^3 (145 pcf) was also specified by Johnson (1992). A summary of all of the concrete parameters is given in the Table 3.2.

Table 3.2 Summary of Concrete Material Properties

MATERIAL PROPERTY	VALUE
Density	2.32 Mg/m^2
Modulus of Elasticity	42700 MPa
Poisson's Ratio	.15
Yield Stress	8.55 MPa
Yield Strain	.0002
Ultimate Compressive Strength	34.9 MPa
Ultimate Tensile Strength	4.25 MPa

3.2.2 Verification

A linear elastic analysis was first conducted by modeling the footing as a simply supported beam and loading it at its center with a 1 MN load. This type of modeling and loading is appropriate because of the known behavior that it exhibits. In a linear elastic analysis, the modulus of elasticity and Poisson's ratio are the only material properties modeled. The theoretical values of the deflection and the stress at the extreme fibers at mid-span were calculated and compared to the values that ABAQUS produces, Table 3.3. This justifies ABAQUS concrete modeling in the elastic range.

Table 3.3 Comparison of Theoretical and ABAQUS values in the Elastic Range

ELASTIC PROPERTIES	THEORETICAL	ABAQUS
Stress (kPa)	630.2	630.6
Deflection (mm)	1.415	1.417

Since concrete is not an elastic material, an inelastic model was constructed. The geometry is the same as the elastic model with the added non-linear relationship of stresses and strains in compression and failure stress in tension. The plain concrete model should fail in tension before reaching the inelastic portion of the compressive stress-strain curve. This model was also simply supported. An incremented displacement was given at midspan in which a reaction (load) was calculated by ABAQUS. This deflection was incremented until failure occurred. A tolerance for the equilibrium of forces occurring at a integration point (PTOL) was investigated and set at 1.0. If this parameter is set too high, the solutions of equations determined by ABAQUS will produce poor results. Furthermore, if the PTOL parameter is set too low, convergence may never be achieved at integration points.

The model failed from cracking in tension since there was no steel to take the tensile forces. A theoretical value for the cracking load and deflection were calculated from Johnson's (1992) values of cracking moment and corresponding curvature. A plot of ABAQUS's values and theoretical values for these loads and deflections are given in Figure 3.3. These two plots show that the cracking behavior of concrete provided by ABAQUS is slightly higher than theoretical values due to the smearing effect of the cracks; however, the stresses and strains observed prove to be adequate for this modeling.

3.4 Reinforced Concrete

3.4.1 Modeling

Reinforcing steel was added to the plain concrete model through ABAQUS's rebar option. Rebars form a layer within two-dimensional continuum elements which were used for the concrete model. These rebar elements are one dimensional taking only axial strain. The amount of reinforcing added is two no.4 bars placed in the top and bottom of the footing shown in Figure 3.4. This amount corresponds to the amount placed in the footing at Herron Road. Testing of the

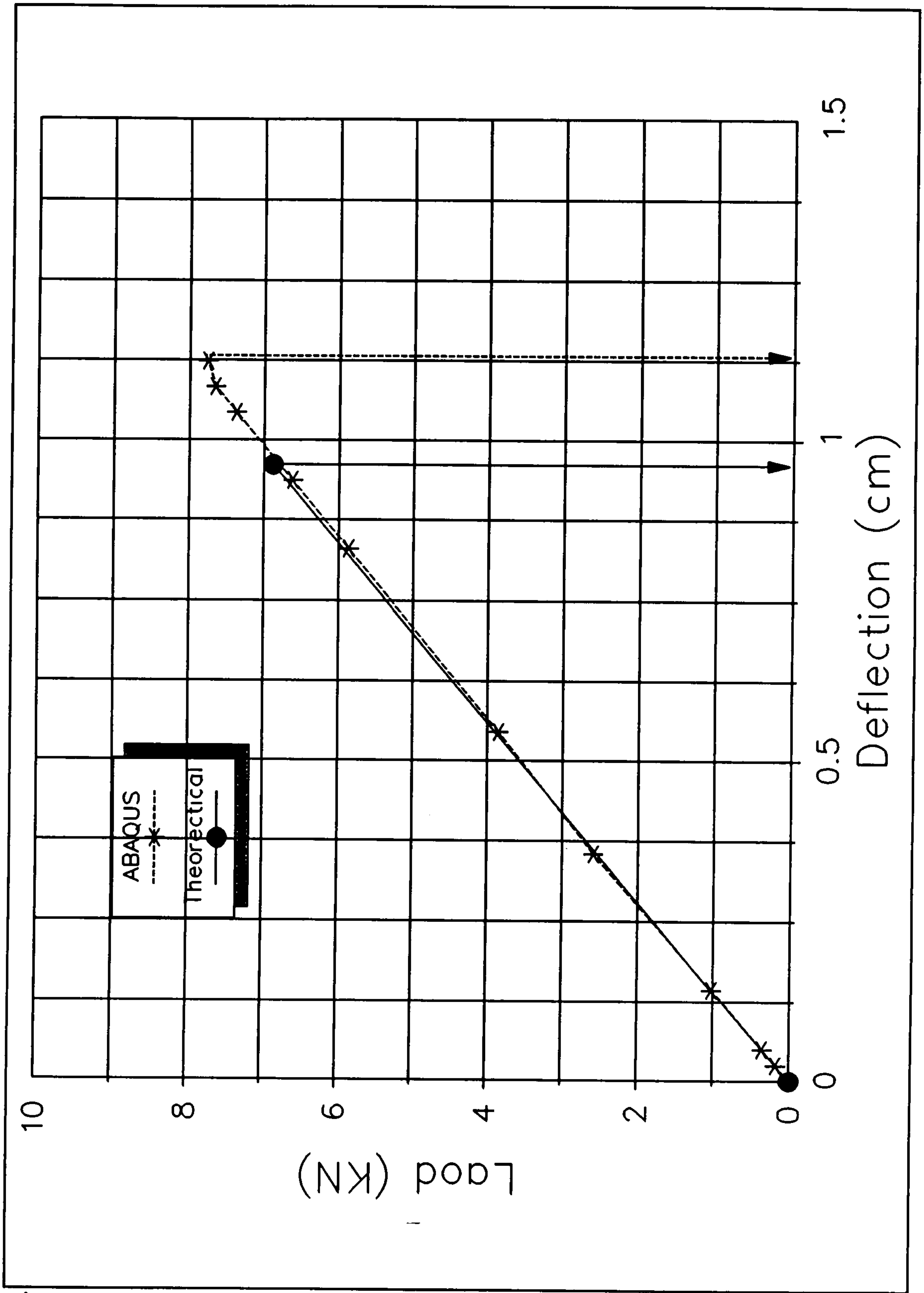

Figure 3.3 Load Deflection Curves for Plain Concrete Footing

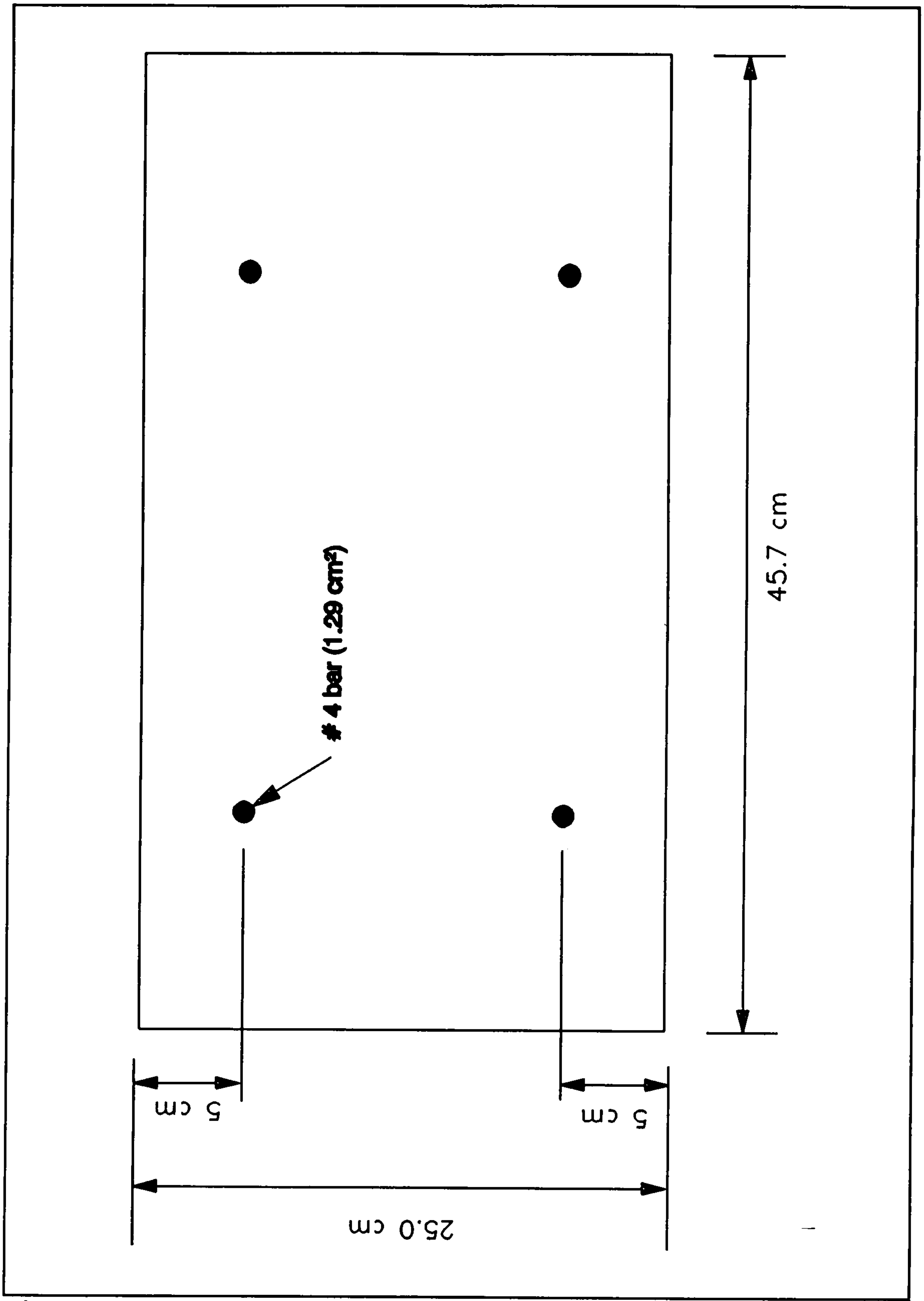

Figure 3.4 Cross-Section of Reinforced Concrete Footing

reinforcing by Johnson (1992) produced a yield stress of 465 MPa (68 ksi) with a modulus of elasticity of 200 GPa (29000 ksi) which are incorporated within this model as elastoplastic behavior. A Poisson's ratio of .3 is used for the reinforcing (Gere and Timoshenko, 1984). The density is increased to 2.403 Mg/m^3 (150 pcf) to account for the weight of the rebars. The tension stiffening parameter is increased to .001 to allow for the added effects of concrete/rebar interaction.

3.4.2 Verification

A load defection curve for a specified displacement at midspan was produced by ABAQUS. The type of loading and PTOL were the same as the plain concrete model. The model was only loaded up to just past yielding of the rebar. Since there was no testing for this reinforced footing, the model is compared to theoretical load-deflection values calculated from Johnson's (1992) moment and curvature values for cracking and yielding, Figure 3.5. It shows that tensile forces are being taken by the added reinforcing after cracking. This figure also shows that results produced from ABAQUS and theoretical calculations are similar. The stresses and strains within the reinforced concrete model were examined and proved to behave properly for this model.

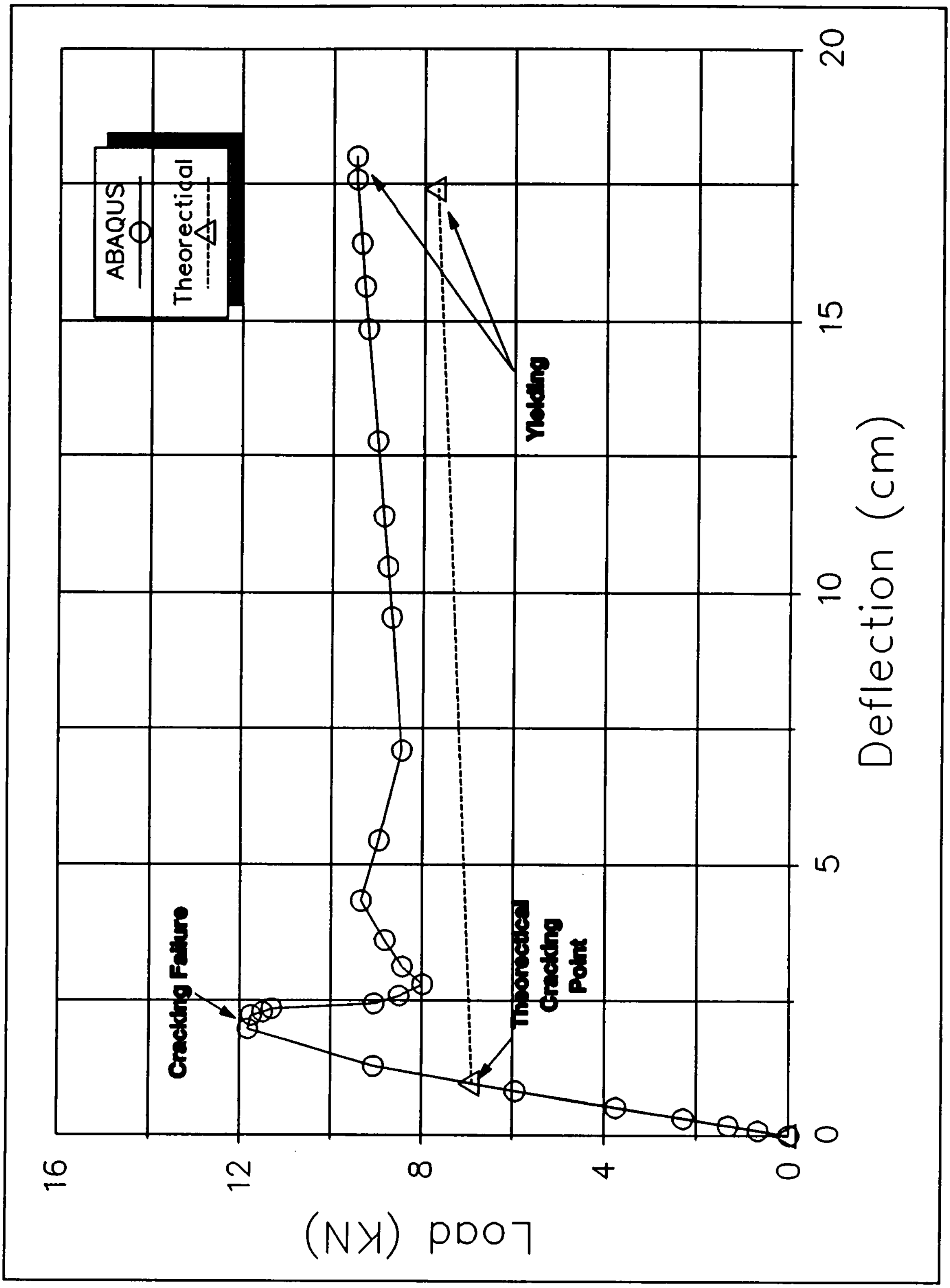

Figure 3.5 Load Deflection Curves for Reinforced Concrete Footing to Yielding

3.5 Masonry

3.5.1 Modeling

The masonry wall is modeled after an analysis of masonry infilled steel frames on ABAQUS conducted by Jamal (1992). Plane stress elements were used. The concrete option along with its sub-options, failure ratios and tension stiffening, were used in his masonry model. A simplified stress-strain curve was adopted which is shown in Figure 3.6. Results from Jamal's modeling proved to be sufficient for modeling masonry in a inelastic fashion; therefore, the ABAQUS (HKS, 1984a) concrete option with its sub-options, plane stress elements, and simplified stress-strain curved used by Jamal (1992) are used for this masonry model.

This model uses gross areas with corresponding properties. The masonry mesh consists of two rows of 16 two-dimensional plane stress, biquadratic, interpolation elements. This mesh is illustrated in Figure 3.7. Actual stress-strain compressive relationships are given in Figure 3.8 from testing of a masonry prism by Johnson (1992). The compressive behavior for this type of testing is appropriate when dealing with masonry assemblages (Schneider and Dickey, 1987). The simplified curve used with this model is also defined in Figure 3.8 according to Jamal's (1992) specifications. The

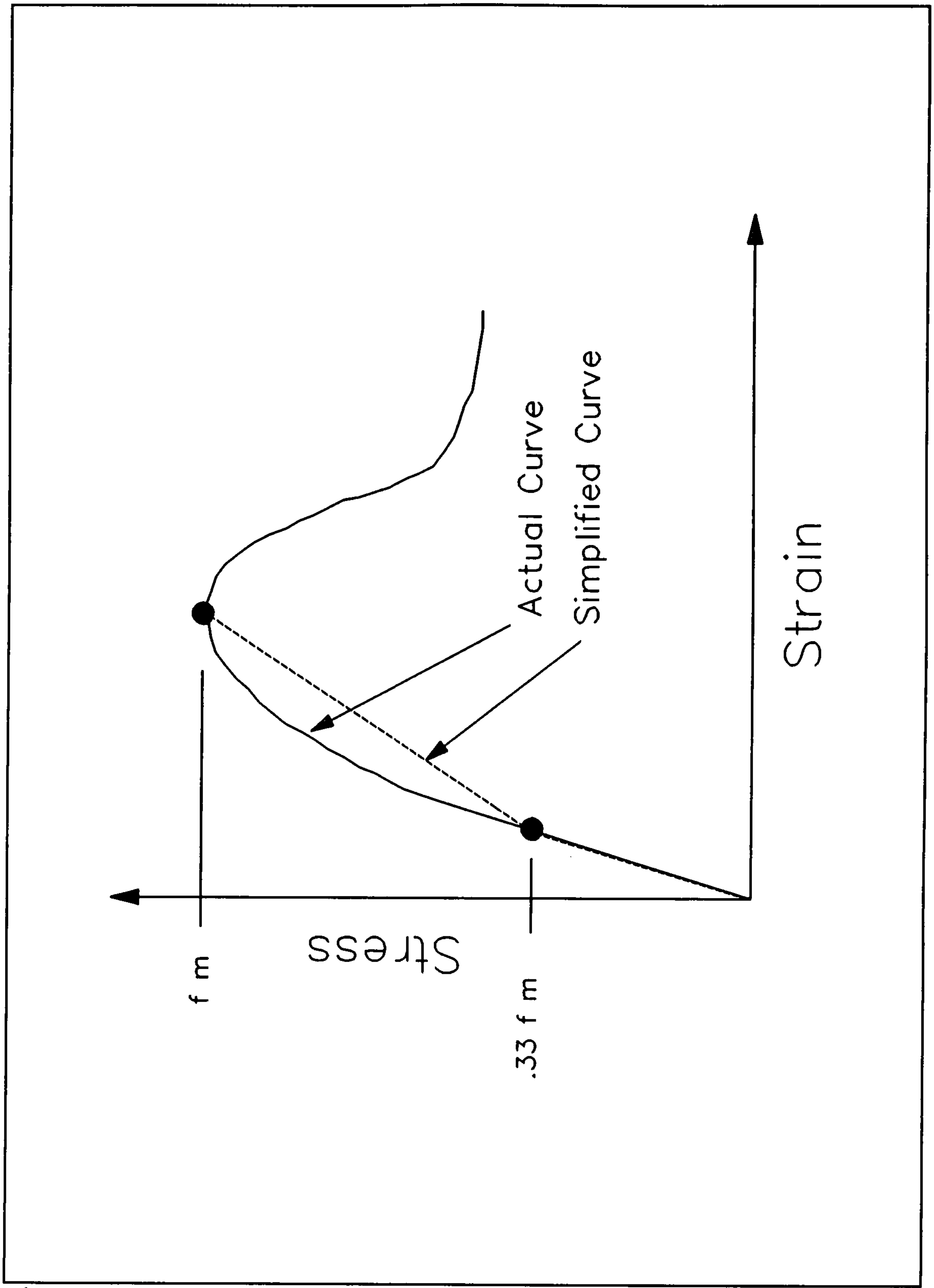

Figure 3.6 Jamal's Simplified Compressive Stress Strain Curve for Masonry (after Jamal, 1992).

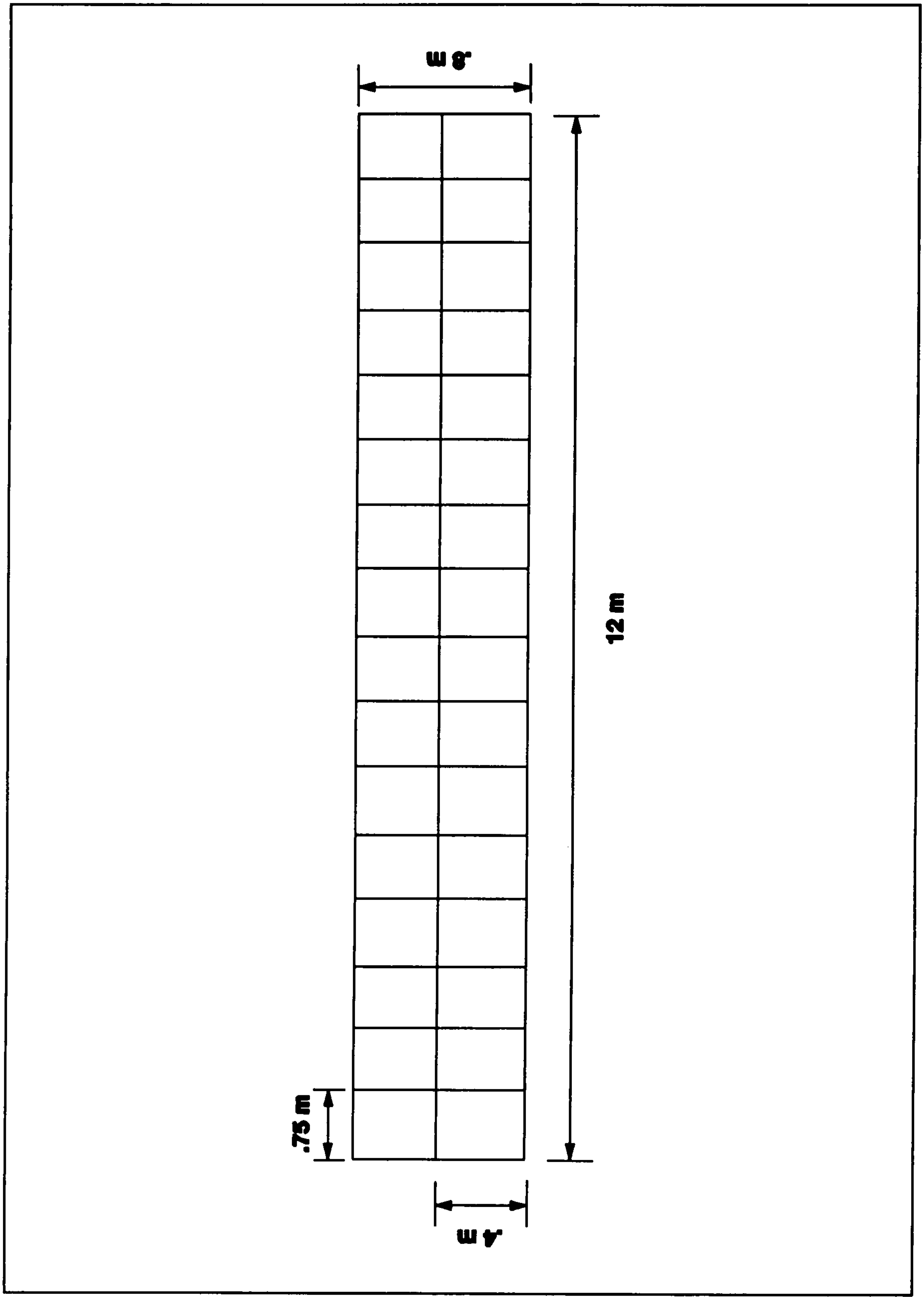

Figure 3.7 Masonry FEM Mesh (not to scale)

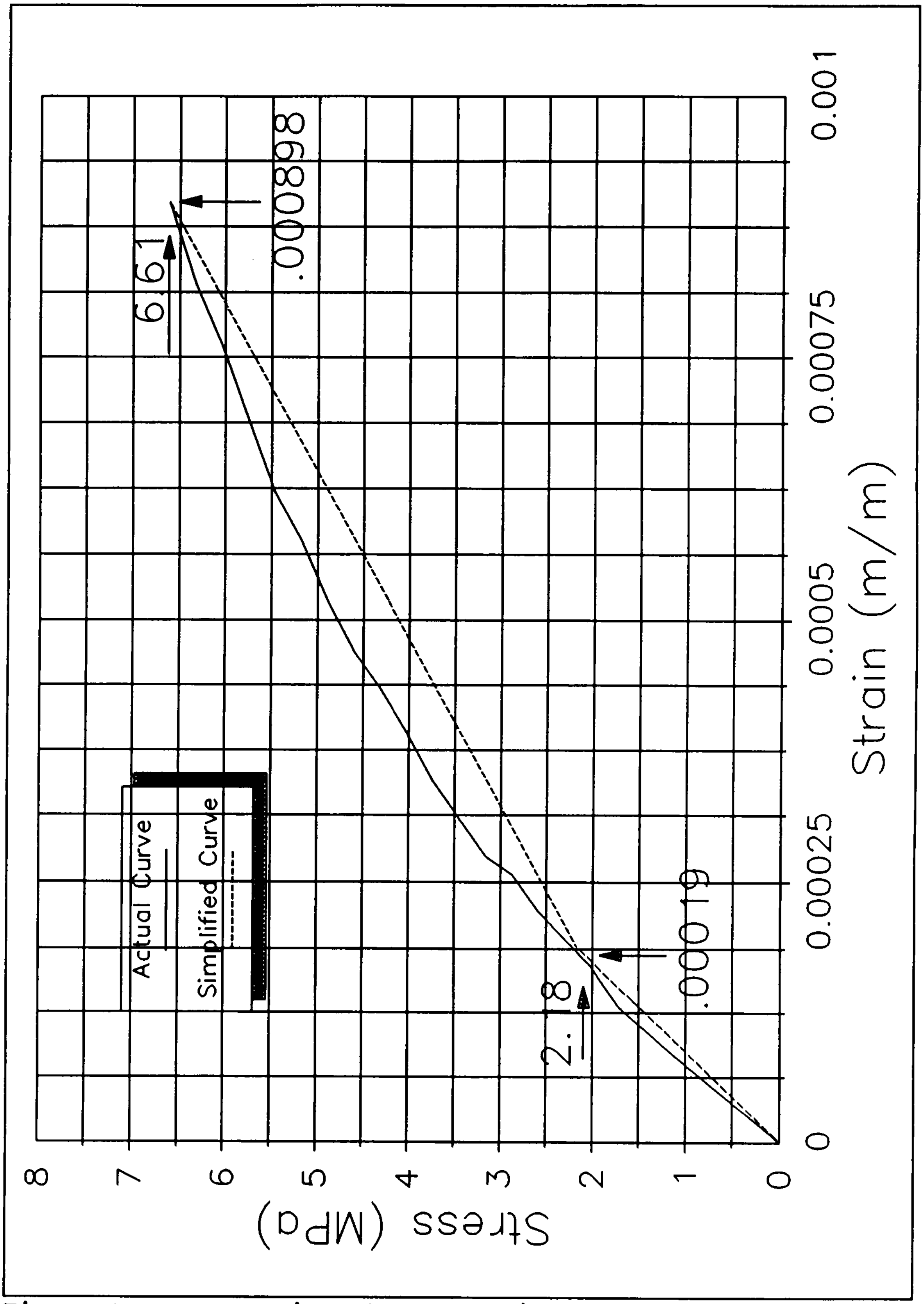

Figure 3.8 Compressive Stress-Strain Curves for Masonry

modulus of elasticity of the simplified curve is 11,500 MPa (1670 ksi) which is close to a suggested modulus of 9,900 MPa recommended by Johnson (1992). According to Johnson (1992) cracking generally did not occur in the masonry blocks, rather a cracking pattern occurred in the bed and head joints. This was also the behavior that Littlejohn (1974) noticed when observing brick walls subjected to mining subsidence. Littlejohn (1974) concluded that failure from cracking occurred as result of the breakdown of the brick-mortar bond due to tensile strains. Drysdale and Hamid (1984) performed tests on masonry walls with N type mortar joints. These tests should reflect the type of cracking behavior that was associated at Herron Road. They concluded that the shear and tensile bond strengths of the mortar have a considerable effect on the tensile capacity a masonry wall forming this cracking pattern. From their test results a tensile capacity of 350 kPa (50 psi) was produced. This almost corresponds to the split tension tests performed earlier by Drysdale et al. (1979) that produced a tensile capacity of the bed joints of 300 kPa (43 psi). From these observations a tensile capacity of 350 kPa is used for the masonry wall unit. Furthermore, a Poisson's ratio of .28 is used (Schneider and Dickey, 1987). The density was recorded by Johnson (1992) to be 1.15 Mg/m^3. A summary of the masonry material properties are given in Table 3.4.

Table 3.4 Summary of Masonry Properties

MATERIAL PROPERTY	VALUE
Density	1.15 Mg/m^3
Poisson's Ratio	.28
Modulus of Elasticity	11500 MPa
Yield Stress	2.18 MPa
Yield Strain	.00019
Ultimate Compressive Strength	6.61 MPa
Ultimate Compressive Strain	.000898
Ultimate Tensile Strength	350 kPa

Convergence problems from high tensile forces were encountered during the subsidence event due to the limitations of the continuum masonry model. When this phenomenon was encountered, the masonry mesh was modified by placing interface elements within the masonry mesh, Figure 3.9. These interface elements are placed within the masonry mesh to simulate "real" vertical cracks or openings between masonry elements. The interface elements are given the tensile capacity of the mortar joints through a modified pressure clearance relationship.

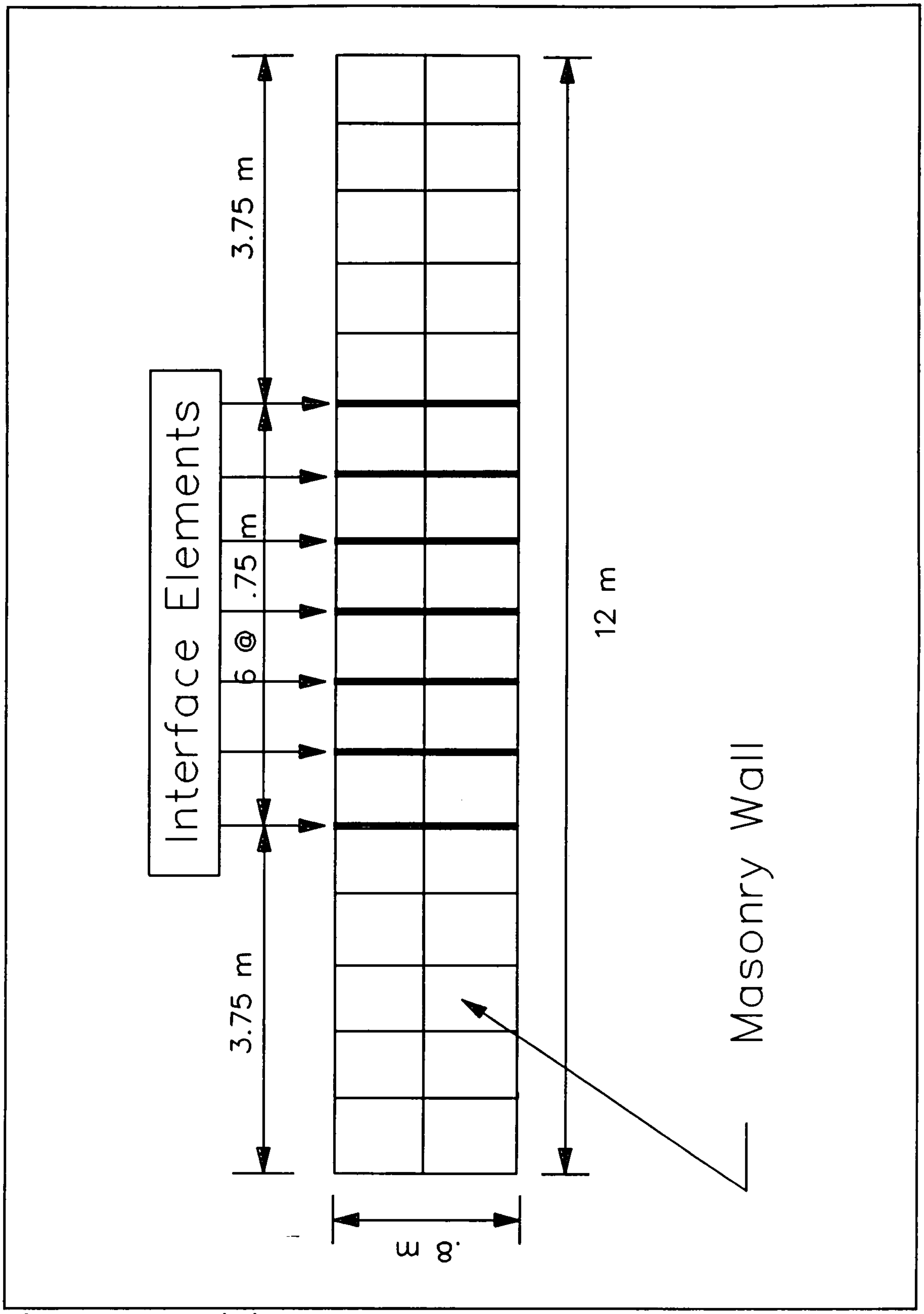

Figure 3.9 Modified Masonry Mesh (not to scale)

3.5.2 Combined Footing/Wall Behavior

The masonry mesh is placed on top of the reinforced concrete mesh to form a partially composite section which is shown in Figure 3.10. This was done to insure that the masonry wall acted appropriately when connected to the footing. The actual interface between the footing and masonry wall was not modeled because it is beyond the scope of this modeling. Displacements were incremented at midspan and corresponding reactions (loads) were calculated by ABAQUS. The section was loaded in two ways in order to produce both tension and compression in the masonry. The deflected shapes for both types of loading are given in Figures 3.11 and 3.12.

There was no test data available for comparison with load deflection curves produced by ABAQUS; therefore, stresses and strains were examined in the footing and masonry during the loading. The stress-strain behavior produced during the tests proved to display proper behavior for these models.

The load deflection curves produced by ABAQUS for the combined masonry and reinforced concrete footing are given in Figure 3.13 and Figure 3.15. These curves are compared to the reinforced concrete footing's load deflection curve to illustrate that the reinforced concrete footing with the masonry wall should be stiffer than just the reinforced concrete footing. Figure 3.13 shows that the composite section is much stiffer when the masonry is in compression. However, Figure 3.14 shows that the composite section has

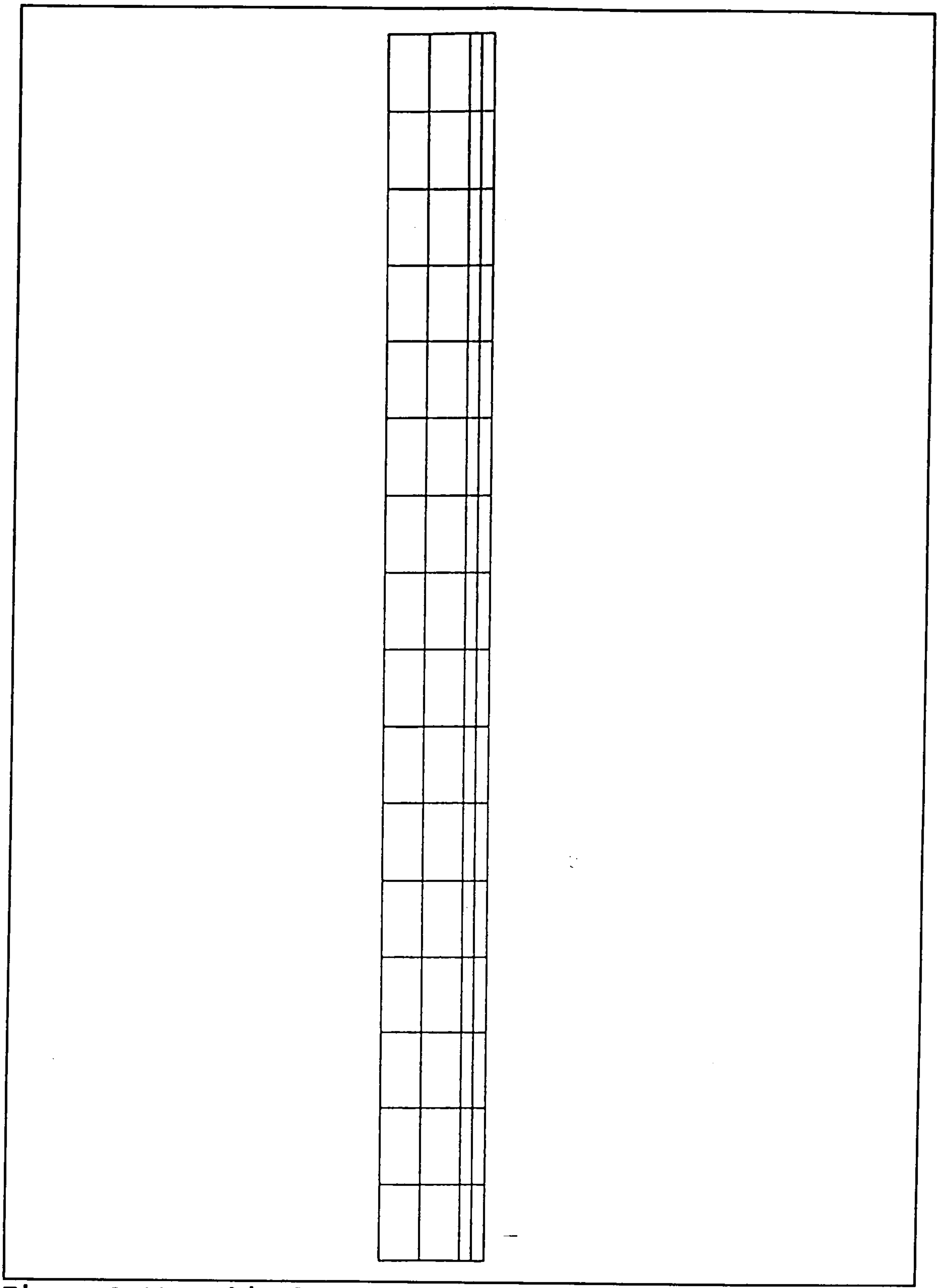

Figure 3.10 Combined Masonry and Reinforced Footing FEM Mesh

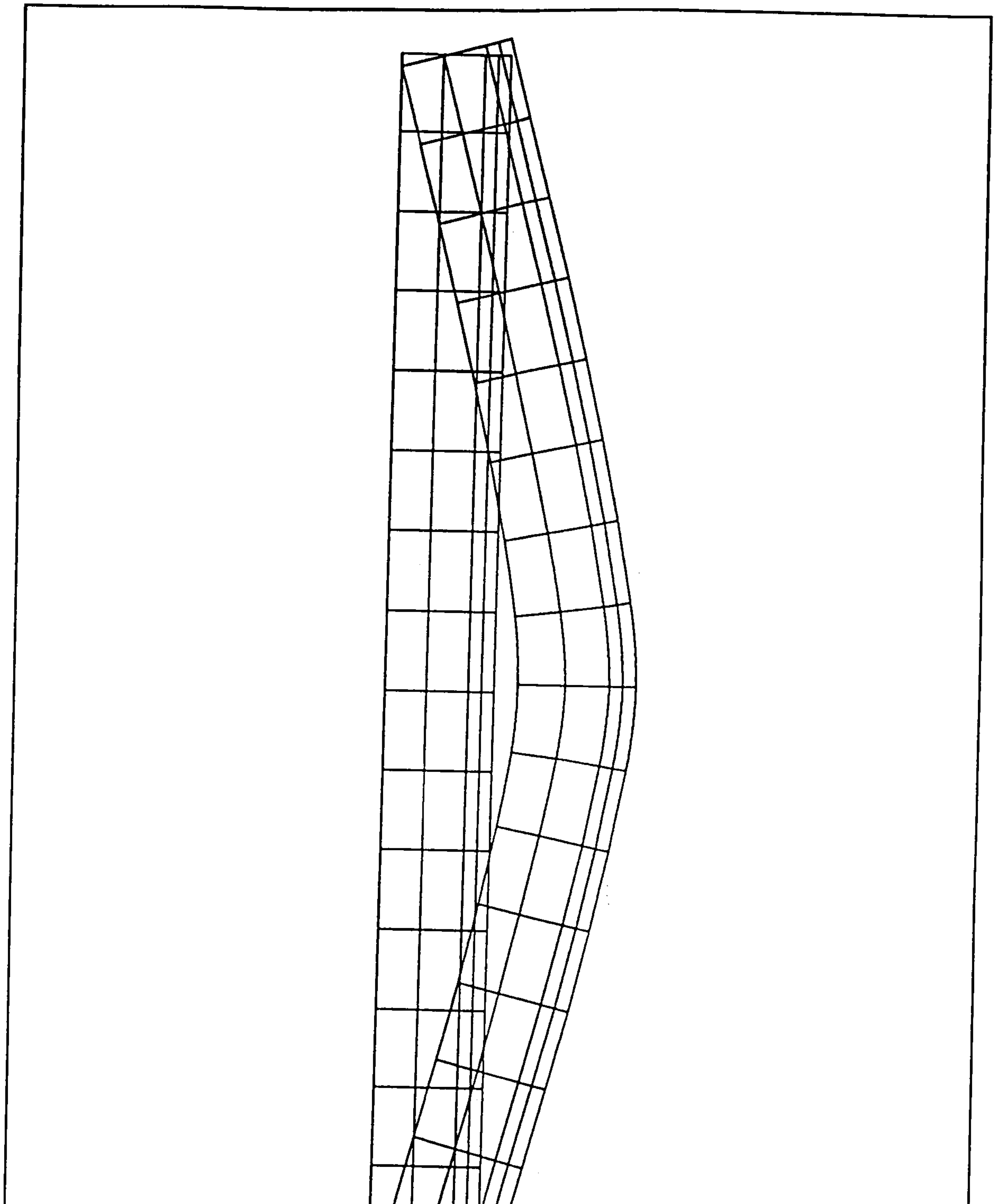

Figure 3.11 Deflected Shape of Partially Composite Section for Masonry in Compression

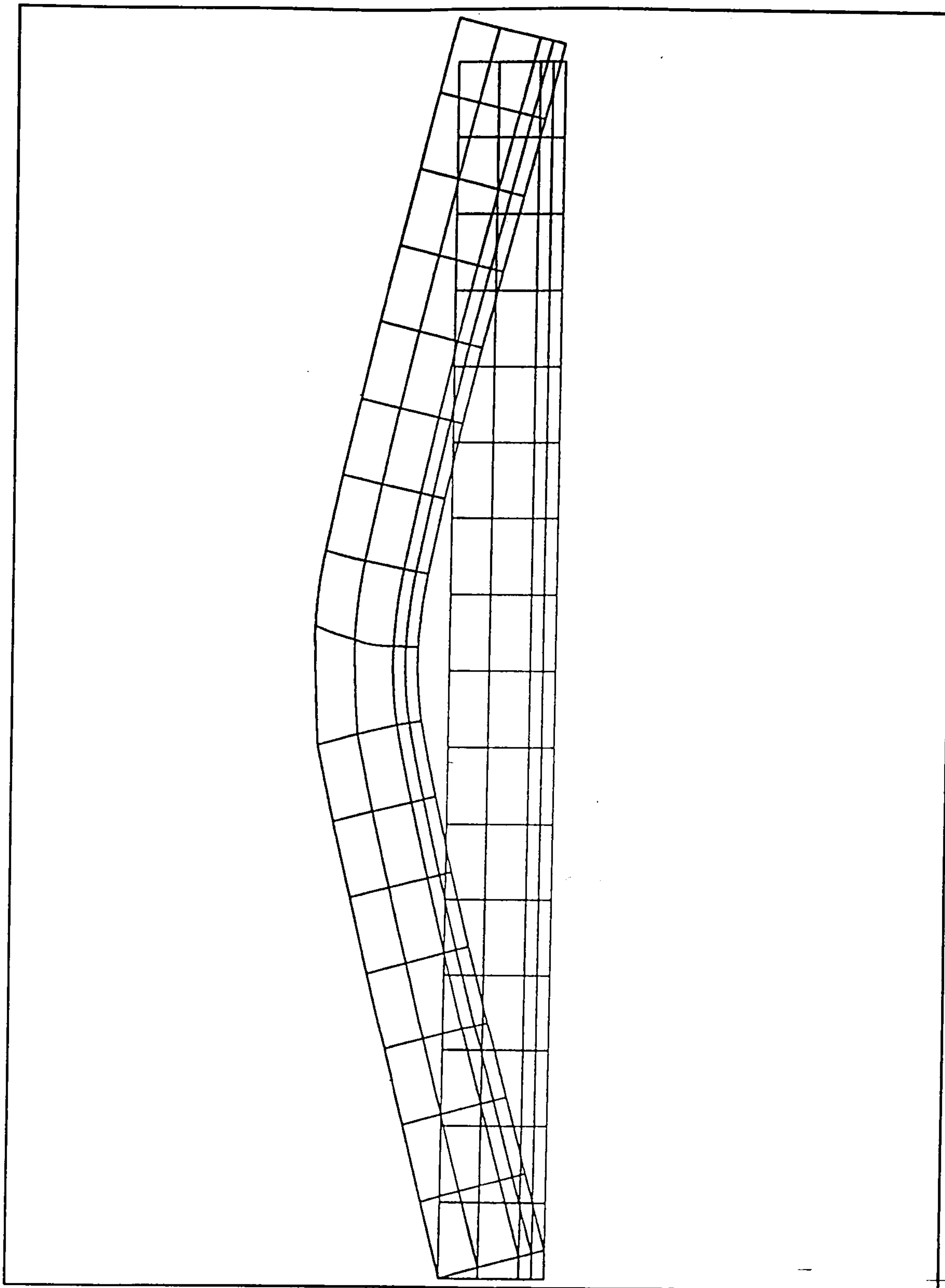

Figure 3.12 Deflected Shape of Partially Composite Section for the Masonry in Tension

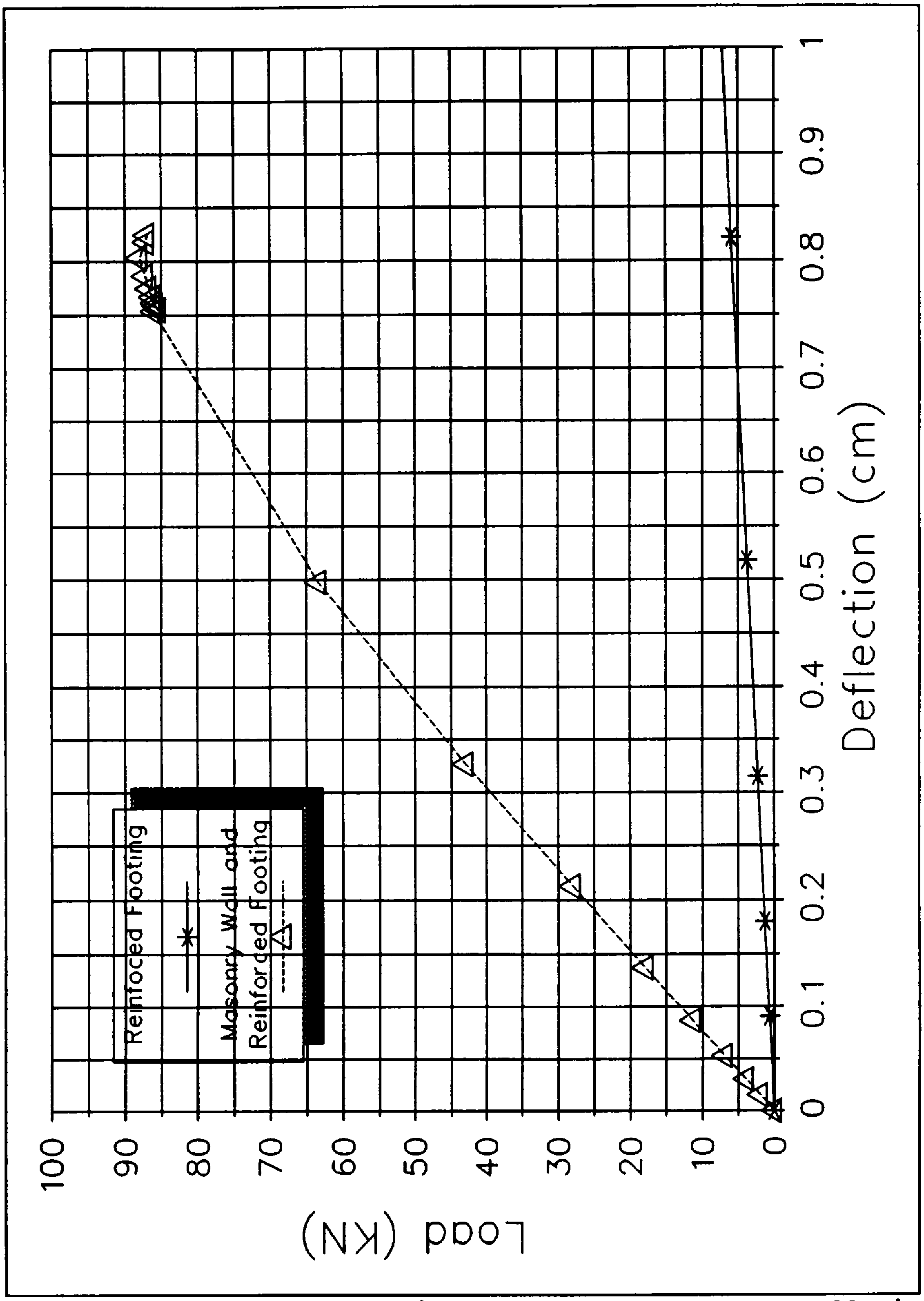

Figure 3.13 Load Deflection Curve for Masonry Wall in Compression

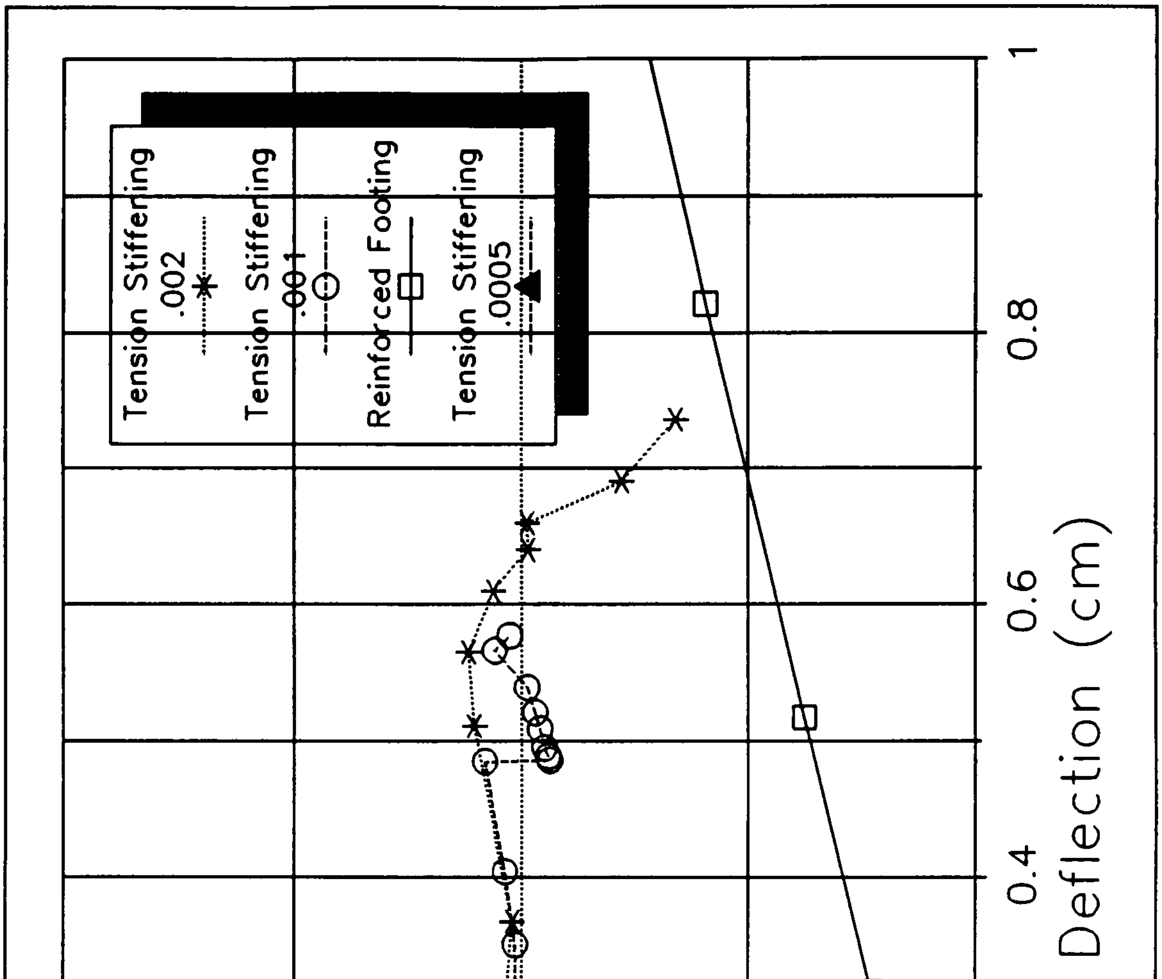

Figure 3.14 Load Deflection Curve for Masonry Wall in Tension.

nearly the same stiffness as the masonry in compression until failure occurs when the masonry reaches its cracking limits. Several tension stiffening values are used to give the masonry different stress-strain paths to follow after cracking. Cracking occurred in the masonry wall for each tension stiffening value. The tension stiffening value of .002 produced the largest deflection before convergence problems were encountered from severe cracking in the masonry. Tension stiffening values higher than .002 did not increase deflections for the masonry wall in tension; therefore, the tension stiffening value of .002 is used to give the masonry model the largest capacity for taking tensile forces in the continuum masonry mesh.

The modified masonry mesh (incorporating interface elements) was placed on the reinforced footing and loaded at midspan to produce tension in the masonry. Stress-strain behavior within the masonry and reinforced footing was observed to insure proper behavior. The load deflection curve produced from this loading is given in Figure 3.15. The results are compared to the reinforced footing with and without the continuum masonry model. Gapping and cracking occurred within the modified masonry mesh at the masonry cracking limit. The stiffness of the modified composite section diminishes at a lower load than the continuum composite section due to the limitations of the model. However, Figure 3.15 shows that the modified masonry still

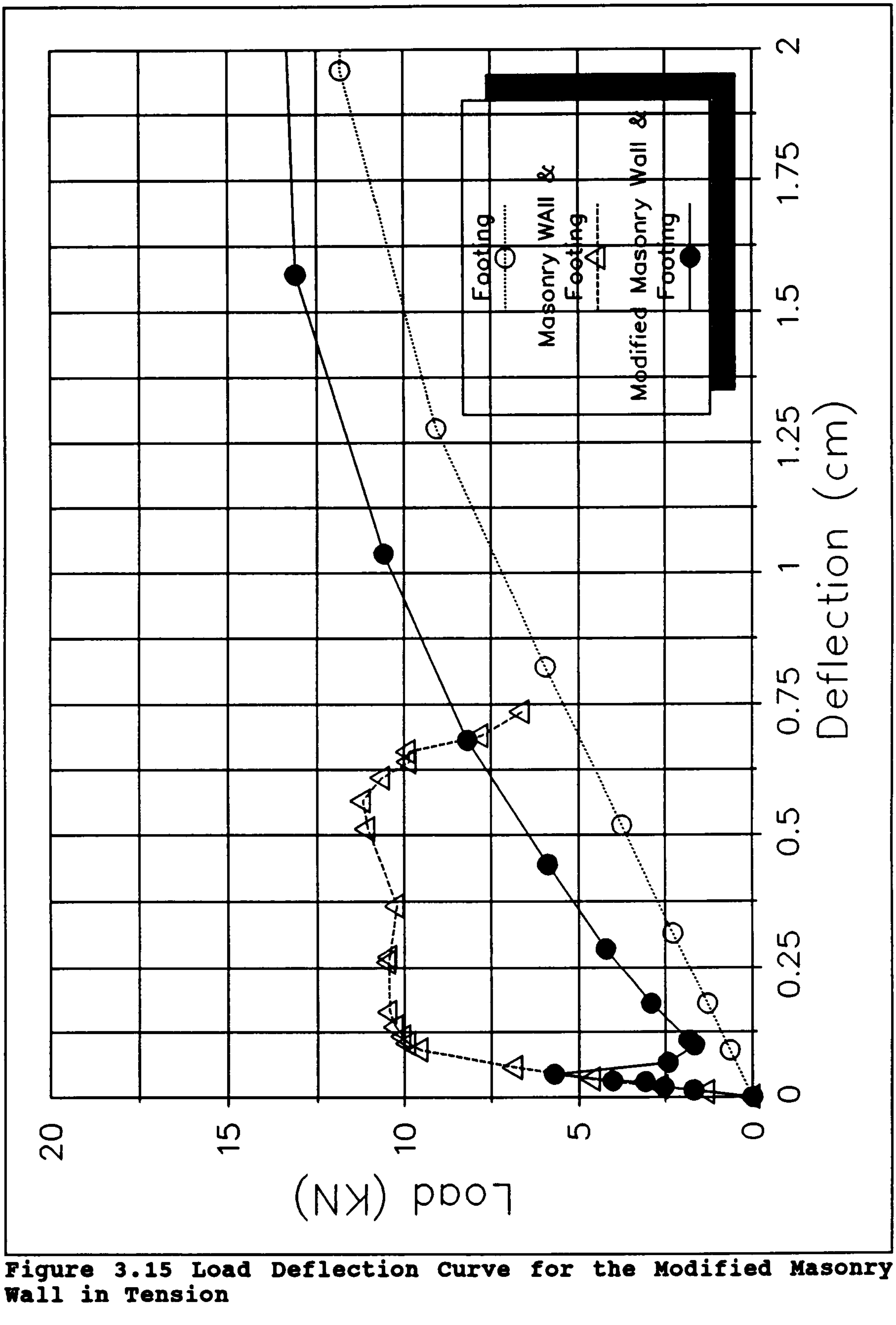

Figure 3.15 Load Deflection Curve for the Modified Masonry Wall in Tension

contributes to the stiffness of the foundation after cracking has occurred in the masonry. This modified masonry mesh is a good solution for eliminating convergence problems when the masonry is subjected to high tensile stresses; therefore, it was used during the tension phase of analysis.

3.6 Soil-Structure Interface

3.6.1 Modeling

Either gap or interface elements could be used to model the interface between the soil and foundation. Both of these elements will allow openings and closure as well as slippage between the soil and footing; however, the output given for these elements are different. Stresses are associated with the interface elements while forces are output variables for gap elements. Three-noded interface elements were chosen to model the interface because the output produced is more beneficial than gap elements. A width corresponding to the footing width and the directions for gapping and slippage are input for these elements. A friction sub-option can also be used with these elements.

The friction option utilizes a classical Coulomb envelope along with a "stiffness in stick" parameter (HKS, 1989). The "stiffness in stick" parameter refers to how much displacement is allowed at the interface according to how much shear stress is present. These displacements are relatively small when compared to the displacements associated with slippage due to shear failure. In addition, an optional shear stress limit can be incorporated in this sub-option; however, it is not needed in this model.

The default value was used to model the surface contact behavior associated with gapping at the interface. The interface elements use a pressure-clearance relationship in which any amount of pressure can exist at the interface when in contact while any amount of clearance can exist when no pressure is present. This phenomenon is illustrated in Figure 3.16.

Direct shear testing was performed by Lee (1989) for a rough concrete-soil interface from soil obtained at the Sesser site. Several "stiffness-in-stick" relationships were determined according to the amount of normal pressure applied. According to Johnson (1992) the normal pressure supplied by the load bins and foundations in the centerline was 34 kPa (4.9 psi). A value of 36.6 MPa/m (133.5 psi/in) was observed by Lee (1989) for this normal pressure; therefore, this value is used for the "stick-in-stiffness" parameter.

A coefficient of friction is needed to specify a basic Coulomb failure envelope for the interface. The failure envelope determined by Lee (1989) would best describe the failure at the interface due to shearing stress; however, the cohesion value determined in the testing can not be

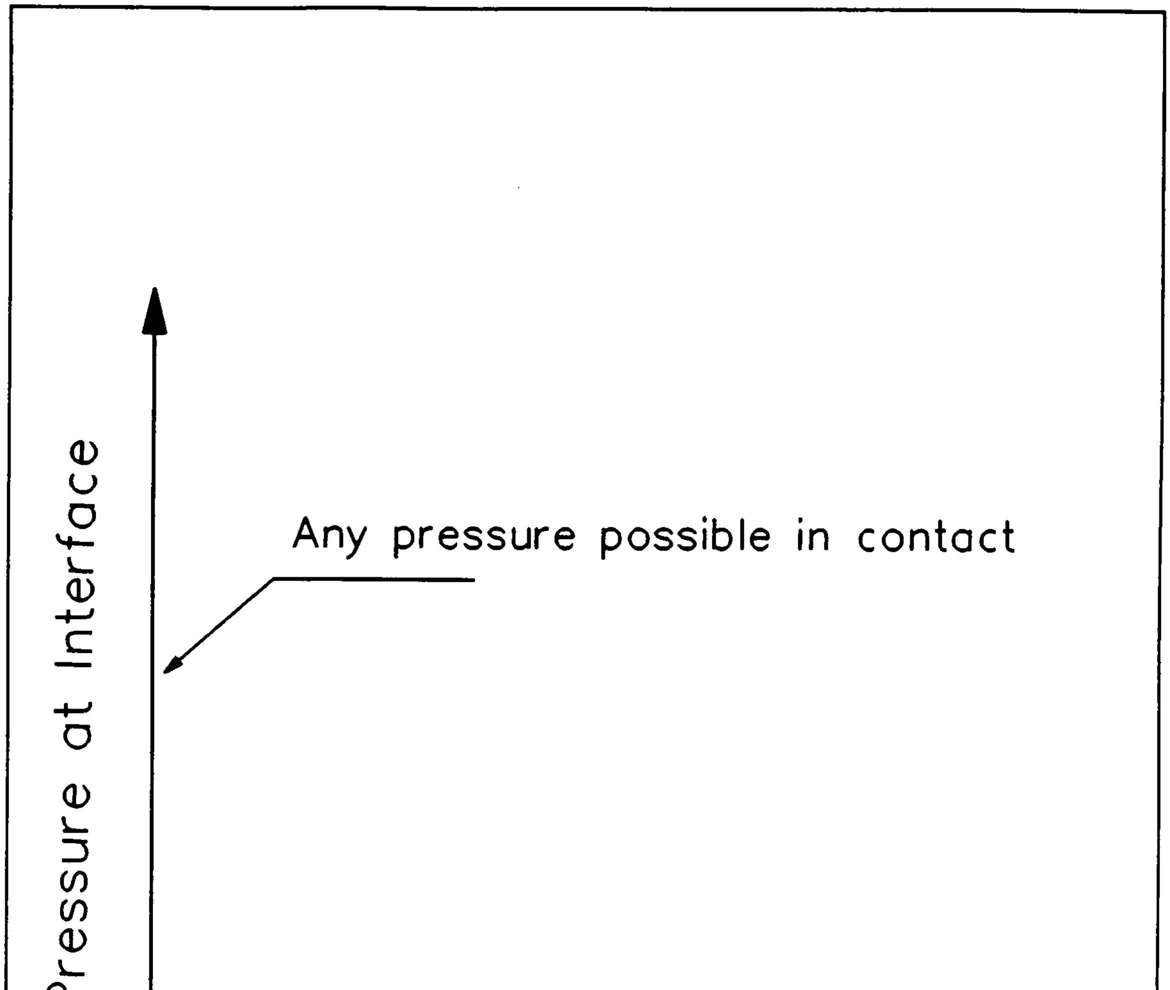

Figure 3.16 Pressure-Clearance Relationship for Interface Elements (after HKS, 1984).

incorporated into the model. An alternative value to be used is the coefficient of friction of the soil. Lawrence (1992) observed a friction angle of 37° which corresponds to a coefficient of friction of 0.7. According to Bowles (1988) the full friction angle of the soil should be used when designing for slippage of a retaining wall at its base. This is to insure that no slippage will occur; therefore, using the full friction angle of the soil will produce the maximum amount of shear stress transferred to the foundation. The value determined by Lawrence will be used in the analysis; however, this value is subject to adjustment after a preliminary analysis is performed. The interface failure envelope produced from the coefficient of friction is illustrated in Figure 3.17.

3.6.2 Verification

A simple model was constructed with an interface element placed between a footing and soil element. Elastic properties are given to both the soil and footing. The soil element was constrained from movement. A surcharge was placed on the footing element to give a pressure of 34 kPa. A horizontal load was given to the footing in increments to produce a corresponding shear stress calculated by ABAQUS at the interface. This modeling and procedure is illustrated in Figure 3.18. When the shear force resulted in a shear stress

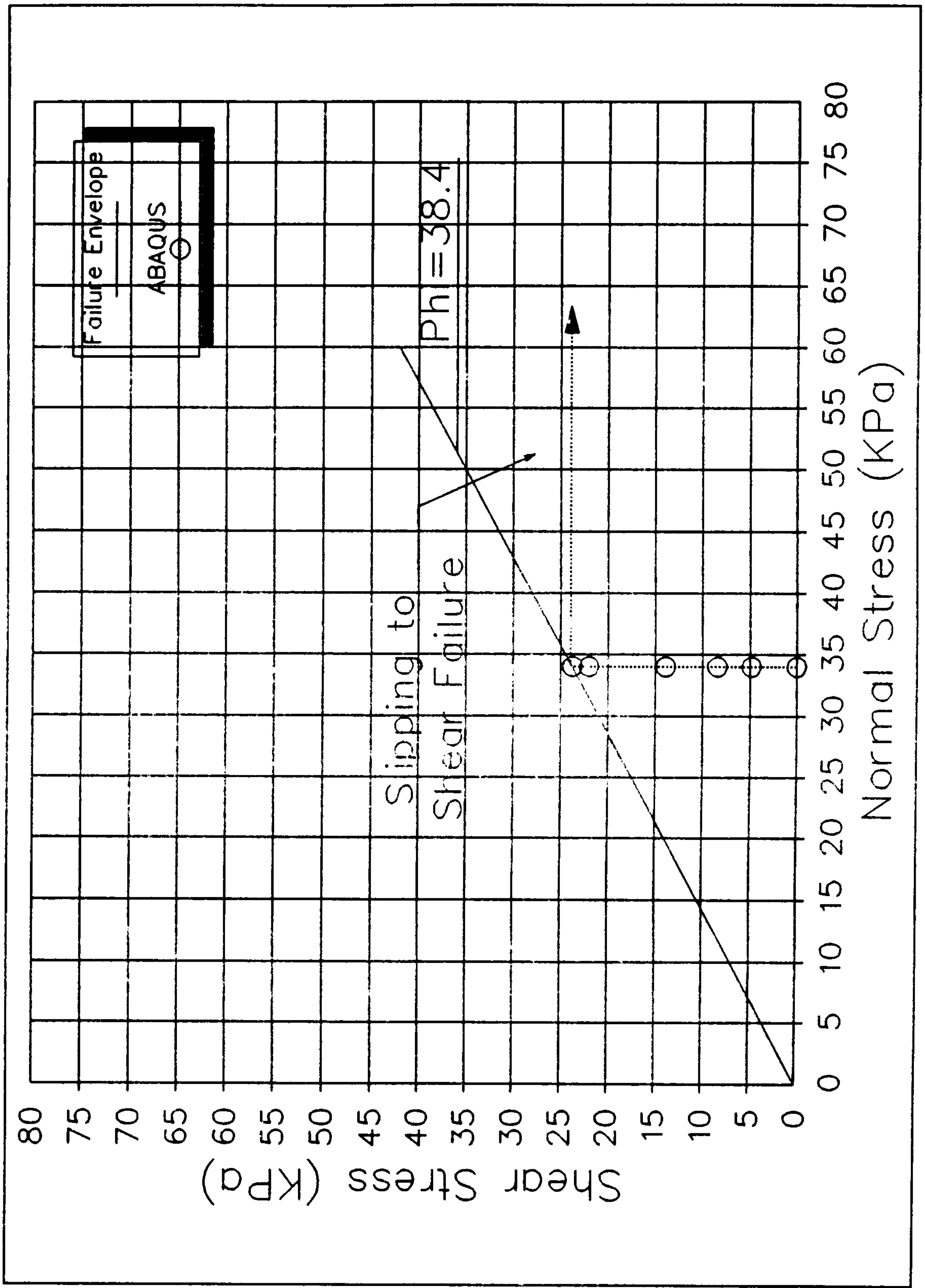

Figure 3.17 Interface Failure Envelope

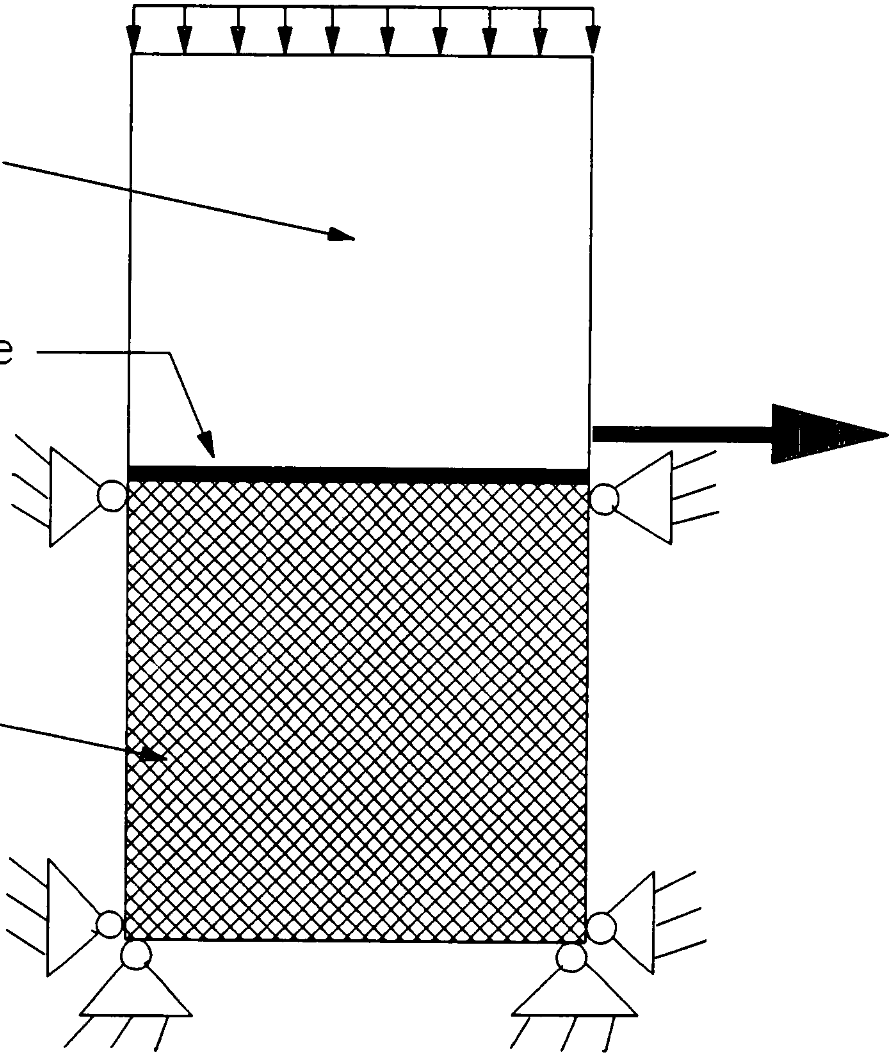

Figure 3.18 Test Diagram for Interface Testing in ABAQUS

of about 24 kPa, failure occurred because the block simply tried to slide off. This failure is illustrated in Figure 3.17. The effect of the "stick-in-stiffness" is illustrated in Figure 3.19 for this model. This figure shows that small displacements are occurring at the interface until failure occurs. The shear stress at which failure occurs corresponds to value at which failure occurs in Figure 3.17.

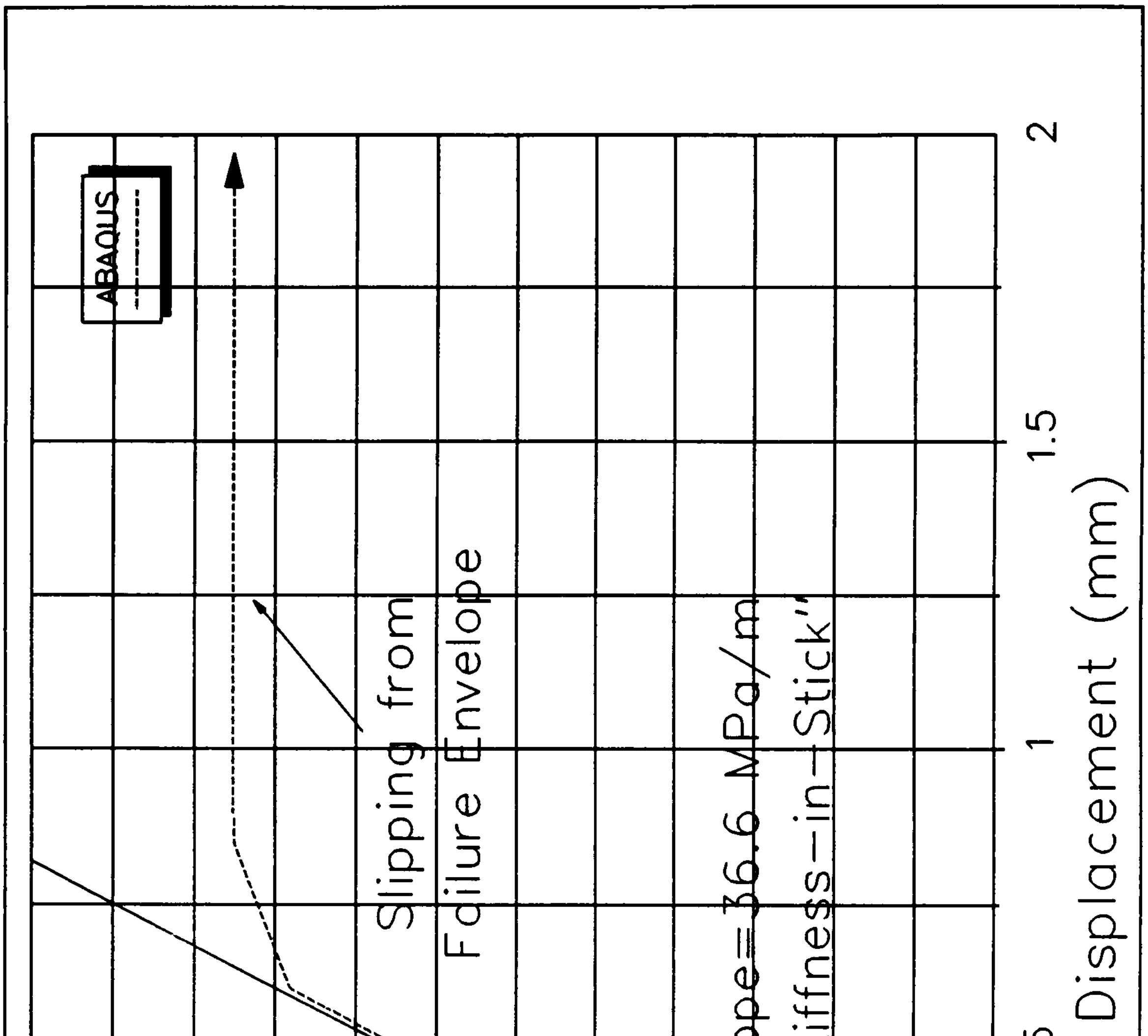

Figure 3.19 Shear Stress vs. Displacement at the Interface

CHAPTER 4

NUMERICAL ANALYSIS

4.1 Free Field Analysis

A free field analysis was conducted by Lawrence (1992) using the ABAQUS (HKS, 1984a) finite element code. A two dimensional plane strain soil mesh was constructed, Figure 4.1. The optimum size of the soil mesh was determined to produce adequate stresses and strains at the surface of the soil mesh for the free field analysis. The size of the mesh is refined at the top center where the foundation would be located, which allows for the addition of the foundation and interface with minimum complications. The size of the mesh is 60 m wide by 13.75 m deep with a total of 258, 8-noded reduced integration, isoparametric elements. Horizontal constraints were given to the side of the mesh while vertical constraints were given to the bottom of the mesh. The domain proved to be adequate for inducing strains and stress without boundary effects.

The analysis was performed for the subsidence event that occurred at the center line of the West Frankfort Project. This subsidence event was captured through a subsidence wave produced from vertical free field survey data, Figure 4.2 (Ben

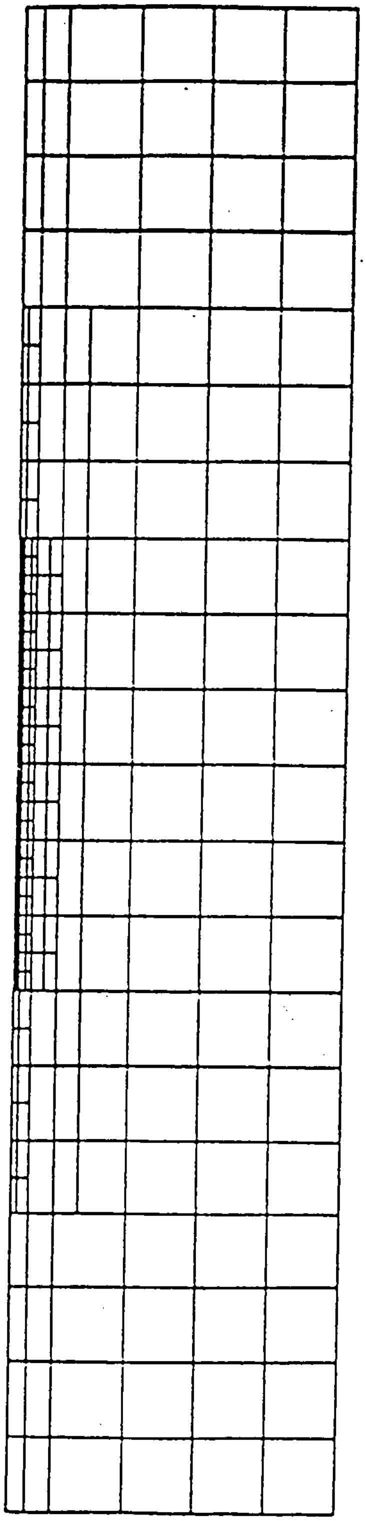

Figure 4.1 Soil Mesh for Free Field Analysis

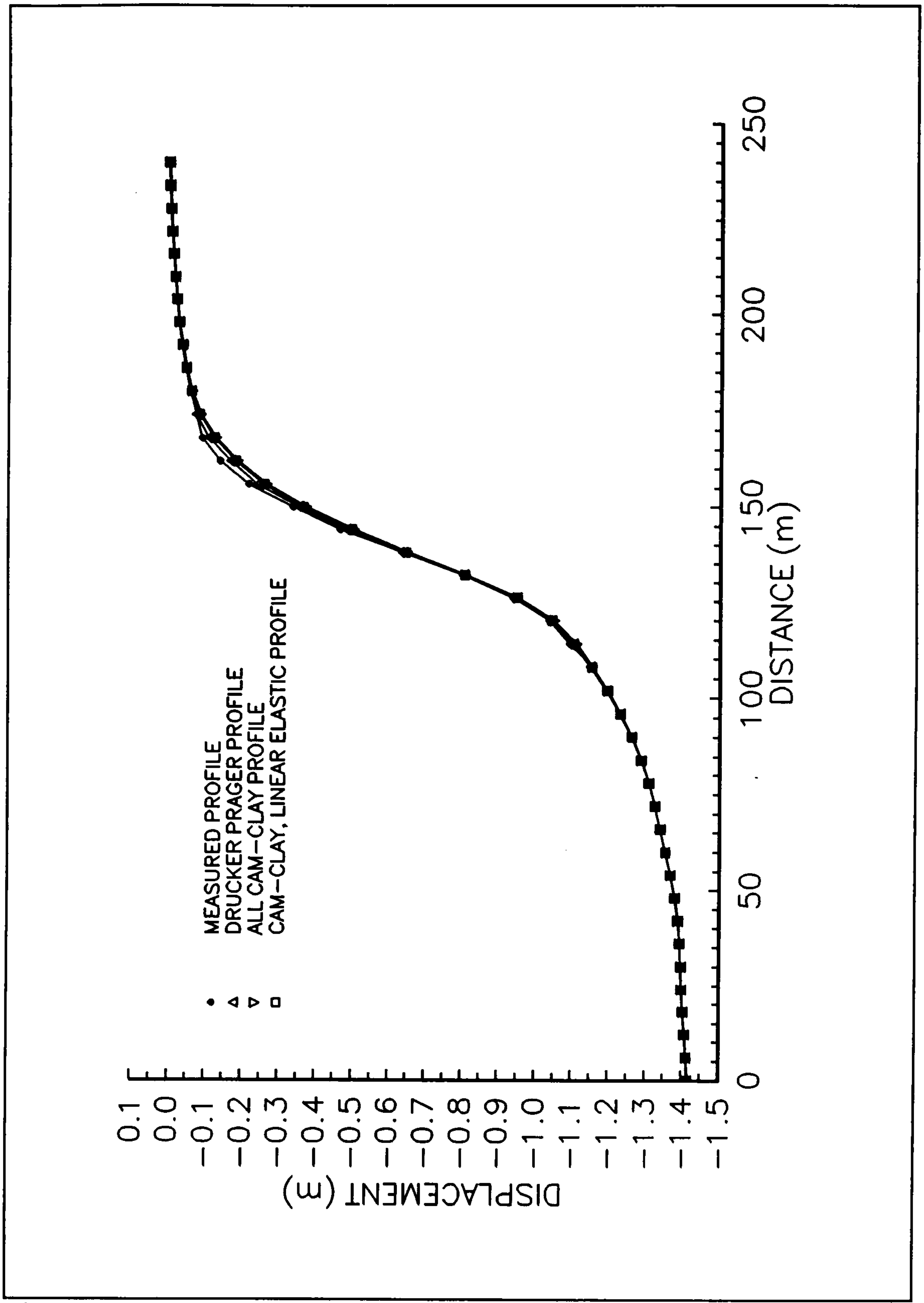

Figure 4.2 Centerline Subsidence Wave (Lawrence, 1992)

Hassine, 1992; Lawrence, 1992). The wave was moved through the soil mesh by applying vertical displacements at the bottom of the mesh to achieve the proper surface displacements. A trial and error process was used to determine the necessary bottom displacements. The soil domain was marched along the subsidence wave in 3 m steps. It took 100 of these steps to simulate the full wave analysis. The illustration of a profile created from applying bottom displacements during one of the steps is shown in Figure 4.3 at a magnification of 8. The comparison of the entire subsidence wave produced numerically is compared to the subsidence wave from field data in Figure 4.2.

After much experimenting with different plasticity models, the Cam-Clay model was used at the top of the soil mesh and a linear elastic model was used at the bottom where stresses and strains are not of concern. The soil mesh was placed in a geostatic stress state before the analysis was performed.

The results were compared to vertical strains measured with Bison soil strain gages in the field. Some discrepancy in comparison can be attributed to several factors. Discrete cracking behavior of the soil could not be captured in the FE analysis due to the continuum elements used to model the soil. Therefore, if cracking occurred near a bison gage, the strain induced in the gage is affected significantly. The extension behavior of the soil in the field was not investigated and

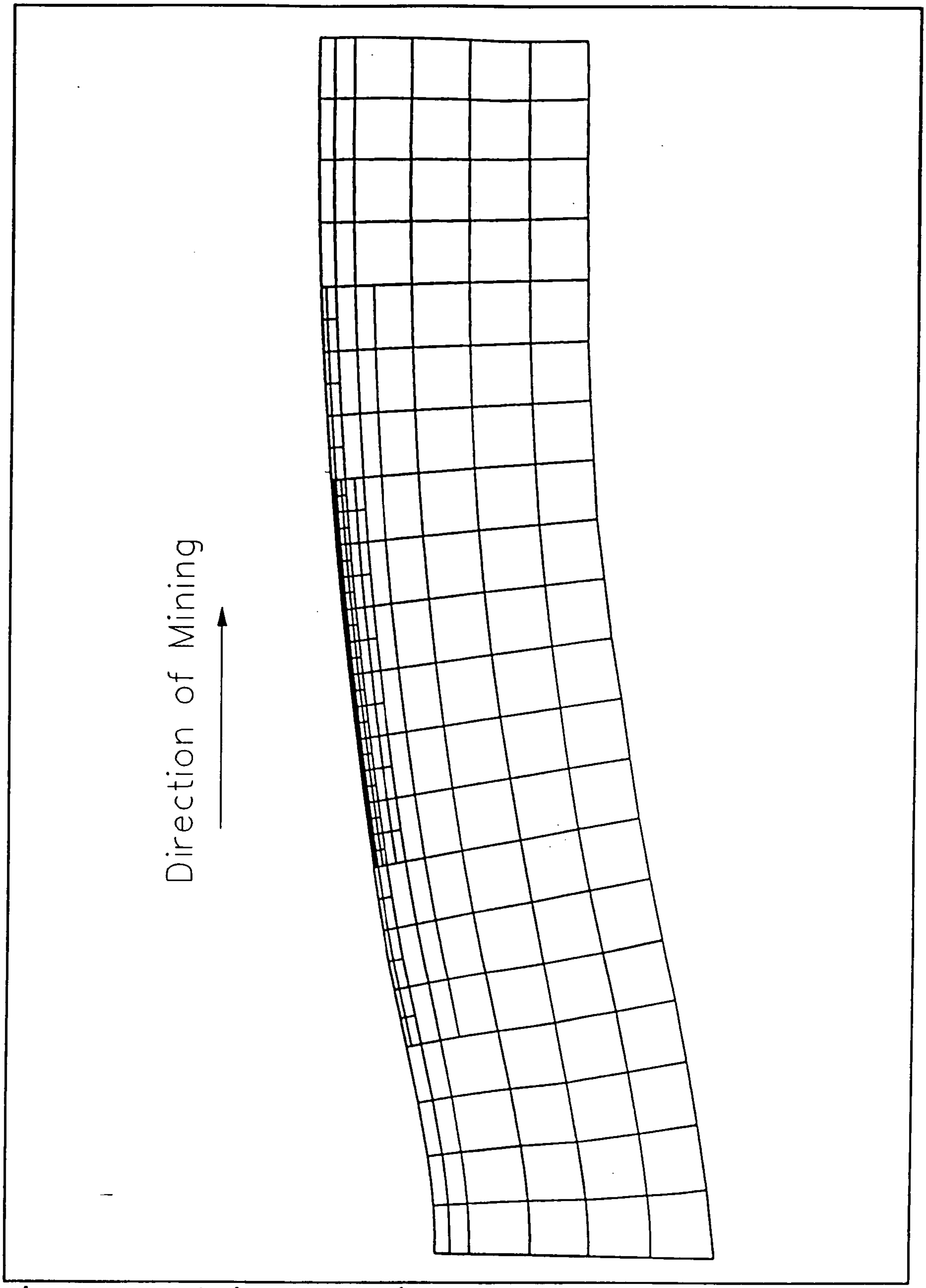

Figure 4.3 Subsidence Profile (mag X 8)

therefore may cause some margin of error. In addition, soil disturbance was created upon the installation of the gages. With these sources of error in mind, the comparison of the FE analysis and bison gages proved to be adequate. The Cam-Clay soil modeling is only an approximation of soil behavior due to limitations in the model.

The effect of non-linear geometry was tested by using a finite strain analysis. No significant difference was observed between the finite strain and small strain free field analysis.

In conclusion, Lawrence (1992) recommends using the Cam-Clay model for the plasticity modeling of soil along with his suggested material parameters. It is suggested that the Cam-Clay modeling be used at the top of the soil mesh and only a linear elastic model be used at the bottom of the mesh.

4.2 Foundation Analysis

4.2.1 Foundation/Soil Modeling

The foundation analysis is conducted by simulating the subsidence event that occurred in the centerline of the West Frankfort Project. This was first achieved by incorporating the foundation modeling performed in Chapter 3 within the top center of Lawrence's (1992) soil finite element mesh. The footing is placed in the top two layers, Figure 4.4. Out of

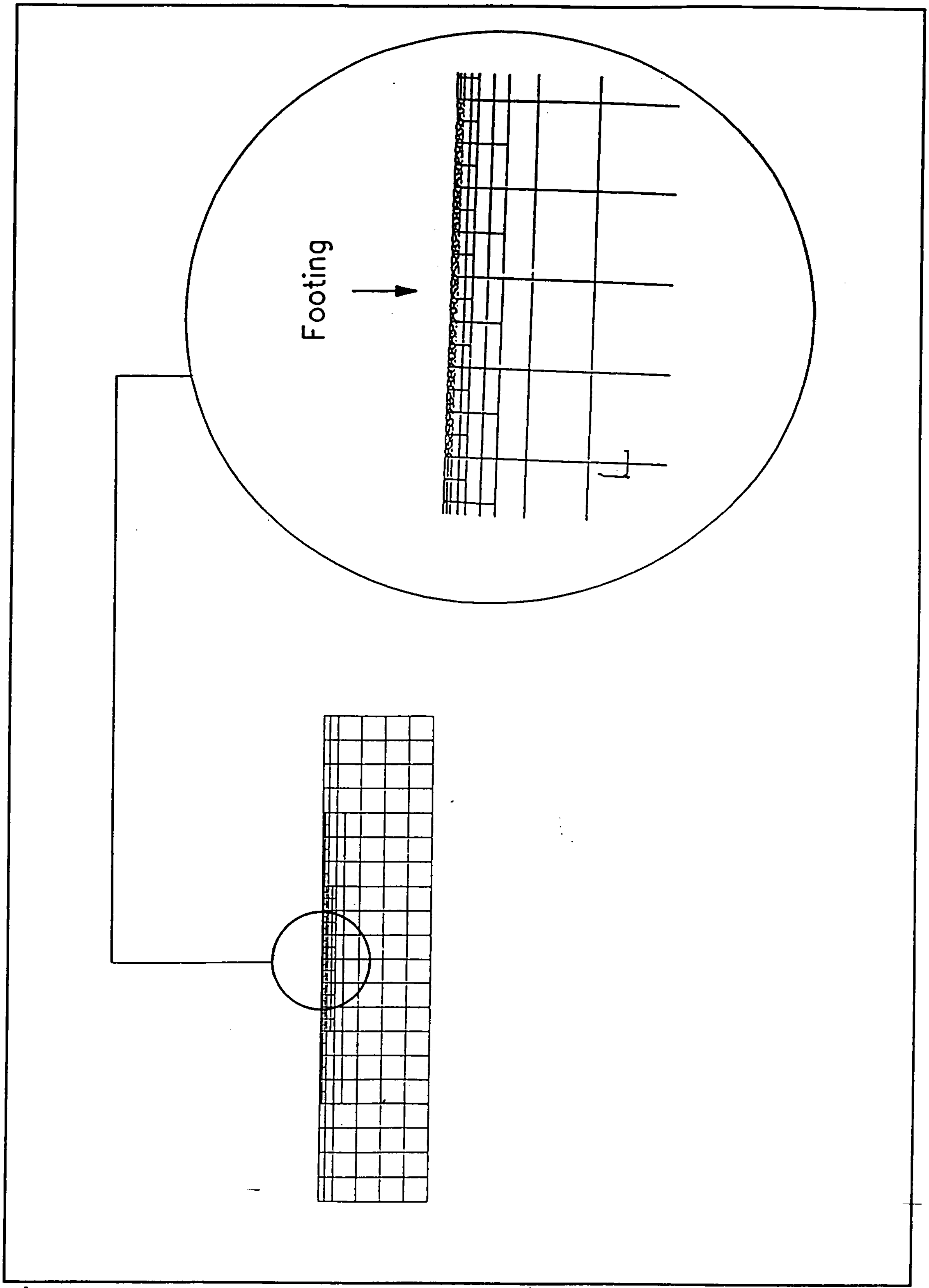

Figure 4.4 Placement of Footing Within the Soil Mesh

plane movements are not considered in these analyses. The same boundary conditions used in Lawrence's (1992) free field analysis were used for the foundation analyses.

Since the type of loading associated with this subsidence event is unique, the PTOL parameter was investigated with values ranging from 1.0 to 0.1. ABAQUS supplied appropriate results with a value of 0.5; therefore, it was used for all analyses.

Five different types of analyses were performed to give appropriate indications of foundation response, Table 4.1. The elastic footing was used to give some indication of an elastic response without cracking effects in the footing. This would simulate a post-tensioned footing. Two other analyses using inelastic concrete behavior, one without and the other with reinforcing bars, were performed to give an

Table 4.1 Summary of Analyses Performed

Footing Type	Masonry Wall Type
Reinforced Concrete Footing 2 #4 bars top and bottom (Control Analysis)	None
Elastic Footing	None
Plain Concrete Footing	None
Reinforced Concrete Footing 2 #4 bars top and bottom	Elastic Properties
Reinforced Concrete Footing 2 #4 bars top and bottom	Inelastic Properties

inelastic response of the footing. Since the effect of reinforcing placed in the footing is of primary concern, the reinforced footing was used as the control analysis. The reinforcing used was the same amount as used in the field. The last two analyses involved the addition of a masonry wall to the reinforced concrete footing. They were performed to show the behavior of the composite masonry wall and footing. One masonry wall used only linear elastic properties while the other used the inelastic and strength limit properties associated with the masonry. The linear elastic masonry wall was used to give a complete composite action while the plain masonry will involve cracking thereby diminishing the stiffness of the section.

The plasticity soil modeling used by Lawrence (1992) in the free field analysis did not produce sufficient stresses and strains to cause any cracking or damage to the foundation in the reinforced footing analysis. The plasticity soil model produced a "softness" behavior during analysis. The footing experienced a large settlement of 6.5 cm under the surcharge loading causing the soil to deform greatly. The footing acted as a rigid body "floating" within the soil model during the analysis which allowed the footing to experience only about one third of the cracking stress.

Since the plasticity model suggested by Lawrence (1992) did not achieve sufficient results in the reinforced footing analysis, the plasticity soil modeling was abandoned and a linear elastic soil model was used for all analyses. The linear elastic soil modeling did induce significant stresses and strains in all analyses to cause damage; however, the linear elastic soil will not give the effects of the plastic deformations produced in the soil from subsidence.

Interface elements were used between the footing and soil with interface properties determined in chapter 3. The behavior of contact pressure at the interface used the default behavior provided by the interface elements. This phenomenon is illustrated in Chapter 3. Due to ABAQUS's capabilities of interface modeling, gapping at the interface was only allowed in the global Y direction and the transfer of shear stresses and sliding effects in the global X direction. The effects of interface rotation in global space during the analysis is assumed not to be a factor because of the small angle of rotation that occurred in the field. No interface was provided at the ends of the footing because only gapping and not shear transfer occurs at this location.

4.2.2 Analysis Procedure

Before a subsidence event was employed in all analyses, the soil was placed in a geostatic stress state due to the effects gravity present in the field. In addition, a uniform surcharge was then applied to the foundation to obtain the bearing pressure that was applied in the field. After these initial steps were completed, subsequent steps involved subjecting the foundation to the center line subsidence wave. This was achieved by applying the same displacements to the bottom of the soil mesh that were used in Lawrence's (1992) free field analysis.

The full wave was used for the control analysis of reinforced concrete footing. The footing was stepped along the full wave in 3 m increments. Since applying the full wave required long computational time, a reduced subsidence event was created to reduce computing time for other analyses. This was achieved by using only a portion of the wave to capture only the peak stages during the tension and compression phases.

The first step of the reduced subsidence wave began by placing appropriate displacements to the bottom of the mesh causing immediate subsidence to occur along the surface of the entire mesh. This immediate subsidence corresponds to placing the leading edge of the mesh 75 m along the wave in one step. From this position the mesh was moved along the wave in 3 m steps allowing the foundation in the center of the mesh to experience the peak stages of both the tension and compression phases. The subsidence event was terminated when the mesh reached a position of 174 m along the wave. Analysis was repeated for the reinforced concrete footing using the reduced subsidence event. The results produced from the reduced subsidence event were the same as applying the full wave;

therefore, analyses can be achieved by using the reduced subsidence event.

The reduced subsidence event was used for all analyses except with the analysis using the inelastic masonry modeling. Termination of this analysis was encountered from convergence problems occurring during the end of the tension phase. To overcome this problem, the compression phase of this analysis was simulated by starting the subsidence event over at 114 m along the subsidence wave. Before restarting the analysis at this position, the modified masonry mesh used in the tension phase was replaced with the continuum mesh since the masonry wall primarily experiences compressive stresses during the compression phase. The wave was then introduced in 3 m increments until reaching the same ending position as the other analyses.

4.2.3 Tension Phase Results

Before the reinforced footing was subjected to the effects of subsidence, the application of the surcharge load produced an initial settlement of 6.5 mm. This resulted in an uniform distribution of pressure of about 35 kPa transmitted throughout most of the interface; however, some stress concentrations formed at the bottom corners of the footing. The surcharge caused the reinforced footing to experience 15% of its cracking limit thereby producing insignificant tensile effects at the beginning of analysis. All other analyses produced virtually the same settlement and distribution of stresses at the interface from the applied surcharge.

The start of the tension phase was produced first as the reduced subsidence event was initiated. Concave curvature is produced in the ground during the tension phase causing tensile stresses to develop in the top of a foundation. The maximum tension produced in the reinforced footing during the tension phase occurred 4.5 m from the leading edge of the footing. The distribution of the stresses at this location is shown in Figure 4.5. The maximum tensile stress at an integration point was 4.0 MPa near the top which is less than the cracking limit of 4.25 MPa. Integration points are not located at the extreme fibers of the footing. Due to the crack detection mechanism of ABAQUS's concrete modeling, no crack predictions were given to the reinforced footing during the tension phase of its analysis. However, contour lines produced by ABAQUS's post processing capabilities showed that the maximum stress at the extreme fibers of the reinforced footing was estimated at 4.4 MPa. These contour lines are produced by a weighted distribution of stresses and strains. The possibly of a crack formation occurring at the extreme fibers of the footing is also suggested from the linear extension of stress distribution in Figure 4.5. The maximum tensile stress induced in the reinforcing is 13.2 Mpa which is far below the its yield stress.

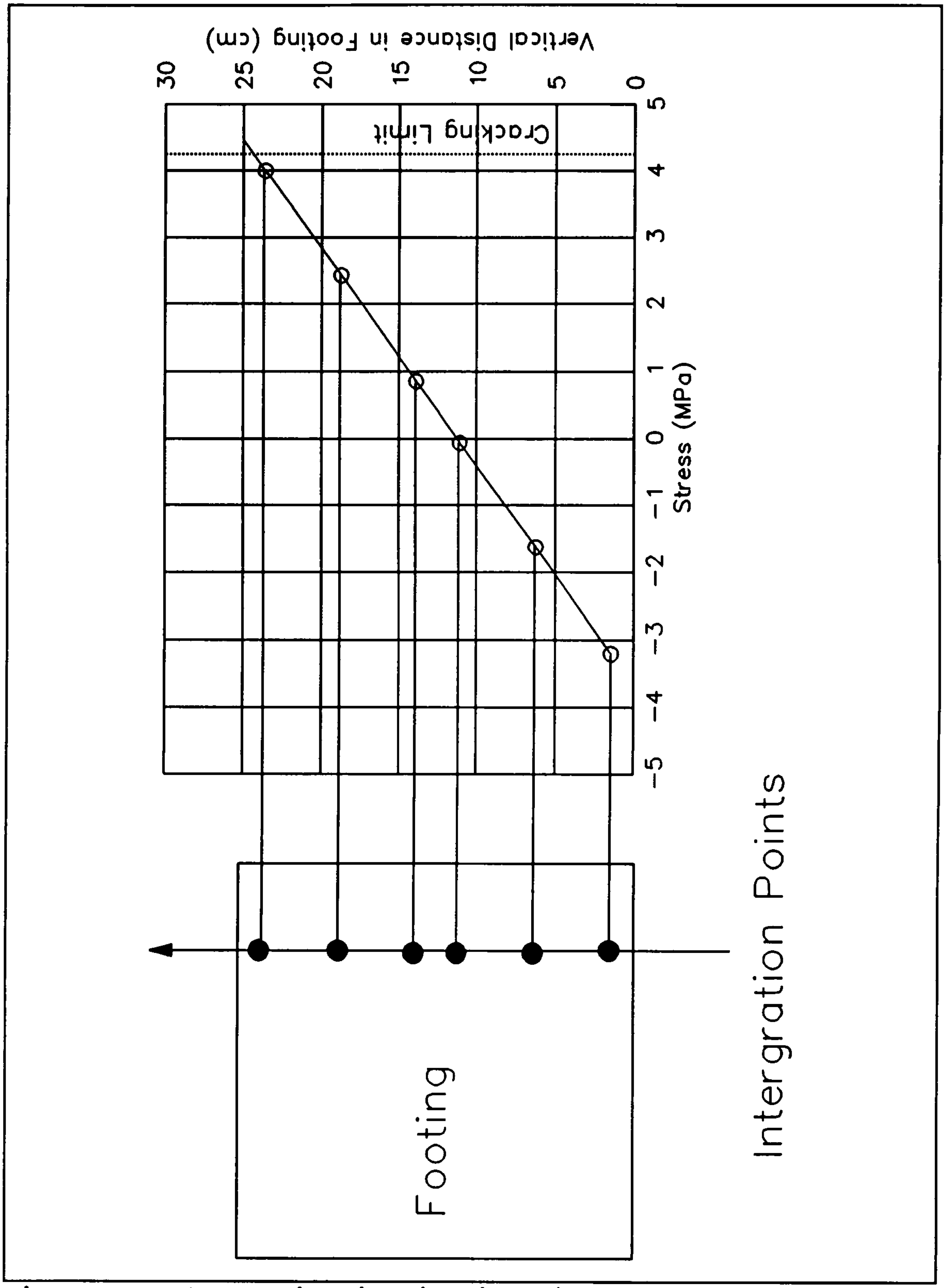

Figure 4.5 Stress Distribution in Reinforced Concrete Footing at Peak Stage of Tension Phase

Results of the other foundation models subjected to the tension phase are compared to the reinforced concrete footing in Table 4.2 in terms of location and amount of maximum tensile stress produced. The stresses produced in the elastic and plain concrete footings are similar to the reinforced concrete footing. This suggests that the concrete footing behaved in a linear fashion in the tension phase.

Table 4.2 Maximum Amount and Location of Tensile Stresses of the Tension Phase Analyses

Analysis		Distance from Leading edge (m)	Tensile Stress (MPa)
Reinforced Footing		4.5	4.0
Elastic Footing		4.5	4.0
Plain Concrete Footing		4.5	4.0
Reinforced Footing with Elastic Masonry Wall	Footing	6	.20
	Wall	6	1.85
Reinforced Footing with Inelastic Masonry Wall (modified)	Footing	3.75	4.25 (crack)
	Wall	3.75	.350 (crack)

The addition of the masonry wall produced significant changes in the behavior of foundation response. The stresses produced in the reinforced footing with elastic masonry were quite low because the elastic properties given to masonry allowed the masonry wall to take most of the tensile stresses. The location and as well as the amount of tensile stresses was dramatically affected by the addition of the elastic masonry wall.

The analysis with reinforced footing and inelastic masonry wall was attempted by using the continuum masonry model; however, severe cracking occurred in the masonry wall during early stages of the tension phase. The analysis could not continue because of convergence problems associated with this cracking; henceforth, the footing did not experience the peak stages of the tension phase. To overcome convergence problems from masonry cracking, the continuum mesh was replaced by the modified masonry mesh. The analysis was started over at the beginning of the reduced subsidence event. The placement of the interface elements within the middle of the modified masonry mesh was assumed satisfactory since the elastic masonry model experienced maximum tension in this area. The modified inelastic masonry modeling was sufficient to allow the analysis to continue through the peak stages of the tension phase without convergence problems. The same step that produced initial cracking in the original continuum inelastic masonry mesh produced initial cracking and gapping within the modified masonry mesh. After gapping and cracking occurred within the modified masonry mesh, the footing took the tensile stresses produced during the tension phase. Unlike the other analyses, a crack formation occurred in the reinforced footing as its cracking limit was reached at a integration point. The locations of initial cracking produced in the reinforced footing with the modified masonry wall are given in Table 4.2. The cracking produced in the footing during the tension phase of this analysis shows that the masonry construction affects the footing response during subsidence. Furthermore, an inelastic masonry wall has a different affect on the response of the footing than the elastic masonry model.

The strains induced in the foundations are used to calculate curvature. Curvature values were computed using a plane distribution of strains from one integration point to the next. The distribution of strains at the section of maximum curvature for the reinforced footing are shown in Figure 4.6. This figure shows that the section remained plane during the tension phase analysis. The values of curvature along the reinforced footing's length during the peak tension phase step are shown in Figure 4.7. This figure shows that curvature values are predominately higher in the middle of the footing. The value of maximum curvature produced from the reinforced concrete footing analysis is -.00076 rad/m which is located at the point of maximum tensile stress. This value is below the theoretical cracking curvature of -.0008 rad/m. Since the maximum value of curvature produced in the reinforced footing is slightly smaller than the theoretical cracking limit, cracking would not be expected to form in the footing during this phase of analysis. The maximum curvature for all of the analyses is given in Table 4.3. The elastic

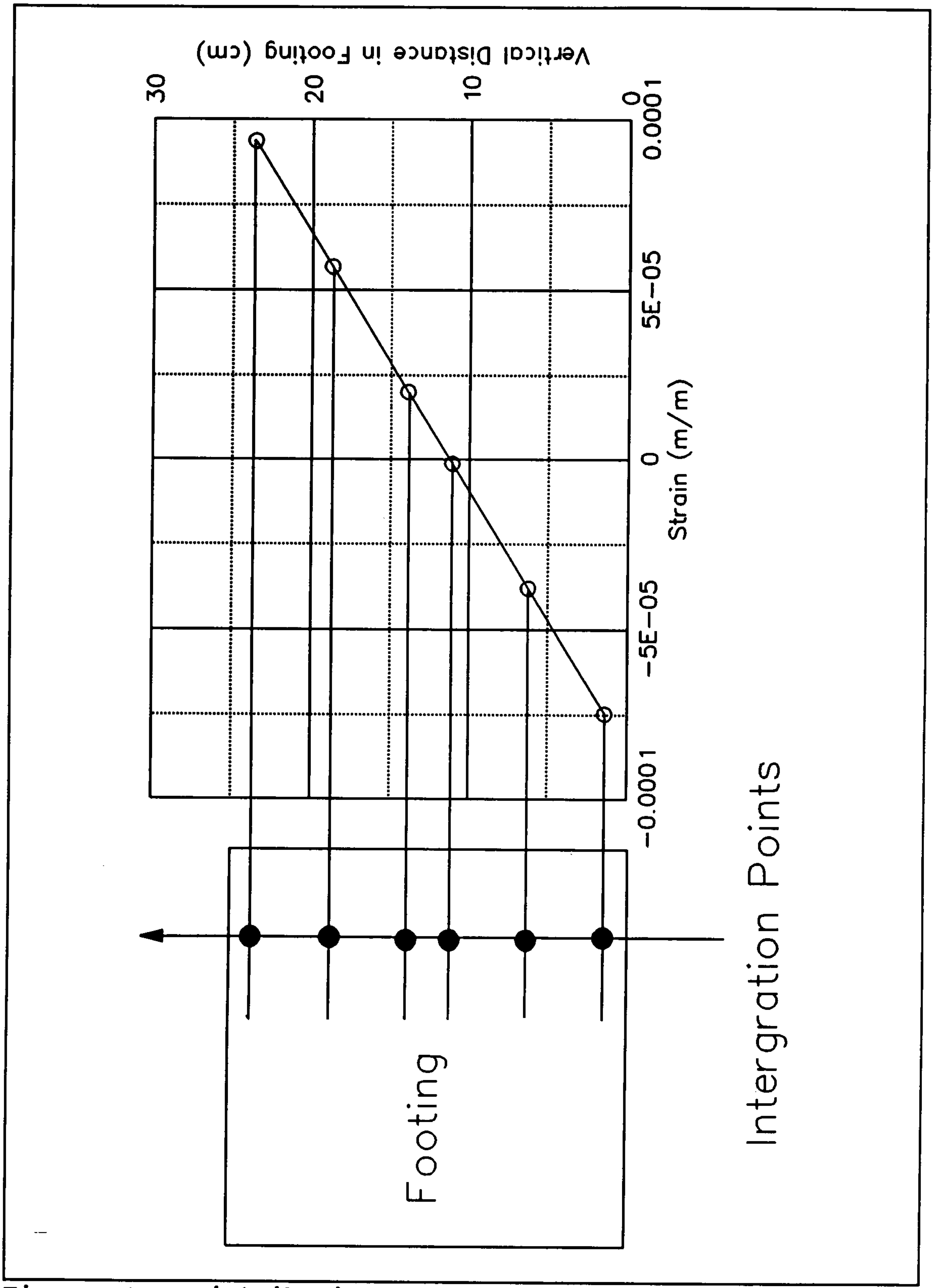

Figure 4.6 Distribution of Strains at Point of Maximum Curvature Within the Reinforced Concrete Footing

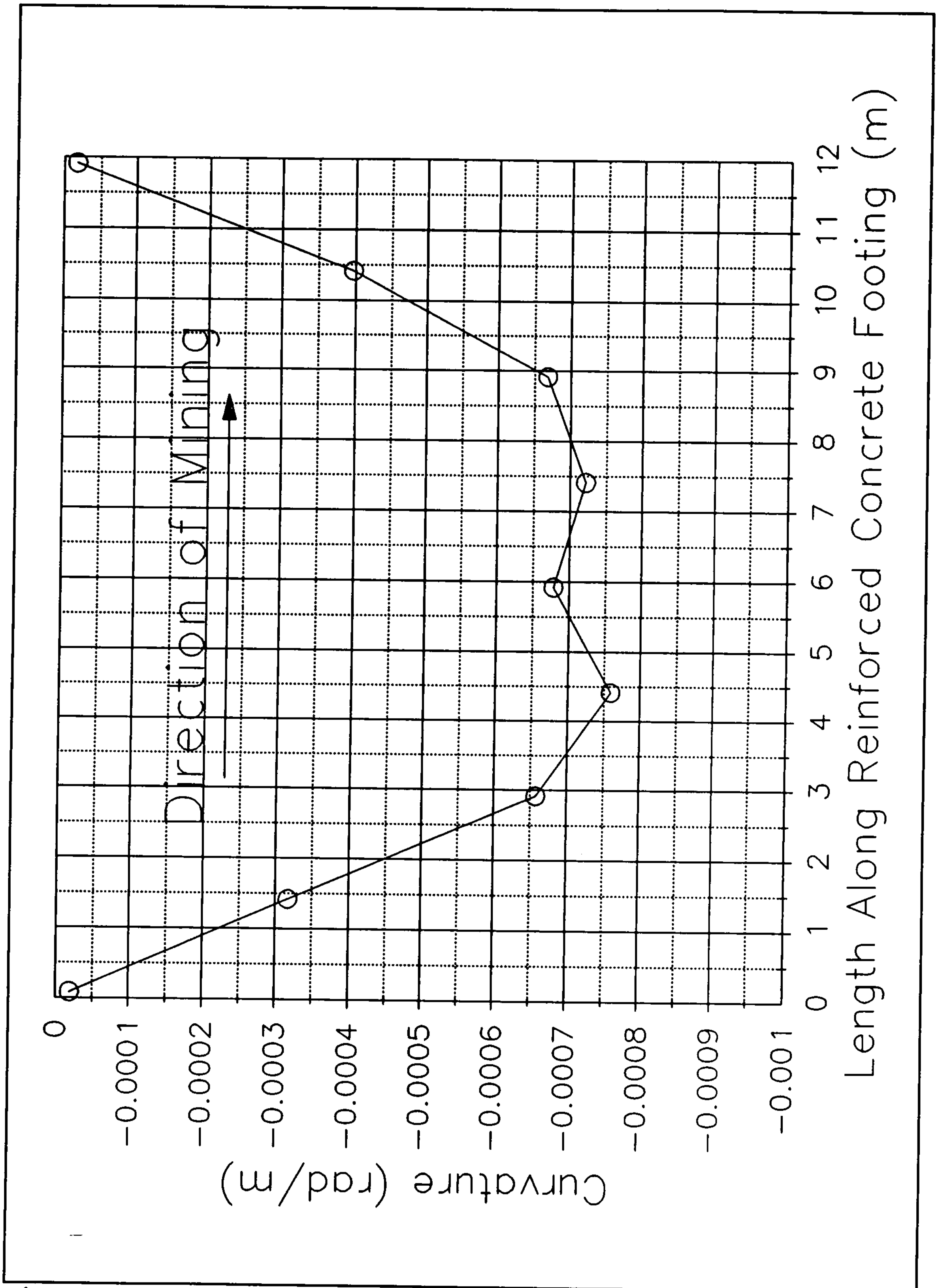

Figure 4.7 Curvature Along the Reinforced Concrete Footing's Length at the Peak Tension Phase Step

Table 4.3 Maximum Curvature Values in the Footings for Tension Phase Analyses

Analyses	Curvature (rad/m)
Reinforced Footing	-.00076
Elastic Footing	-.00076
Plain Concrete Footing	-.00076
Reinforced Footing Elastic Masonry Wall	-.00021
Reinforced Footing Non-linear Masonry Wall (modified)	-.00085

and plain concrete footing analyses produced the same maximum curvatures as the reinforced footing. This also suggests that the concrete behaved in a linear fashion.

The addition of the masonry wall showed a different response in curvature produced in the reinforced footing. The reinforced footing and elastic masonry wall resulted in a much smaller curvature. The distribution of strains at the peak stage in the tension phase is shown in Figure 4.8 for the combined section. This composite section remains plane. Due to the large increase in stiffness, the structure is essentially responding as a rigid body. The modified inelastic masonry wall caused more curvature to be induced in the foundation. This could be contributed to a diminished stiffness produced from the cracking induced in both the masonry wall and footing. This should be expected since the masonry wall is not designed to handle the large tensile

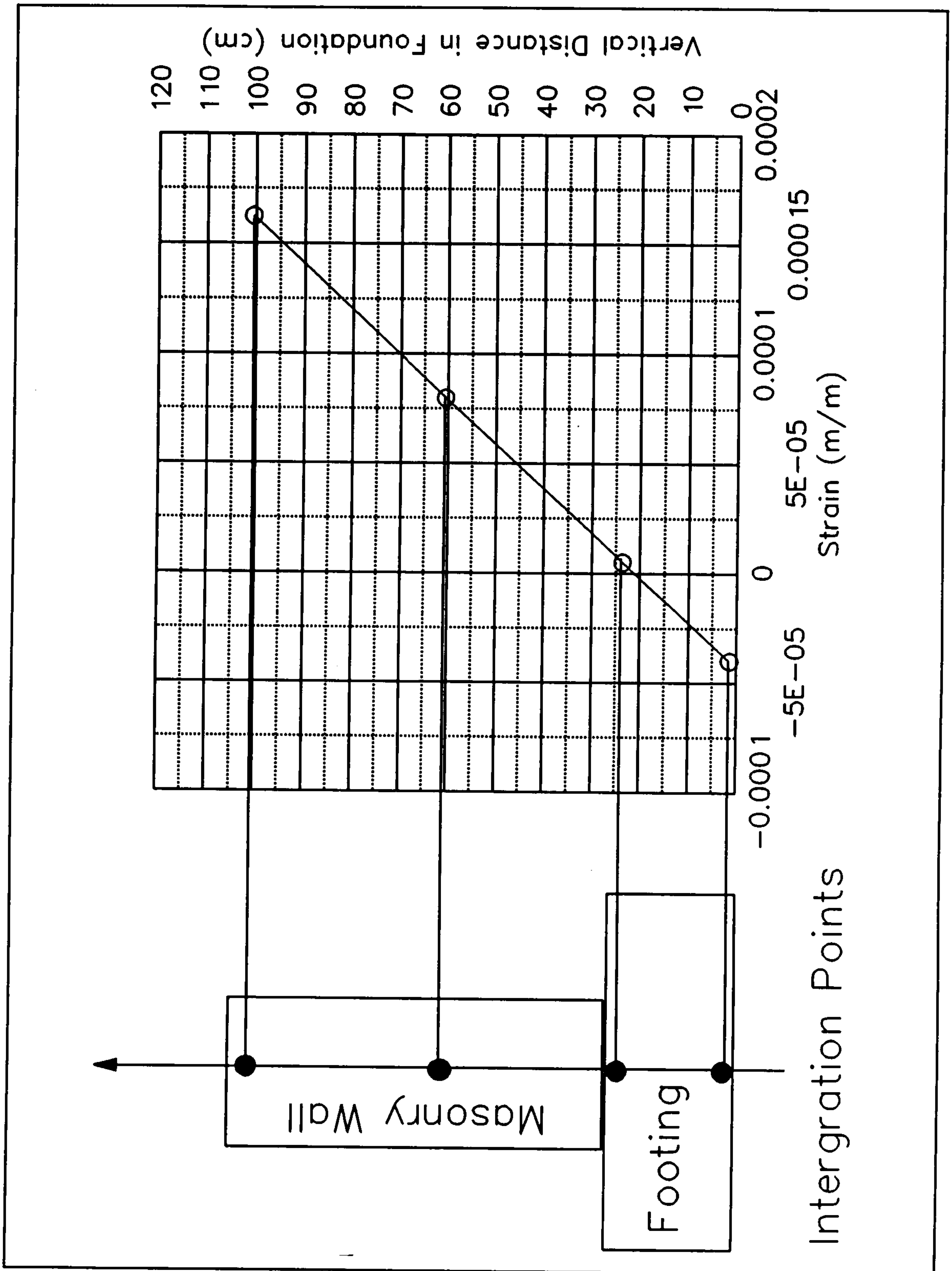

Figure 4.8 Strain Distribution for the Elastic Masonry Wall and Reinforced Concrete Footing Composite Section During the Tension Phase

stresses that were produced during the tension phase of subsidence.

The interface response between the footing and soil was primarily the same for all analyses. Sliding occurred at the interface. The soil behaved in an "expanding" fashion underneath the footings. The soil seemed to "expand" from the center of the footing toward both ends of the footing. This "expanding" phenomenon is illustrated in Figure 4.9. From Figure 4.9 it can seen that gapping only occurred at the ends where no interface was provided. The soil moved a maximum of 3.2 cm horizontally away from the corners of the footing.

The transmission of shear stresses at the interface did not produce lengthening of the reinforced concrete footing. The total horizontal strain produced in the bottom of the footing was -.0000602 m/m, and .000072 m/m in the top of the footing. These strains are caused primarily from the bending effects of the tension phase producing tensile strains in the top and compressive strains in the bottom of the footing. All other analyses responded in the same fashion as the reinforced concrete footing.

4.2.4 Compression Phase Results

As the subsidence event progressed out of the tension phase, the stress and strain state of the foundation was reduced as it experienced primarily tilting during a brief

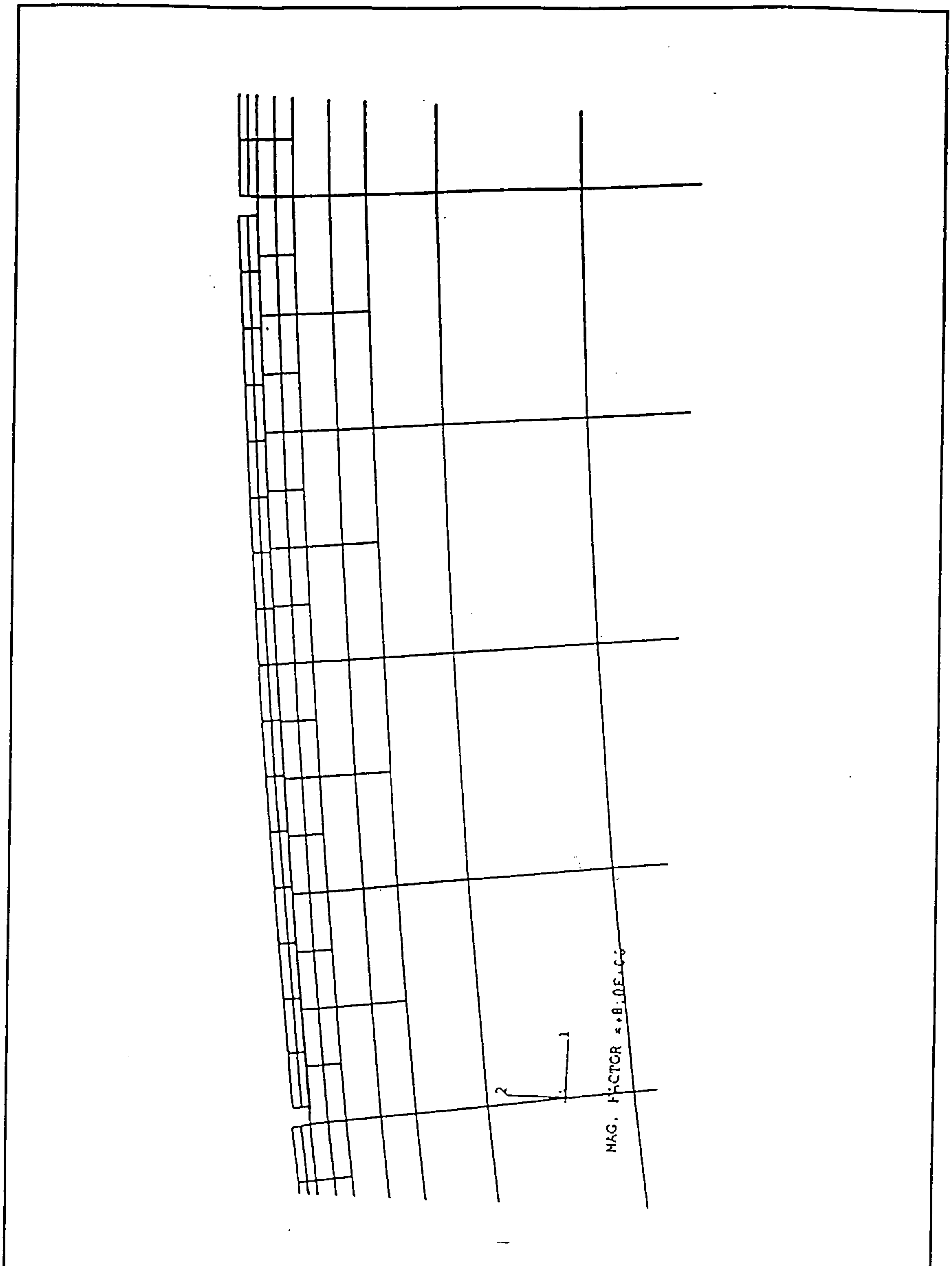

Figure 4.9 Soil Behavior Beneath Footing in Tension Phase

transition state. After experiencing this transition stage, the foundations were introduced to the compression phase of the subsidence event, Figure 4.10. The compression phase of the subsidence event caused a concave soil profile thereby producing tension in the bottom of the foundation and compression in the top of the foundation.

The reinforced concrete footing model exhibited cracks during the compression phase. ABAQUS's crack detection mechanism predicted that cracking initially formed 3.75 m from the leading edge of the footing. Due to ABAQUS's "smear" cracking effect, several cracks formed in this region. As the analysis continued, the cracking region progressed from the leading edge to the middle of the footing and finally terminated at 3.0 m from the trailing edge. The steel in the reinforced footing reached a tensile stress of only 15.0 MPa during this phase.

The plain concrete footing experienced the same initial cracking and subsequent distribution of cracks as the reinforced concrete footing. Since the elastic footing did not crack, maximum tensile stress location and value were recorded, Table 4.4. The location and value of this maximum stress are given with the prediction of initial cracking for other analyses during the compression phase. Since the cracking stress was exceeded in the elastic footing, cracking that occurred within the reinforced and plain concrete footings is justified.

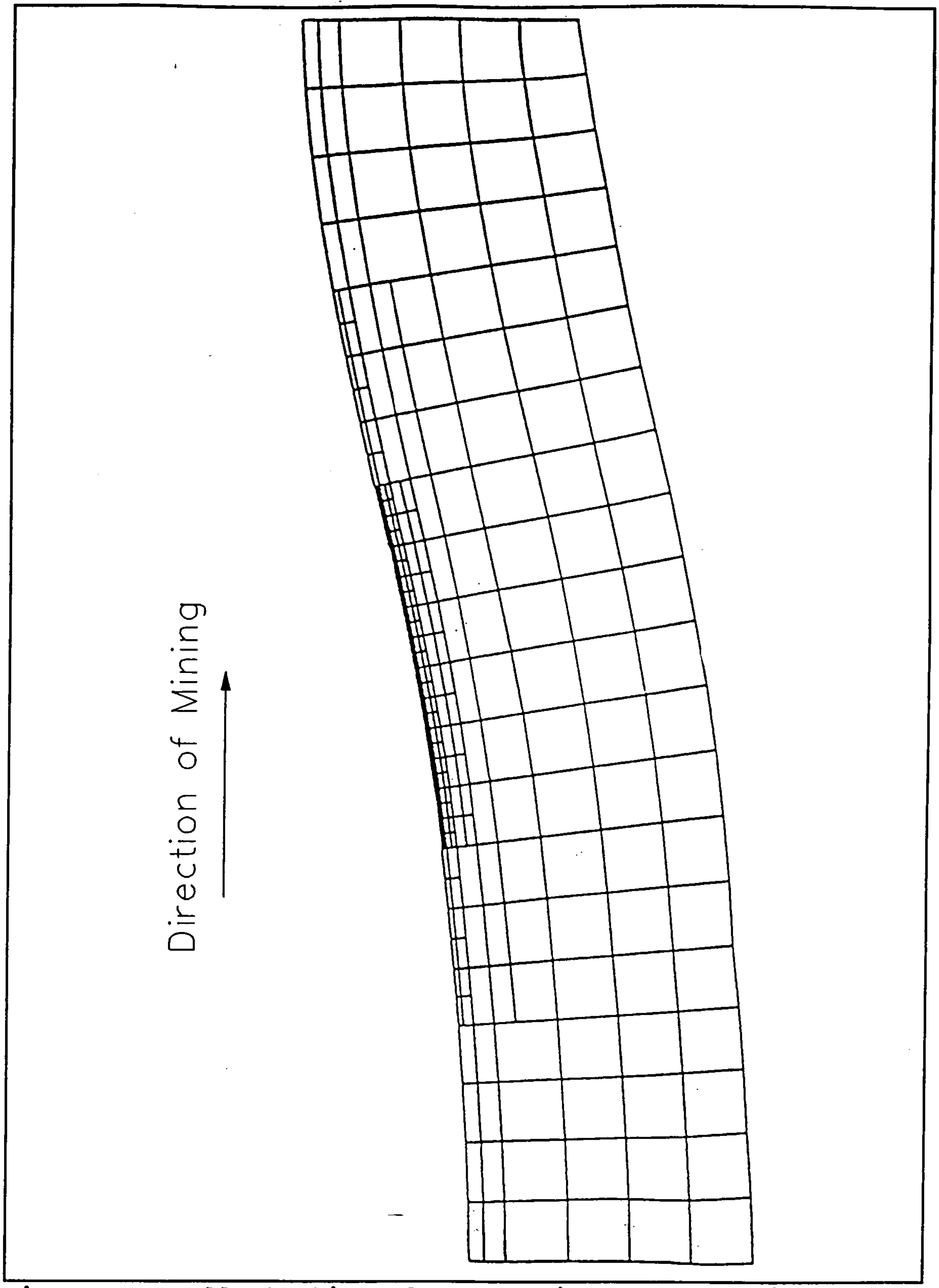

Figure 4.10 Illustration of Compression Phase Profile (mag X 8)

Table 4.4 Location of Initial Cracking and Maximum Tensile Stress During Compression Phase Analyses

Analysis		Location from Leading Edge (m)	Maximum Tensile Stress (MPa)
Reinforced Footing		3.75	4.25 (crack)
Elastic Footing		3.75	4.65
Plain Concrete Footing		3.75	4.25 (crack)
Reinforced Footing Elastic Masonry Wall	Footing	6.0	4.25 (crack)
	Wall	-	-
Reinforced Footing Inelastic Masonry Wall	Footing	6.0	4.25 (crack)
	Wall	-	-

The cracking behavior in the reinforced concrete footing in the compression phase was not effected by the addition of the elastic masonry wall. The reinforced footing experienced the same cracking pattern with or without the elastic masonry wall model.

Analysis termination of the reinforced footing with the modified inelastic masonry occurred at the end of the tension phase due to convergence difficulties. In order to allow this analysis to experience the effects of the compression phase, the analysis was started over. The modified masonry model was replaced with the continuum mesh, since the masonry experiences primarily compressive strains during the compression phase. The tension phase was skipped by initiating the subsidence event at 114 m along the subsidence wave. The cracking that would have been formed in the foundation during the tension phase is not present in this phase; however, this should not the effect the behavior of the masonry wall since it is in a state of compression during this phase. The foundation was then stepped along the wave at the 3 m increments until reaching the termination point of the original reduced subsidence event. The compression phase of the analysis produced the same cracking effects as in the reinforced footing with elastic masonry wall model. Since the addition of both masonry wall models produced cracking behavior in the footing, the masonry wall does not alleviate the cracking that the footing will experience during the compression stage.

Maximum curvature values are calculated at a vertical section of the foundation where the maximum strain distribution exists between integration points. This usually occurs at a section where cracks have been predicted. The distribution of curvature along the reinforced footing length is shown in Figure 4.11 for the peak stage of the compression phase. The higher curvature values lie within the middle of the footing. The reinforced footing's maximum curvature is given in Table 4.5 along with maximum curvature for the compression phase from other analyses.

The elastic footing and plain concrete footing both exhibited virtually the same curvatures as the reinforced footing. Since these values are so close, the amount of

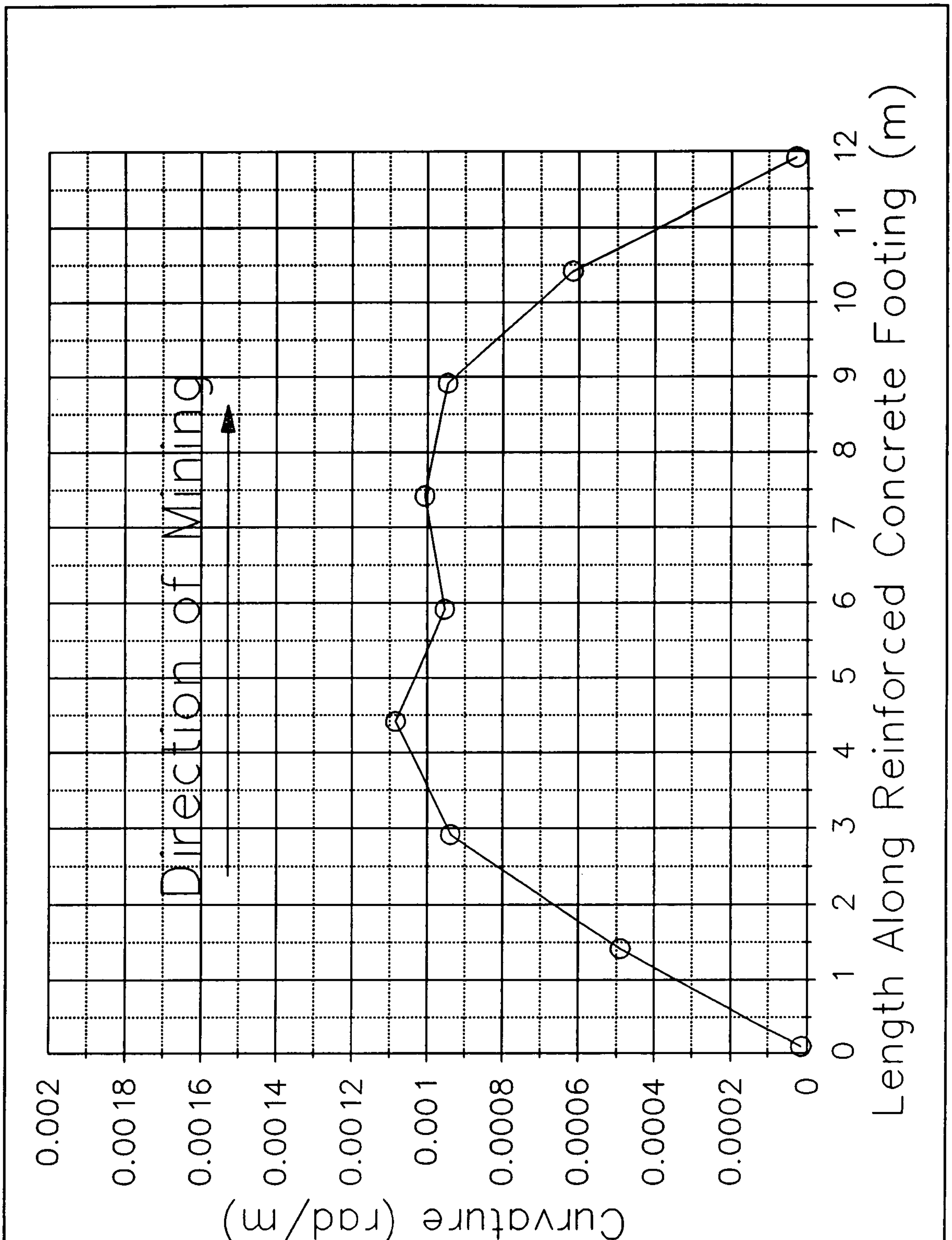

Figure 4.11 Curvature Along the Reinforced Concrete Footing's Length at the Peak Compression Stage

Table 4.5 Maximum Curvature Values during Compression Phase Analyses

Analysis	Maximum Curvature (rad/m)
Reinforced Footing	.00108
Elastic Footing	.00106
Plain Concrete Footing	.00110
Reinforced Footing Elastic Masonry Wall	.000489
Reinforced Footing Inelastic Masonry Wall	.000564

curvature produced by subsidence is not effected by the application of rebars. However, the reinforcing will extend the curvature capacity of the footing after cracking occurs.

The addition of the masonry walls did affect the curvatures produced in the reinforced footing. The elastic masonry provided a slightly more rigid response than the inelastic masonry wall. The wall additions caused the curvature response during the compression phase to be cut by one-half. Unlike the other analyses, the reinforced footing with inelastic masonry modeling experienced lower curvatures during the compression phase than during the tension phase. This behavior is attributed to the large cracks or openings that were present in the modified masonry mesh during the tension phase. These openings allowed larger strains to be induced within the foundation whereas continuum masonry wall was beneficial by adding compression stiffness in the compression phase. Due to this behavior, conventional masonry wall construction is not beneficial when subjected to tensile forces; however, the masonry wall is very beneficial in reducing curvature when it is in a state of compression.

The interface in all analyses showed that the soil slid back or "contracted" to a state of compression. This is illustrated in Figure 4.12. There was sliding at the interface. The soil slid inward toward the middle of the footing in all analyses. The gapping at the ends of the footings closed completely. The overlapping of the soil mesh into the footing mesh at the end was caused because no interface was provided at this location. The amount of overlap is exaggerated in Figure 4.12 since the displacements are magnified by a factor of 8.0. A preliminary analysis that had provided an interface at the ends proved to cause an extreme amount of axial force to occur in the footing during the compression phase. This was due to the elastic soil model not failing at the ends thereby causing too much axial force to be transferred into the footing. Since shear transfer is of primary concern and not axial force transfer, the overlapping of the soil and footing should not be of concern.

The total horizontal strains produced in the reinforced footing analysis are .0000833 m/m and -.0001 m/m in the bottom and top respectively. These strains are consistent with tension being applied in the bottom and compression in the top. All other analyses resulted this same type of behavior.

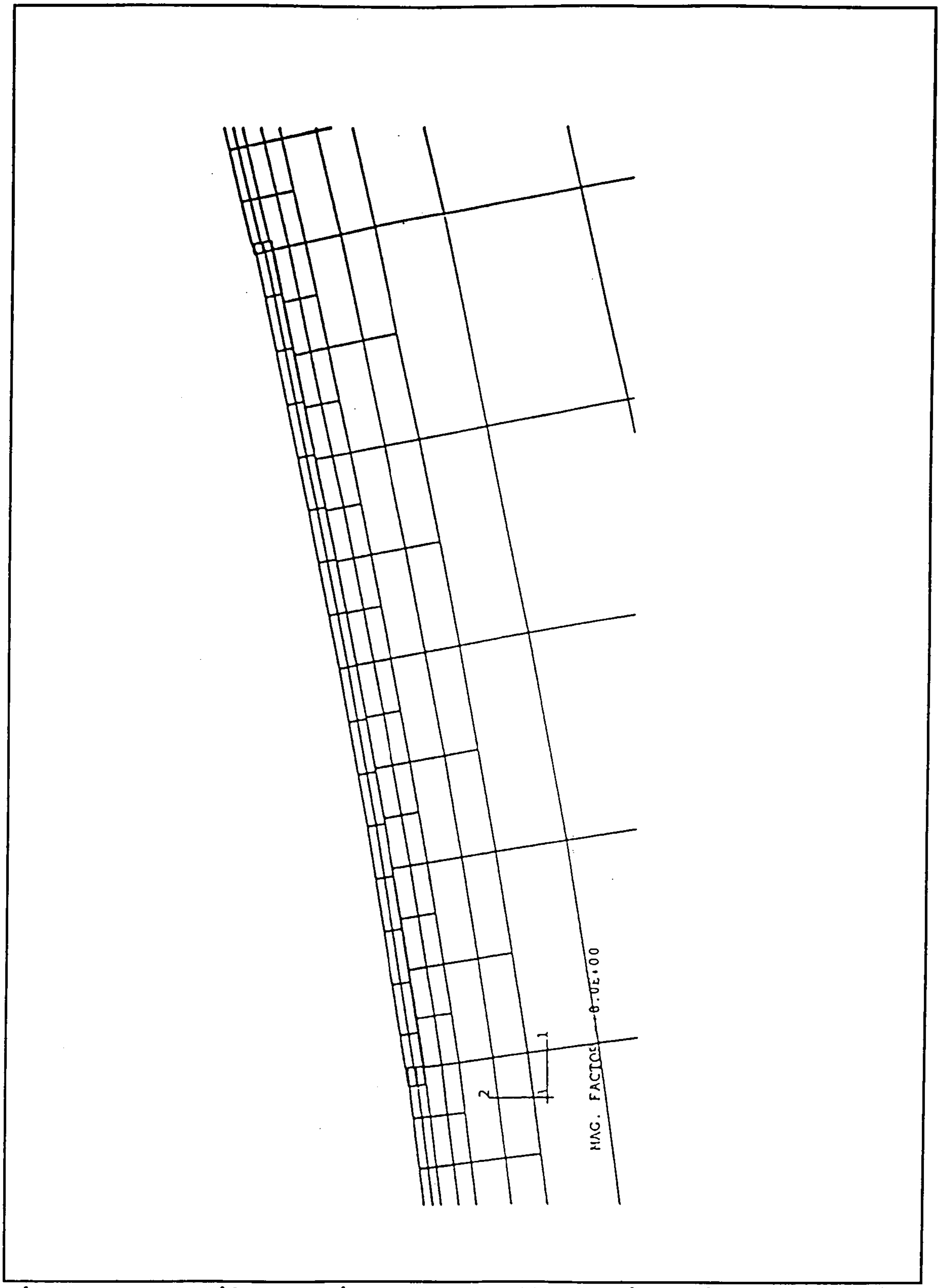

Figure 4.12 Soil Behavior Underneath Footings in Compression Phase Analyses (mag X 8)

4.3 Foundation Analysis Discussion

The application of the reduced subsidence event was successful in reducing computational time of analyses. The elimination of the first 75 m of the subsidence wave had no affect of changing the amount of damage produced in the tension and compression phases. In addition, the elimination of the relation phase at the end of the wave was valid since this phase did not contributed in causing damage. All analyses were successful in using the reduced subsidence event except for the analysis with inelastic masonry modeling. Problems were encountered from limitations of the masonry modeling. If modeling of the mortar joint behavior in the masonry could be refined, perhaps the entire analysis can be achieve with the reduced subsidence event.

The compression phase of analyses represented the highest amount of damage inflicted to the footings. A great amount of cracking was predicted in the footings during the compression phase. Higher curvatures were also present in analyses without masonry construction during the compression phase. This type of behavior was also noticed by Hudging's (1989) numerical analyses. However, the tension phase was most detrimental in causing cracking in the inelastic masonry wall. This was also noticed in field observations.

Crack locations and maximum curvatures predicted in the analyses were not consistent to field observations. Due to ABAQUS's cracking capabilities of its concrete model, one distinctive crack did not form in the analyses as did in the field. The numerical analyses suggests that cracks would form at the leading one third of the foundation whereas the field results produced cracking at the trailing one third of the foundation. However, looking at the curvature plotted along the length of the reinforced concrete footing during the tension phase in Figure 4.7 shows a second concentration of curvature occurring near the trailing one third point of the footing. The numerical modeled foundations may have responded differently to this second concentration if a plasticity soil model was used during analyses. In addition, the interface provided may not have fully captured soil-structure interaction due to the limitations of the interface modeling.

The addition of the masonry walls affected the cracking and curvature behavior of the reinforced concrete footing. The linear elastic and inelastic modeling used for the masonry produced two different behaviors during the tension phase. The elastic masonry wall increased the stiffness of the reinforced footing during the tension phase whereas the inelastic masonry (modified) failed thereby forcing the reinforced footing to take the tensile stresses. These tensile stresses produced cracking in the footing whereas no cracking occurred in the footing for other analyses. If the masonry wall could take higher tensile stresses by increasing its stiffness such as the linear elastic model, the masonry wall would contribute to reducing curvature during the tension phase. Both masonry models virtually behaved the same during the compression phase. The addition of both walls did not reduce cracking of the footing during the compression phase. However, more importantly is that curvature values were reduced in footing during the compression phase with the masonry walls. This in turn would cause less curvature to be inflicted in the superstructure where damage is of primary concern.

The response at the interface was the same for all analyses. The strains induced in the footings in all analyses suggest that primarily bending stresses and not horizontal stresses transmitted at the interface occurred within the footing. This behavior was also noticed by numerical analyses performed by Hudgings (1989).

CHAPTER 5

PARAMETRIC ANALYSIS

5.1 Introduction

A parametric study was conducted to evaluate the effects of changing or modifying parameters within the interface and foundation modeling. Six different studies are performed, Table 5.1. Each study without inelastic modeling used the reduced subsidence event to capture only the peak steps of the tension and compression phases. Studies using inelastic masonry modeling used the same two part subsidence event used in Chapter 4. The same house loading scheme is used in these studies. The results of each study are compared to appropriate analyses performed in Chapter 4.

5.2 Various Rebar Amounts

5.2.1 Footing Without Masonry Wall

The reinforced footing constructed in the field contained two #4 reinforcing bars in the top and bottom of the footing. This investigation analyzes the effects of increasing the amount of reinforcing placed within the footing without any

Table 5.1 Parametric Studies

1	Increasing amounts of reinforcing in reinforced concrete footing
2	Deleting bottom row of reinforcing
3	Increasing depth of reinforced concrete footing
4	Decreasing friction angle at interface
5	Addition of bond beam in Inelastic Masonry Wall
6	Addition of concrete wall to reinforced concrete footing

masonry construction. This is accomplished by replacing the #4 rebars with #5, #6, and #8 rebars within the footing. Two bars will be placed in both the top and bottom as the original design. Rebar location and material properties are not altered. The tension stiffening parameter is not modified for these analyses.

The increase of reinforcement added to the footing did not significantly decrease the amount or change the location of maximum tension stress produced in the top of the footing during the tension phase of the subsidence event. This is illustrated in Table 5.2. The location of initial cracking produced in the bottom of the footing during the compression phase is given in Table 5.3. Initial cracking occurred in the same compression step and location for each amount of reinforcing. Due to the smear cracking effects of ABAQUS, additional cracks are produced throughout the bottom side of the footing as the subsidence event progressed during the

Table 5.2 Comparison in Location and Amount of Maximum Tensile Stress for Various Amounts of Reinforcing for the Tension Phase

Amount of Reinforcing	Distance from Leading Edge (m)	Tensile Stress (MPa)
#4 rebars (control)	4.5	4.0
#5 rebars	4.5	3.98
#6 rebars	4.5	3.97
#8 rebars	4.5	3.94

Table 5.3 Location of Initial Cracking Produced for Various Amounts of Reinforcing in the Compression Phase

Amount of Reinforcing	Initial Crack Location from the Leading Edge (m)
#4 rebars (control)	3.75
#5 rebars	3.75
#6 rebars	3.75
#8 rebars	3.75

compression phase. The same cracking pattern is produced for each amount of reinforcing. This pattern extends from 3.75 m from the leading edge to 3.0 m from the trailing edge. The effects of cracking was terminated as the subsidence events progressed into the relaxation phase. The increase in the amount of reinforcing had no effect on the cracking effects of the footing.

The maximum curvature produced in the footing for the increased amounts of reinforcement is given in Table 5.4 for both the tension and compression phases of subsidence. The curvatures produced in footing are virtually the same for all amounts of reinforcement. The increased amounts of reinforcing proved to have no effect on the curvature produced in the footing.

The maximum tensile stress produced in the reinforcing is given in Table 5.5. The tensile stress given for the tension phase is for the two rebars in the top of the footing and the tensile stress given for the compression phase is for the bottom two rebars. The stresses given in Table 5.5 shows that the reinforcing was not near to the specified yielding stress of 465 MPa (68 ksi).

The observations made from increasing the amount of reinforcing within the footing of the foundation suggest that there is no need for an increase of reinforcing. Only a sufficient amount is needed to increase the curvature capacity of the foundation. Cracking will still occur if there is an

Table 5.4 Maximum Curvature Produced in the Footing for Various Amounts of Reinforcing

Amount of Reinforcing	Curvature (rad/m)	
	Tension Phase	Compression Phase
#4 rebars (control)	.00076	.00108
#5 rebars	.00070	.00109
#6 rebars	.00076	.00109
#8 rebars	.00075	.00109

Table 5.5 Maximum Rebar Tensile Stresses for Various Amounts of Reinforcing

Amount of Reinforcing	Tensile Stress (MPa)	
	Tension Phase	Compression Phase
#4 rebars (control)	13.24	15.0
#5 rebars	13.21	15.14
#6 rebars	13.17	15.13
#8 rebars	13.06	15.09

increase of reinforcing. The increase of reinforcing does not increase the cracking moment capacity of the footing to a great extent. More important is the fact that the same curvature is produced within the footing no matter how much reinforcing is added. The original design with #4 rebars is sufficient to handle this curvature.

5.2.2 Reinforced Footing With Masonry Wall

Since the addition of the masonry wall affected the response of the reinforced footing, the effect of various amounts of reinforcing placed within the footing with the masonry wall is studied. The increased amounts of reinforcing placed in the footing are the same amounts used in the footing without a masonry wall. The modified masonry modeling is used for the masonry wall for tension phase analysis and the plain masonry mesh is used for compression phase analysis.

Cracking occurred in the footing during the tension phase with the #4 rebars and modified masonry wall. The increased amounts of reinforcing did not alleviate this phenomenon. Cracking was produced 3.75 m in the footing from the leading edge for all amounts of reinforcing. The maximum reduction of curvature for the tension phase was supplied by the #8 rebars with -.00083 rad/m. However, this reduction is very small considering a curvature of -.00085 rad/m was produced for the #4 rebars.

The same response was produced for all amounts of reinforcing during the compression phase. Cracking produced in the footing was not prevented by increasing the amount of reinforcing. In addition, curvature response was not changed to any significant extent. There was only a maximum of 2% reduction in curvature provided by the #8 rebars.

From the results produced in this study, an increased amount of reinforcing would not reduce the amount of damage that would be inflicted to the superstructure due to foundation response. The stress produced in each amount of reinforcing did not decrease significantly for both phases of subsidence. The #4 bars are adequate for handling the curvature produced in this study.

5.3 Rebar Placement

The original design of rebar placement suggests that rebar should be placed in both the top and bottom for reverse curvature effects from subsidence. This design only considers the footing for taking stresses with no contribution from the masonry wall. Johnson (1992) suggests that rebar should only be placed in the top of the footing for taking the tensile stresses in the tension phase when the masonry wall does not contribute to great extent. However, the masonry wall does contribute in taking compressive stresses in the compression phase; therefore, the combination of footing and masonry wall should supply a deep beam type action with rebar in the top of the footing for tensile stresses. From Johnson's (1992) suggestion and the observations made from previous analyses, the elimination of the rebar in the bottom of the footing will be studied for this section. The modified inelastic masonry mesh is also used for the tension phase and the continuum inelastic masonry mesh is used for the compression phase with peak stages analyzed.

Cracking was produced in the top of the footing 3.75 m away from the leading edge for the tension phase. This was the same location of cracking of the footing with two rows of reinforcing. Curvature induced in the footing was only slightly increased, 0.2%, which is virtually no change.

The compression phase produced cracks in the footing in the same manner as the original analysis. Curvature within the footing rose only from .000564 rad/m to .000566 rad/m. This amount of increase in curvature is also insignificant.

The rebar stress did not increase to a large extent and they were not close to yielding for both phases. Due to this fact and the other observations made from this study suggests that only one row of #4 rebars placed in the top of the footing is necessary when the masonry wall is considered as a contributing factor.

5.4 Various Footing Depths

This study uses only the reinforced concrete footing analysis with no masonry construction as a base model. The only parameter changed within the model is the footing depth. The same distance of 5.08 cm (2 in.) in rebar placement from the top and bottom surface is used in each analysis. This corresponds to the original placement of rebar. Three depths of 30.5 cm (12 in.), 40.6 cm (16 in.), and 70.0 cm (24 in.) are used in this investigation and compared to the original depth of 25.0 cm (10 in.).

The change in depths of the reinforced footing produced cracking in the top of the footing for certain depths while other depths produced only high tensile stresses during the tension phase of analysis. The footing of 30.5 cm depth produced its initial and only cracking at three integration points in the top of the footing about 4.5 m from the leading edge. The footing with a depth of 40.6 cm produced initial cracking at three integration points about 5.2 m from the leading edge. As the analysis continued for the 40.6 cm depth, more cracks formed in the top of the footing during the tension phase. They extended from the initial cracking point to 7.5 m from the leading edge. The footing of 70.0 cm produced the same behavior as the original depth of 25.0 cm with no cracking during the tension phase; however, the amount and location of maximum tensile stress is changed. This could be due to gapping of 4.5 mm that occurred underneath the corners of the footing at the interface for the footing of 70.0 cm in depth. This would suggest that the footing reached a depth to where its stiffness was large enough to overcome bending effects in the tension phase even though its cracking curvature was decreased. A summary of the cracking behavior and maximum stress for the various footing depths during the tension phase is given in Table 5.6. The cracking produced in the bottom of the footings were virtually the same for all depths analyzed during the compression phase. The final crack pattern produced in the bottom of the footings for the compression phase extended from 3.75 cm from the leading edge to 3 m from the trailing edge.

Table 5.6 Location and Amount of Maximum Tensile Stress for Various Reinforced Footing Depths during the Tension Phase

Footing Depths	Maximum Tensile Stress (MPa)	Location from Leading Edge (m)
25.0 cm (10 in.) (control)	4.0	4.5
30.5 cm (12 in.)	4.25 (crack)	4.5
40.6 cm (16 in.)	4.25 (crack)	5.2 - 7.5
70.0 cm (24 in.)	3.2	6

The summary of maximum curvatures produced in each footing is given in Table 5.7. The curvature values produced in each phase decrease as the depth of the footing is increased. Cracking in some of the footings may have occurred because as the footing depth is increased the value of curvature to cause cracking is decreased. The decrease in curvature suggests that a rigid approach to design would be appropriate in order to reduce bending transmitted to the superstructure.

Table 5.7 Maximum Curvature Values for Various Depths of Reinforced Footings

Footing Depth	Curvature (rad/m)	
	Tension Phase	Compression Phase
25.0 cm (10 in.) (control)	.00076	.00108
30.5 cm (12 in.)	.00068	.00102
40.6 cm (16 in.)	.00055	.00101
70.0 cm (24 in.)	.00022	.00060

The maximum tensile stresses produced in the reinforcing for each depth of footing is given in Table 5.8. This table shows that as the depth increases the tensile stress in the rebars increase. Only a decrease in tensile stress was produced in the 70.0 cm footing depth for the tension phase. This could be attributed to the fact that no cracking was produced in this phase at this depth of footing.

The increase in depth of the reinforced footing proved to give good results. A decease in curvature was produced with an increase in footing depth. Different cracking behaviors were established for different footing depths in the tension

Table 5.8 Maximum Tensile Stress in the Reinforcing for Various Amounts of Footing Depths

Footing Depth	Tensile Stress (Mpa)	
	Tension Phase	Compression Phase
25.0 cm (10 in.) (control)	13.24	15.0
30.5 cm (12 in.)	14.50	18.24
40.6 cm (16 in.)	18.57	32.75
70.0 cm (24 in.)	14.06	37.44

phase; however, cracking behavior was the same for each depth in the compression phase. The amount of reinforcing specified was adequate for each depth as not to reach its yielding limit.

5.5 Interface Reduction

The modeling used in the reinforced concrete footing analysis is used for this study. The interface properties are modified by reducing the friction angle by one-half. This reduction drops the coefficient of friction from 0.7 to 0.315. Note that reducing the friction angle by one-half is not the same as reducing the coefficient of friction by one-half.

The maximum tensile stress produced in the reinforced footing during the tension phase of subsidence was increased from 4.0 Mpa to 4.13 MPa. The strains induced in the footing cause an increase in maximum curvature from .00076 rad/m to

.00083 rad/m. Even though the strains and stresses were increased with the reduction in the coefficient of friction, no cracking was produced during the tension phase. The tensile stresses in the rebars were only slightly elevated from 13.24 Mpa to 13.38 Mpa.

The compression phase produced the same cracking behavior in both analyses. The reduced friction angle produced a higher maximum curvature. There was an increase from .00108 rad/m to .00111 rad/m. The tensile stress in the rebars was increased from 15.0 MPa to 16.65 MPa.

The reduction in the friction angle at the interface primarily caused an increase in stresses and strains within the reinforced footing.

5.6 Bond Beam Addition

A bond beam is placed in the top of the modified masonry mesh. This is accomplished by placing truss elements across the length of the masonry wall. The truss elements use the area of a #6 rebar along with material properties proposed by Johnson (1992) for reinforcing. This amount of reinforcing used was to simulate the stiffness provided by the double sill plates installed on top of the masonry wall during construction of the West Frankfort test foundations. Material properties of the wood sill plates and slippage that occurred at sill plate connections are used for this estimation of rebar size. Since the purpose of the bond beam is to carry tensile stresses when the masonry is in a state of tension, the tension phase analysis is only relevant to the use of this masonry construction.

The bond beam contributed to a significant increase in the stiffness of the foundation. A reduction of cracking was evident within the masonry wall. Furthermore, gapping within the modified mesh at interface element placement was reduced. The resulting maximum tensile stress that formed in the reinforced concrete footing was 3.1 MPa occurring 5.25 m from the leading edge. The bond beam only experienced 65.3 MPa of stress which is far below yielding. The use of the bond beam reduced the tensile stresses in the footing whereas the conventional masonry wall produced cracking in the footing.

The curvature produced in the foundation was reduced with the use of the bond beam. The maximum curvature that existed during the tension stage was .000626 rad/m. The bond beam caused a 26% reduction in curvature over the use of the conventional masonry construction.

The use of a bond beam is an effective technique to carry tensile stresses produced in the tension phase of subsidence. The occurrence of cracking within the masonry wall was reduced. Finally superstructural damage would decrease due to diminishing curvatures produced in the foundation.

5.7 Concrete Wall Addition

This study involved the addition of a concrete wall to the reinforced concrete footing. The concrete properties used for the footing and the geometry and elements used for the masonry modeling were given to the concrete wall. This analysis studies the footing reactions to an increase in stiffness of the foundation from the concrete wall.

The combined section of the concrete wall and reinforced footing experienced no cracking during both phases of analysis. The foundation cantilevered during the tension phase producing gapping at both ends of the interface. The gapping between the footing and soil produced a maximum vertical gap of 6.6 mm. The compression phase produced a bridging effect in the foundation at the middle 1/3 of the interface. A maximum gap of 1.17 mm was produced between the bottom of the footing and soil.

The tension phase produced tensile stresses in the concrete wall and compressive stresses in the reinforced footing. The maximum tensile stress that was obtained in the wall was 2.39 MPa which is far above the cracking stress of 350 kPa occurring in the mortar joints of conventional masonry. This stress was located 6 m from the leading edge which was the location of maximum stress produced in the elastic masonry wall. However, the tensile stress produced in the concrete wall is 30% greater than that in the elastic masonry wall. In addition, only compressive stresses were produced for this phase in the reinforced footing, whereas the reinforced footing with the elastic masonry took some tensile stresses.

The compression phase produced tension in both the reinforced footing and concrete wall. Maximum tensile stresses only reached 3.43 MPa in the footing. The location of this maximum stress was 6 m from the leading edge which was the same location of maximum stress in the footing with the elastic masonry wall. The maximum tension that the concrete wall experienced in this phase was 991 kPa. Unlike previous analyses no cracking was produced in the footing from the compression phase. This may be attributed to the increase in stiffness provided by the concrete wall.

The maximum curvatures produced in the combined section were -.000086 rad/m and .00020 rad/m for the tension and compression phases respectively. The curvatures were reduced 100% and 65% over the curvatures produced in the non-linear masonry wall with reinforced footing for the tension phase and compression phase. The reduction of curvatures could be attributed to the increase in stiffness allowing the structure to act as a rigid body thereby cantilevering and bridging over the soil.

The addition of the concrete wall produced a significant increase in stiffness as compared to conventional foundation construction. The behavior of this foundation construction was different from other analyses performed. Unlike typical masonry, no cracking was produced within the concrete wall. Furthermore, the concrete wall reduced tensile stresses in the reinforced footing thereby eliminating cracking. Curvatures were also reduced significantly in both phases of analysis, thereby reducing superstructure damage. This was accomplished by the rigid body behavior of the combined section that allowed it to "ride out" the subsidence event.

CHAPTER 6

CONCLUSIONS AND RECOMMENDATIONS

6.1 Conclusions

The numerical analyses performed in this work simulated the foundation response from subsidence. Even though the exact response of the field foundations was not duplicated due to the limitations and availability of the material models, certain behavioral responses such as cracking and curvature were induced in the foundation. From the responses presented in these analyses, valuable information was obtained as to how each component of the foundation contributes to the complete foundation response. In addition, the effect of changing certain parameters within the modeling furnished an insight as to how damage associated with subsidence can be reduced.

The effect of increasing reinforcement within the footing did not show promise as to decreasing damage and curvature. The addition of the masonry wall to the footing showed also that increased amounts of reinforcing produced no significant influence in foundation behavior. The cracking behavior and curvature response for both models was virtually the same for all amounts of reinforcing studied. However, a minimum amount of reinforcing is needed to maintain foundation integrity after cracking. The maximum amounts of curvature induced in these analyses suggests that the two #4 rebars is sufficient. Hudgings (1989) analysis suggests that two rows of reinforcing is needed for reverse curvature produced in the footing; however, his analyses did not include any masonry wall modeling. The analyses performed in this study suggests that if typical masonry construction is considered acting compositely with the footing, only one row of reinforcement should placed in the top of the footing. This amount of reinforcing corresponds to 0.22%.

The change in footing depth suggests that a foundation will experience damage according to curvature or moment resisting designs. As the footing depths were increased, the curvature capacity was diminished while the moment capacity was increased. This phenomenon was illustrated as curvature produced by the subsidence event induced higher tensile stresses in the footing as its depth was moderately increased. However, the footing depth was increased to an extent that its increase in moment capacity allowed it to "ride out" the curvature effects by acting as a rigid body. This was also noticed when the masonry wall was replaced with a concrete wall producing virtually a large deep beam.

The addition of the masonry wall to the foundation played a vital role in affecting foundation response. The traditional masonry block proved to be very weak when subjected to tensile stresses. The masonry wall did not relieve tensile stresses produced in the footing at a cracked section during the tension stage. However, the masonry wall could contribute to relieving these tensile stresses by increasing its tensile capacity. This could be accomplished through the use of placing a bond beam in the top of the wall or by replacing the masonry wall with a concrete wall. The masonry was very useful when it was subjected to compressive forces during the compression phase of subsidence. The addition of the wall did not reduce cracking in the footing; however, curvature was reduced dramatically. The masonry wall and footing were working together to act as a deep beam. Further reduction in curvature and the elimination of cracking in the footing was accomplished with the concrete wall.

The change in reducing the friction angle at the interface produced a surprising effect. The tensile forces and curvature effects induced in the footing were increased with a decrease in friction angle. This is not what was expected. As to why this behavior occurred can not be explained at this point since limited information has been compiled as to the effects of shear transfer at the interface.

6.2 Recommendations

The soil modeling used in these analyses was only elastic behavior, since difficulties were encountered with the plasticity model. The damage from the analyses did not correspond exactly to the damage produced in the field. A plasticity soil model should be used that would induce significant strains and stresses in the foundation to cause damage. Since unrecoverable deformations are associated with plasticity models, the entire subsidence event may need to be use for analysis. In addition, more information needs to be gathered about shear transfer at the interface so that an improved interface can be provided for in future analysis.

From the analysis performed in this work and literature reviewed, it is suggested that a residential footing should be designed either flexible or rigid. The field footings represent a flexible design with a minimum amount of reinforcing incorporated for post cracking behavior. The analyses performed in this work in conjunction with Hudging's (1989) analyses suggest that the amount of reinforcing used within the footing should only be enough to produce a yield moment slightly greater than the cracking moment. In addition, analyses suggest that only one row of reinforcing is needed in the top of the footing to satisfy post cracking behavior and minimum clear cover requirements for reinforcing. However, if this flexible approach is used, then measures should be taken to design the superstructure for curvature effects that it will experience during subsidence. If reduced measures are desired in designing the superstructure, then a semi-ridge approach suggested from analyses is to use a bond beam placed in the top of the masonry wall. One #6 rebar proved to be sufficient for these analyses; however, due to limitations of the numerical model and that the analysis assumed perfect bond between the masonry and bond beam, the use of two #6 bars may be more appropriate for the bond beam. The installation of the bond beam will reduce cracking within the masonry wall and footing during the tension phase; however, the same curvature will still exist from the compression phase. To further increase the tensile carrying capacity of the masonry wall, the masonry should be dowelled into the footing. This can be accomplished by embedding vertical rebars in the footing and extending these bars through the holes of the masonry. These holes should then be filled with grout. In addition, rebar location in the footing should be placed in only one layer at 7.75 cm (3 in.) from the bottom where it would be most beneficial during the compression phase.

A complete rigid approach would require the least of any superstructure modifications. The entire foundation and superstructure would act as a rigid body, with tilt as the only movement experienced. The analysis performed in this work suggests that this rigid approach can be accomplished by replacing the masonry wall with a concrete wall. The concrete wall should be dowelled in place so that the wall and footing can perform as a deep beam. This method of foundation construction would cost the most as far as foundation construction is concerned; however, the cost of incorporating superstructure modifications would probably be offset. The suggestion of using a concrete wall is certainly valid for these analyses by increasing the stiffness of the foundation to an extent to where it predominantly acts as a rigid body; however, a plasticity soil model may show that the concrete wall may induce more curvature or even cracking within the foundation. Therefore, this type of design should be tested with a plasticity soil model to insure its credibility.

BIBLIOGRAPHY

BIBLIOGRAPHY

ACI Committee 318 (1989). Building Code Requirements for Reinforced Concrete (ACI 318-89). American Concrete Institute, Detroit, Michigan.

Awasthi, R. (1992). "Structural Deformation, Tilt and Curvature," Subsidence Effects on Structures. Institute for Geotechnology, Dept. of Civil Engineering, University of Tennessee, Knoxville, Tennessee, TN., Report #92-01, Vol. 2(8), 1-50.

Basham, K.D., Suprenant, B.A., Karfakis, M.G., and Johnson, W.L. (1989). "Suggested Guidelines and Recommendations for Residential Construction to Minimize Subsidence Related Damage." Proc., Evolution of Abandoned Mine Land Technologies, Riverton, Wyoming, 1-14.

Bell, S.E. (1977). "Successful Design for Mine Subsidence." Large Ground Movements and Structures. John Wiley and Sons, New York, NY, 562-578.

Ben Hassine, J. (1992). "Numerical Analysis," Subsidence Effects on Structures. Institute for Geotechnology, Dept. of Civil Engineering, University of Tennessee, Knoxville, Tennessee, TN., Report #92-01, Vol. 2(13), 1-29.

Ben Hassine, J., and Drumm, E.C. (1991). User Manual for UTGTECH, Version 1.9. Institute for Geotechnology, Dept. of Civil Engineering, Univ. of Tennessee, Knoxville, TN.

Bennett, R.M. (1990). "Structural Damage and Remedial Measures." Workshop on Mine Subsidence and Structures, 1990 National Symposium on Mining, Friedrich, N.O., and Kane, W.F. (Eds). Institute for Geotechnology Publication #90-91, University of Tennessee, Knoxville, TN. 55-65.

Boscardin, M.D., and Ahmed, I. (1992). "Subsidence Effects on Buildings and Buried Pipelines." 3rd Subsidence Workshop Due to Underground Mining, 106-112.

Boscardin, M.D., and Cording, E.J. (1989). "Building Response to Excavation-Induced Settlement." Journal of Geotechnical Engineering., ASCE, Vol. 115(1), 1-21.

Bowles, J.E. (1988). Foundation Analysis and Design., 4th ed., McGraw-Hill Publishing Company, New York, New York.

Burland, J.D., Broms, B.B., and de Mello, V.F.B. (1977). "Behavior of Foundations and Structures." State of the Art Report., Proc., International Conference on Soil Mech. and Found. Engr., Vol. 3, Tokyo, Japan, 495-546.

Chen, C.Y., Chen, Y.M., and Gaffney, D.V. (1974). Architectural Measures to Minimize Subsidence Damage. Appalachian Regional Commission, 130 pp.

Drumm, E.C., and Bennett, R.M. (1992). Subsidence Effects on Structures. Institute of Geotechnology, Dept. of Civil Engineering, University of Tennessee, Knoxville, TN., Report #92-01, Vol. 1-3.

Drumm, E.C., Bennett, R.M., and Kane, W.F. (1988). "Mechanisms of Subsidence Induced Damage and Techniques for Analysis." Mine Induced Damage: Effects on Engineered Structures. Geotechnical Special Publication No. 19, ASCE, New york, NY, 168-188.

Drysdale, R.G., Hamid, A.A., and Heidebrecht, A.C. (1979). "Tensile Strength of Concrete Masonry." Journal of the Structural Division., Vol. 105(ST7), 1261-1276.

Drysdale, R.G., and Hamid, A.A. (1984). "Tension Failure Criteria for Plain Concrete Masonry." Journal of Structural Engineering., ASCE, Vol. 110(2), 228-244.

Freyermuth, C.L. (1987). "Residential and Industrial Floors Benefit from Post-tensioning." Concrete Construction. Vol. 32(1), 14-18.

Geddes, J.D. (1977a). "The Effect of Horizontal Ground Movements on Structures." Large Ground Movements and Structures. John Wiley and Sons, New York, NY, 623-646.

Geddes, J.D. (1977b). "The Behavior of a CLASP-System School Subjected to Mining Movements." Large Ground Movements and Structures. John Wiley and Sons, New York, NY, 579-596.

Geddes, J.D. (1977c). "Construction in Areas of Large Ground Movement." Large Ground Movements and Structures. John Wiley and Sons, New York, NY, 949-974.

Geddes, J.D. (1984). "Structural Design and Ground Movements." Proc., Ground Movements and Their Effects on Structures. Glasgow, 243-267.

Gere, J.M., and Timoshenko, S.P. (1984). Mechanics of Materials, 2nd Ed., Wadsworth,Inc., Belmont,California, 744 pp.

Hall, H.C. (1978). "Masonry Buildings: Construction on Subsidence Sites." Proc., North American Masonry Conference. The Masonry Society, 84-1 to 84-13.

Heathcote, F.W.L. (1965). "Movement of Articulated Buildings on Subsidence Sites." Proc., Institute of Civil Engineers, Vol. 30, 347-368.

Hibbitt, Karlsson, and Sorensen, Inc. (1989a). ABAQUS Theory Manual, Version 4.8.

Hibbitt, Karlsson, and Sorensen, Inc. (1989b). ABAQUS User Manual, Version 4.8.

Hudgings, R.A. (1989). "Numerical Investigations of Mitigation Techniques for Damage to Structures Subjected to Mining Subsidence," thesis presented to the University of Tennessee, Knoxville in partial fulfillment for the degree of Master of Science.

Jamal, B.D., Bennett, R.M., and Flanagan, R.D. (1992). "Numerical Analysis for In-Plane Behavior of Infilled Frames," Proc., of the Sixth Canadian Masonry Symposium, Saskoon, Saskatchewan, 609-620.

Johnson, D.C. (1992). "Structural Behavior and Damage Assessment of Residential Foundations Subjected to Subsidence," thesis presented to the University of Tennessee, Knoxville in partial fulfillment of the requirements for the degree of Masters of Science.

Kane, W.F., Triplett, T.L., Yarbrough, R.E. and Murphy, E.W. (1989). "Earth-Structure Interaction Analysis for Subsidence Damage Mitigation." Proc., Evolution of Abandoned Mine Land Technologies, Riverton, Wyoming, 79-98.

Karmis, M., Yu, Z. and Jatosz, A. (1990). "Design Considerations for Subsidence Control." Proc., of the Annual Meeting of Society for Mining, Metallurgy, and Exploration, Salt Lake City, Utah, 1-6.

Lawrence, T.S. (1992), "Soil Testing and Numerical Modeling of a Subsidence Event," thesis presented to the University of Tennessee, Knoxville, in partial fulfillment of the requirements for the degree of Masters of Science.

Lee, P.A. (1989). "Interface Parameters for Earth-Structure Interaction During Mining-Induced Subsidence," thesis presented to the University of Tennessee, Knoxville in partial fulfillment for the Degree of Master of Science.

Lin, G. (1992a). "Structural Deformation: Strain," Subsidence Effects on Structures. Institute for Geotechnology, Dept. of Civil Engineering, University of Tennessee, Knoxville, Tennessee, TN., Report #92-01, Vol. 2(10), 1-19.

Lin, G. (1992b). "Structural Damage Assessment," Subsidence Effects on Structures. Institute for Geotechnology, Dept. of Civil Engineering, University of Tennessee, Knoxville, Tennessee, TN., Report #92-01, Vol. 2(12), 1-12.

Littlejohn, G.S. (1974). "Observations of Brick Walls Subjected to Mining Subsidence," Proc., Conference on Settlement of Structures, John Wiley and Son, New York, New York, 384-393.

Marino, G.G., Mahar, J.W., and Murphy, E.W. (1988). "Advanced Reconstruction for Subsidence-Damaged Homes." Mine Induced Subsidence: Effects on Engineering Structures, Geotechnical Special Publication, 1987-106.

National Coal Board (1975). Subsidence Engineers' Handbook. NCB Mining Dept., United Kingdom.

Park, R., and Paulay, T. (1975). Reinforced Concrete Structures. John Wiley and Sons, New York, NY.

Peng, S.S. (1986). Coal Mine Ground Control: 2nd Ed. John Wiley and Sons, New York, 491 pp.

Powell, L.R., Triplett, T.L., and Yarbrough, R.E. (1986). Foundation Response to High Extraction Mining in Southern Illinois. Unpublished Report of Investigation, U.S. Bureau of Mines, Twin Cities Research Center.

Schneider, R.R., and Dickey, W.L. (1987). Reinforced Masonry Design., 2nd Ed., Prentice-Hall, Inc., Englewood Cliffs, New Jersey.

Treworgy, C.G., and Hindman (1991). The Proximity of Underground Mines to Residential and Other Built-up Areas in Illinois. Illinois State Geological Survey.

Triplett, T.L., Yarbrough, R.E., and Powell, L.R. (1986). "Foundation Response to Subsidence Induced by High Extraction Mining in Southern Illinois." Proc., of the 27th U.S. Symposium on Rock Mechanics, Tuscaloosa, AL., 283-290.

VITA

Robert Earl Gatlin, son of Earl S. and Barbara Gatlin, was born in Dyersburg, Tennessee on January 6, 1968. He graduated from Dyersburg High School in May 1986. He attended the University of Tennessee, Knoxville in the pursuit of a degree in civil engineering. During the completion of his degree of Bachelor of Science in May 1991, he accepted a position with the U.S. Bureau of Mines, Twin Cities Research Center to further his education in graduate school. In May of 1993, he received his Master of Science Degree in Civil Engineering.